2022

ESIPT-Enabled Alkyne Migration Provides Rapid Access to Benzoxazinones

Andrés G. Muñoz
University of Denver

ESIPT-Enabled Alkyne Migration Provides Rapid Access to Benzoxazinones

Abstract

Benozoxazinones have long been of interest to agrochemical scientists and medicinal chemists because of their widespread biological activity. These scaffolds are also of interest to synthetic chemists, who recognize the utility of benzoxazinones for accessing functionalized heterocycles. The use of efavirenz, a benzoxazinone-based reverse transcriptase inhibitor used in the treatment of HIV-1, has brought increased attention to this privileged pharmacophore. While there exist numerous strategies for synthesizing benzoxazinones, methods that do not require the use of acutely toxic and environmentally hazardous reagents are lacking. Consequently, there is a need to develop new methods for constructing this valuable scaffold. Herein, we report a photochemical alkyne migration that provides rapid access to the benzoxazinone scaffold. This is the first reported photochemical synthesis of a benzoxazinone, and, to our knowledge, the first reported photochemical alkyne migration.

Document Type

Thesis

Degree Name

M.S.

Department

Chemistry and Biochemistry

First Advisor

Andrei G. Kutateladze

Second Advisor

Brian Michel

Third Advisor

John Latham

Keywords

Organic synthesis, Photoassisted synthesis, Photochemistry

Subject Categories

Chemistry | Organic Chemistry | Other Chemistry

ESIPT-Enabled Alkyne Migration Provides Rapid Access to Benzoxazinones

_____

A Thesis

Presented to

the Faculty of the College of Natural Sciences and Mathematics

University of Denver

_____

In Partial Fulfillment

of the Requirements for the Degree

Master of Science

_____

by

Andrés G. Muñoz

August 2022

Advisor: Dr. Andrei G. Kutateladze

Author: Andrés G. Muñoz
Title: ESIPT-Enabled Alkyne Migration Provides Rapid Access to Benzoxazinones
Advisor: Dr. Andrei G. Kutateladze
Degree Date: August 2022

ABSTRACT

Benozoxazinones have long been of interest to agrochemical scientists and medicinal chemists because of their widespread biological activity. These scaffolds are also of interest to synthetic chemists, who recognize the utility of benzoxazinones for accessing functionalized heterocycles. The use of efavirenz, a benzoxazinone-based reverse transcriptase inhibitor used in the treatment of HIV-1, has brought increased attention to this privileged pharmacophore. While there exist numerous strategies for synthesizing benzoxazinones, methods that do not require the use of acutely toxic and environmentally hazardous reagents are lacking. Consequently, there is a need to develop new methods for constructing this valuable scaffold. Herein, we report a photochemical alkyne migration that provides rapid access to the benzoxazinone scaffold. This is the first reported photochemical synthesis of a benzoxazinone, and, to our knowledge, the first reported photochemical alkyne migration.

ACKNOWLEDGEMENTS

Undertaking a graduate degree in organic chemistry was daunting given my background in biology. However, I knew success was possible so long as I surrounded myself with the right people. The people mentioned hereafter had a profound impact on my professional and personal life. Without their guidance, friendship, and support, this thesis would not have been possible.

First, I would like to thank my advisor, Dr. Andrei Kutateladze, who took a chance on me and allowed me to conduct research in his group. His support, especially when I failed for months on-end, reminded me that scientific research is not just about publishing papers – it is about perseverance, fortitude, and commitment to a mission greater than ourselves.

Second, I would like to thank my friends at the University of Denver. Mitchell Ellinwood and Samir Rezgui were the first to train me in synthetic organic techniques. Without their guidance and patience, I would not be the chemist I am today. Further, I would like to thank Morgan Schneider, whose friendship, support, and sense of humor got me through some of the toughest times in the lab. To Alex Volkova and Maxwell Freeman, I thank you for providing much needed comic relief and necessary distractions throughout my time as a graduate student.

Finally, I would like to thank my fiancée, Rhyan, whose unending support, encouragement, and confidence in my abilities pushed me to complete my graduate work and thesis. Without her, none of this would have been possible.

TABLE OF CONTENTS

LIST OF FIGURES

Chapter One

Chapter Two

1. INTRODUCTION

1.1 PHOTOCHEMICAL TRANSFORMATIONS IN ORGANIC SYNTHESIS

Photochemical transformations hold unparalleled potential for the construction of complex scaffolds and molecular architectures. While a historically esoteric discipline, photochemistry has gained significant traction in the synthetic community in the last two decades. Herein are several examples highlighting the use of photochemical reactions as key steps in the synthesis of complex molecules and natural products.

The earliest example dates to 1908, when Ciamician and Silber utilized an intramolecular photochemical [2+2]-cycloaddition in the synthesis of carvone camphor from carvone (Figure 1.1).[1] This example also served to demonstrate the utility of photochemistry to access structures otherwise forbidden by thermal cycloadditions; orbital symmetry in thermal cycloadditions do not allow [2+2]-cycloadditions to form cyclobutanes. Cyclobutanes are commonly found in natural products, making photochemical [2+2]-cycloadditions an important tool for the synthesis of these scaffolds.

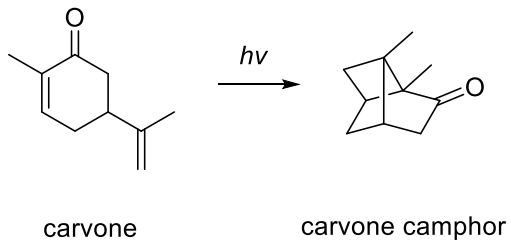

Figure 1.1. Photochemical [2+2]-cycloaddition to access carvone camphor.[1]

In the total synthesis of biyouyangagin A by Nicolaou, Sarlah and Shaw, a photochemical [2+2]-cycloaddition was a key step in constructing a cyclobutane moiety central to the scaffold (Figure 1.2).[2]

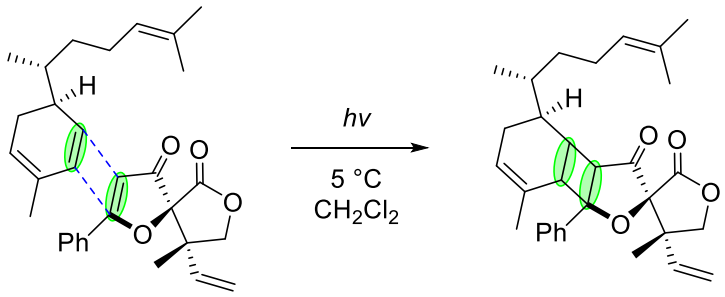

Biyouyangagin A

Figure 1.2. Photochemical [2+2]-cycloaddition in the synthesis of Biyouyangagin A.[2]

As depicted in Figure 1.3, a photochemical [2+2]-cycloaddition was also employed as a key step in the total synthesis of (+)-Solanascone by Srikrishna and Ramasastry.[3]

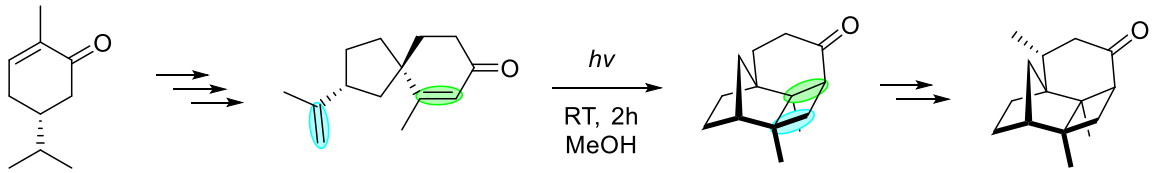

(+)-solanascone

Figure 1.3. Photochemical [2+2]-cycloaddition in the synthesis of (+)-solanascone.[3]

In addition to formal cycloadditions, photochemistry also allows access to more complex architectures that are otherwise inaccessible via thermal methods alone. For example, β,γ-unsaturated ketones are capable of undergoing oxa-di-π-methane rearrangements as depicted in Figure 1.4.[4]

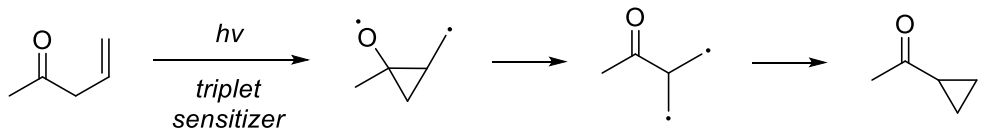

Figure 1.4. Oxa-di- π-methane rearrangement of β,γ-unsaturated ketone.[4]

As shown, a β,γ-unsaturated ketone, when irradiated in the presence of a triplet sensitizer, will undergo a 1,2-acyl migration, closing a cyclopropyl ring between the original α and γ atoms.

Yates and coworkers were the first to employ the oxa-di-π-methane rearrangement as a key step in the total synthesis of cedrol, as depicted in Figure 1.5.[5]

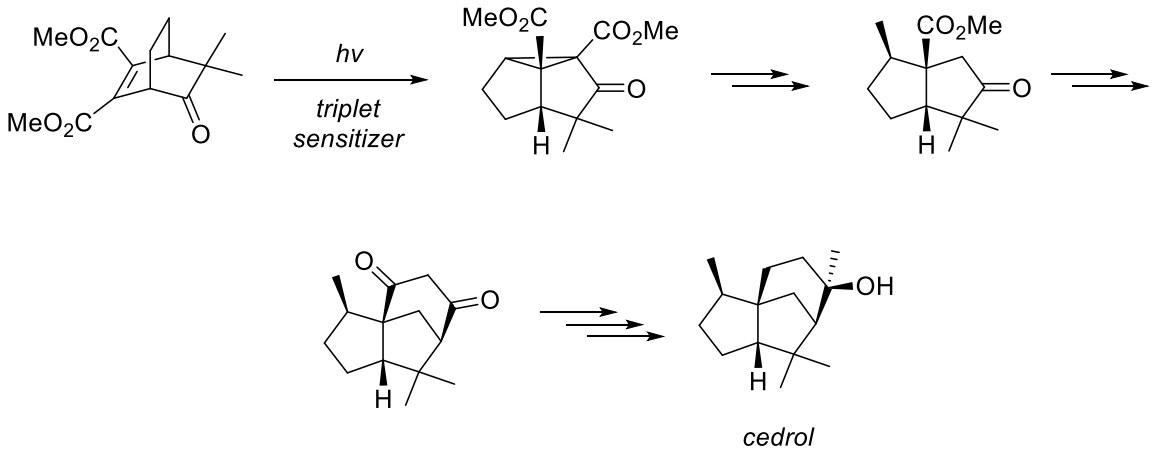

Figure 1.5. Oxa-di-π-methane rearrangement in the total synthesis of cedrol.[5]

These examples are only a select few in a growing body of work utilizing photochemical transformations as key steps in complex syntheses. That said, photochemistry remains largely underutilized by most synthetic chemists. Consequently, there is an urgent need for the continued development of experimentally simple photochemical transformations to construct complex scaffolds that are otherwise difficult to access by thermal methods alone.

1.2 EXCITED-STATE INTRAMOLECULAR PROTON TRANSFER

1.2.1 DISCOVERY OF ESIPT

An important tool in modern photochemistry is the excited-state intramolecular proton transfer (ESIPT), discovered in the 1950's by Weller. He found that irradiation of salicylic acid with UV light induced a proton transfer from the hydroxyl to the carbonyl oxygen, which, after relaxation from the excited-state, would undergo a ground-state back-transfer of the proton to reinstate the original molecule (Figure 1.6).[6]

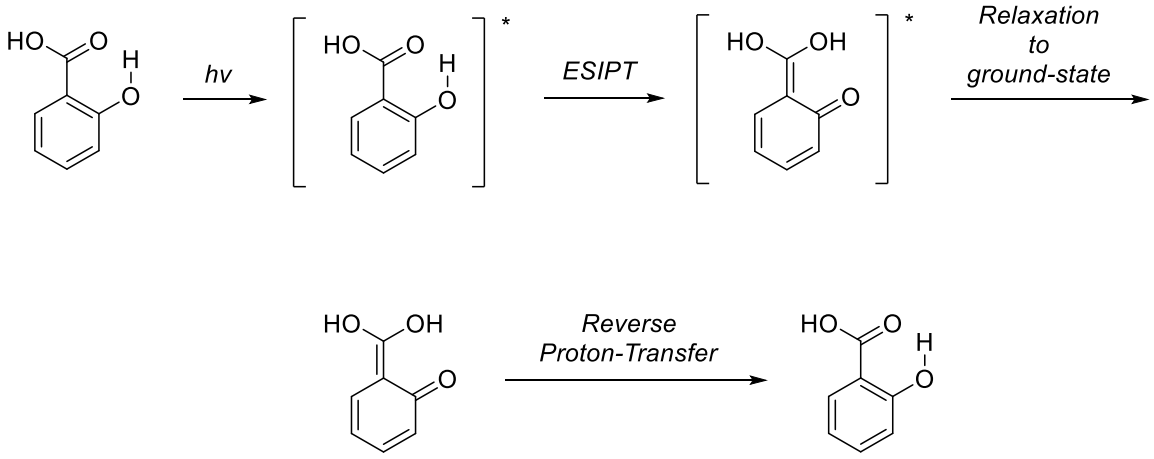

Figure 1.6. Weller's discovery of ESIPT in salicylic acid.[6]

Weller's pioneering work demonstrated that ESIPT occurs through intramolecular hydrogen bonding, and can therefore occur between H-bonding donors and acceptors, so long as geometry is favorable.[7] It was also established that acidic or basic moieties within a molecule become more acidic or basic upon excitation with light, thus making ESIPT more likely to occur, again with the caveat that the proximity and geometry of donors and acceptors is favorable.[8]

1.2.2 THE PHOTOPHYSICS OF ESIPT

An energy diagram depicting ESIPT in 2-(2-hydroxyphenyl)-benzothiazole (HBT), a common chromophore, is shown in Figure 1.7.

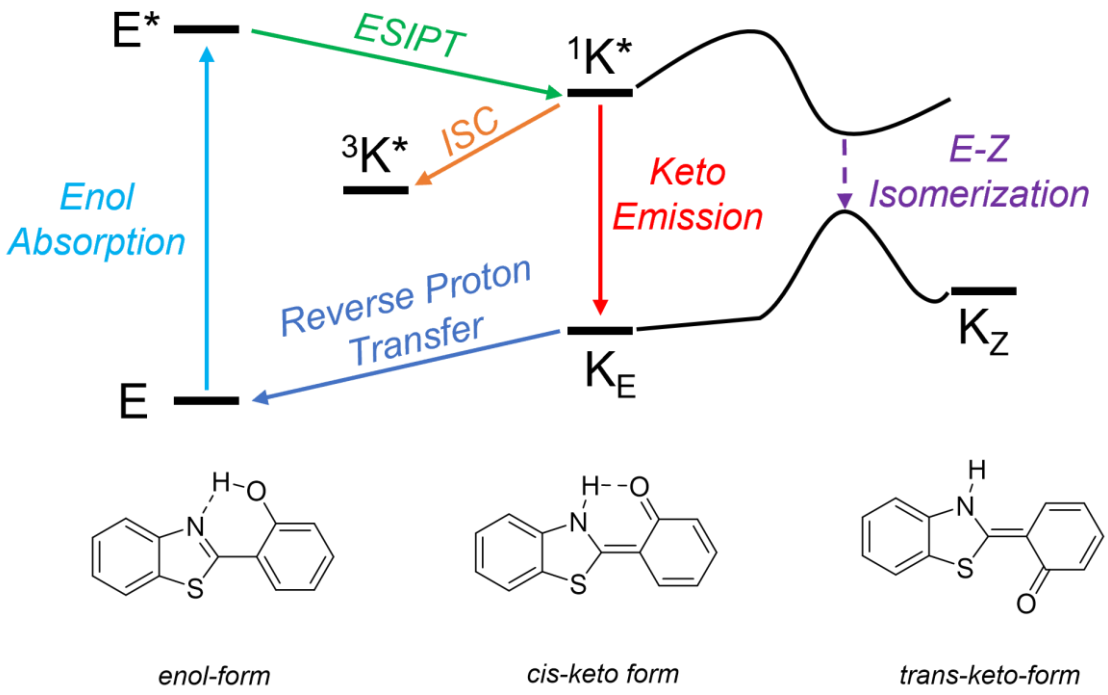

Figure 1.7. Energy diagram depicting the photophysics of ESIPT using HBT.

Beginning with the enol-form in the ground state **E**, absorption of UV light leads to the singlet excited-state enol, **E***. ESIPT occurs from **E***, producing the singlet excited-state cis-keto form **^{1}K***. Intersystem crossing to the triplet-excited state also occurs from **^{1}K*** to **^{3}K***. Keto emission from the singlet excited-state **^{1}K*** to the ground-state **K_E** emits fluorescence, after which a reverse proton transfer can occur, reconstituting the ground-state enol **E**. *E-Z* isomeratization is also possible from the singlet excited-state **^{1}K***, resulting in the ground-state trans-keto form **K_Z**.

A unique property of ESIPT is that it exhibits a large Stokes shift, whereby relaxation from the single-excited state **^{1}K*** to the ground-state emits fluorescence at a significantly higher wavelength than the wavelength absorbed by the ground-state enol. This feature of ESIPT makes it an attractive mechanism for fluorescent sensors and imaging agents.[9]

It is important to note that intersystem crossing (ISC) from the singlet-excited state to the triplet-excited state also produces a triplet 1,4-biradical, as depicted using salicylic acid in Figure 1.8. This triplet 1,4-biradical relaxes to the ground-state to yield an *o*-oxa-xylylene before reverse proton-transfer reconstitutes the starting molecule.

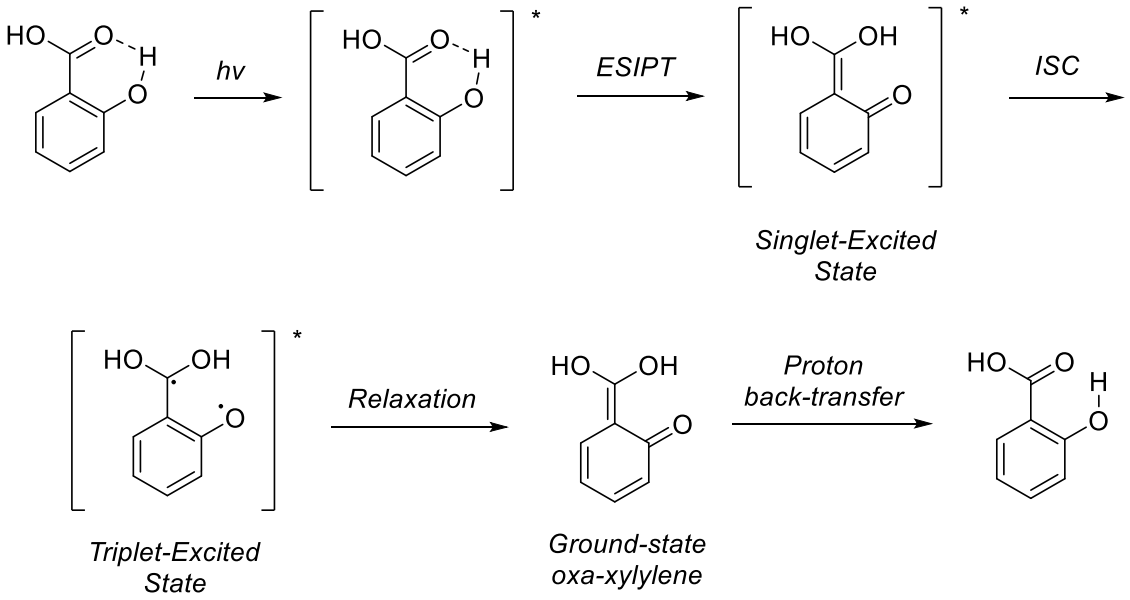

Figure 1.8. ISC produces a triplet-state 1,4-biradical.

1.3 UTILITY OF ESIPT IN THE SYNTHESIS OF COMPLEX MOLECULES

1.3.1 ESIPT-GENERATED XYLYLENES IN ORGANIC SYNTHESIS

Ortho-quinodimethanes, from here on referred to as *ortho*-xylylenes, have been important intermediates in synthetic organic chemistry for over 70 years.[10-13] Photochemical generation of *o*-xylylenes was first reported in by Sammes in 1976, and is depicted in Figure 1.9.[14]

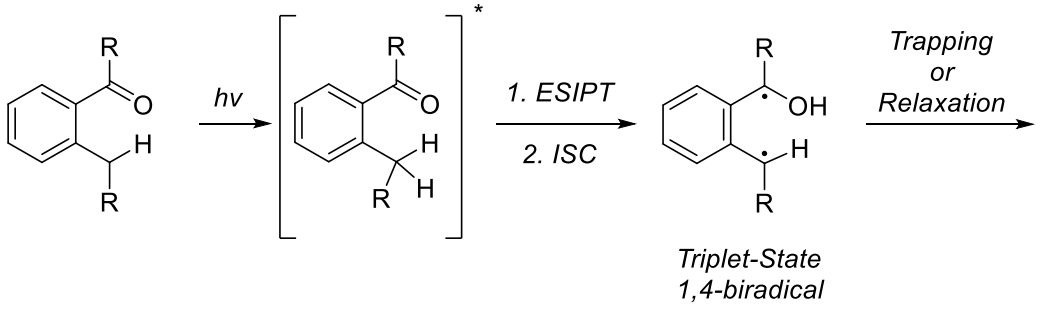

Figure 1.9. ESIPT-generated *o*-xylylenes.[14]

The ESIPT-generated triplet-state 1,4-biradical or ground-state *o*-xylylene can be trapped using a Diels-Alder reaction, making it a powerful intermediate for organic synthesis. Below are examples demonstrating the utility of photogenerated *o*-xylylenes in the synthesis of natural products.

In the total synthesis of estrone, a naturally produced steroid, Quinkert and coworkers utilized a photogenerated *o*-xylylene and subsequent [4+2]-cycloaddition to access its fused polycyclic scaffold (Figure 1.10).[15]

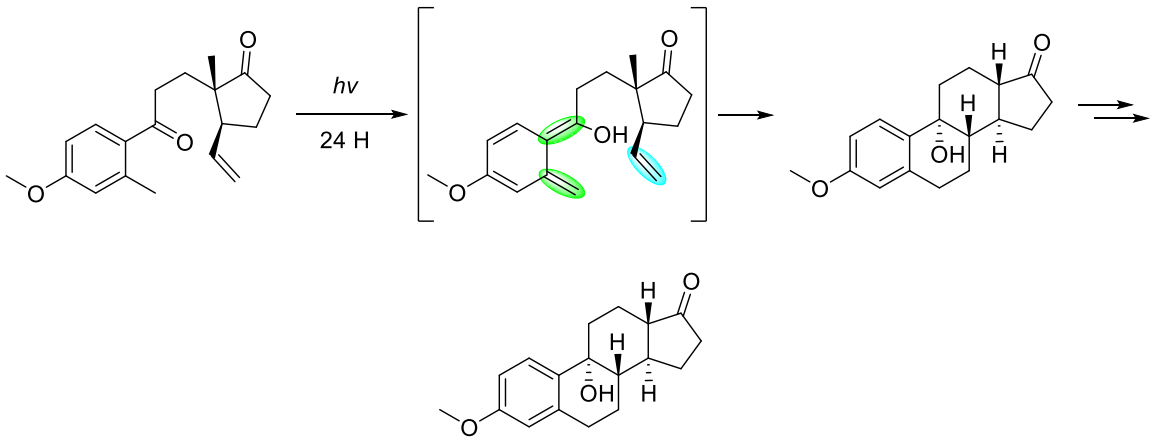

Figure 1.10. Synthesis of estrone using ESIPT-generated *o*-xylylene.[15]

An ESIPT-generated *o*-xylylene was also utilized in a [4+2]-cycloaddition in the total synthesis of podophyllotoxin by Kraus and Wu (Figure 1.11).[16]

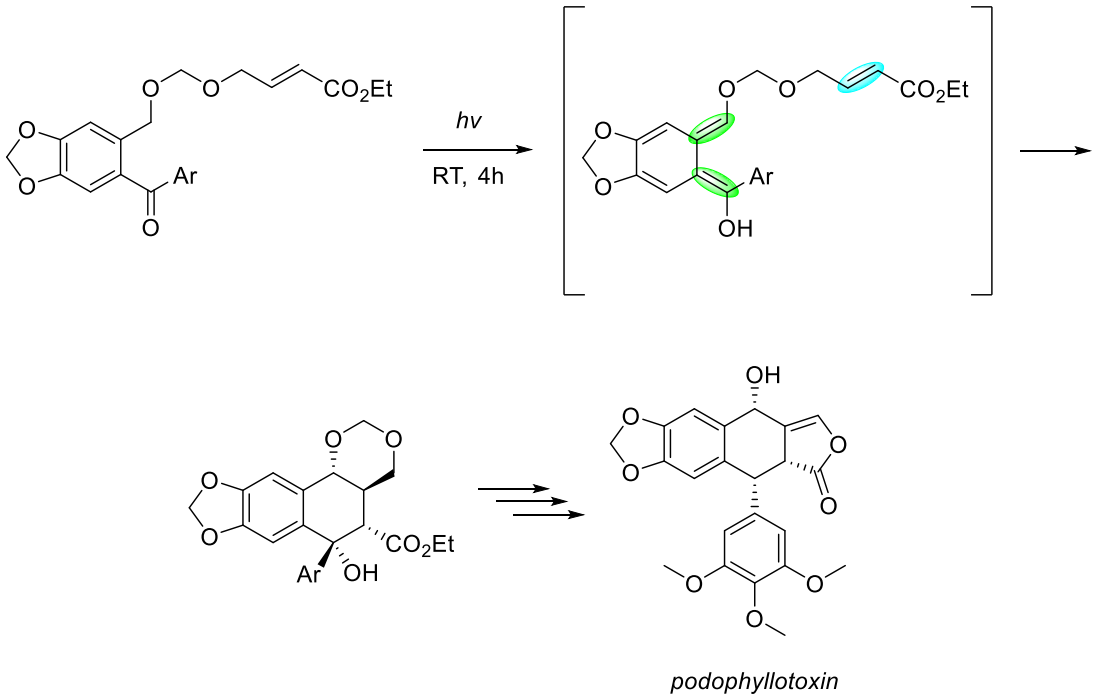

Figure 1.11. Synthesis of podophyllotoxin using ESIPT-generated *o*-xylylene.[16]

1.3.2 ESIPT-GENERATED *O*-AZAXYLYLENES IN ORGANIC SYNTHESIS

The Kutateladze group has published extensively on the use of ESIPT-generated *o*-azaxylylenes to undergo formal cycloadditions.[17-30] Much like their carbon analogues, ESIPT proceeds smoothly when *o*-amidoketones are irradiated with UV-light and the photogenerated *o*-azaxylylenes can be trapped using tethered dienophiles. Figure 1.12 shows an intramolecular [4+4]-cycloaddition between the photogenerated *o*-azaxylylene and a tethered furan to produce a polycyclic heterocycle.[22]

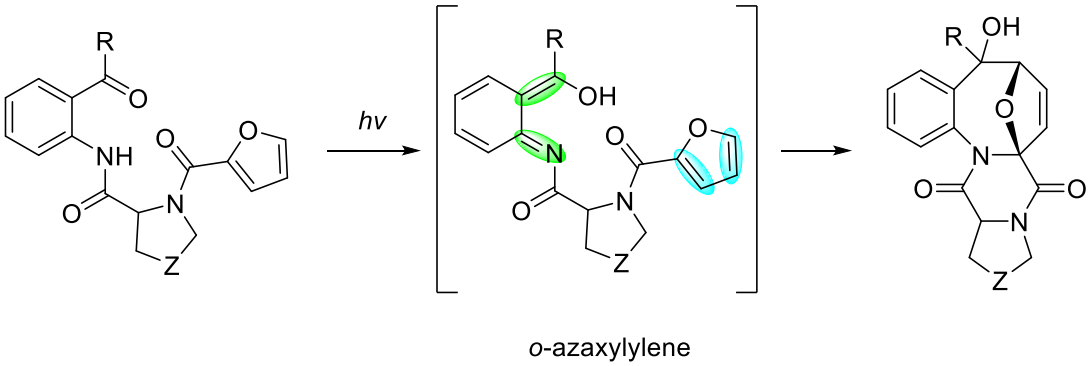

Figure 1.12. Intramolecular [4+4]-cycloaddition of a photogenerated *o*-azaxylylene.[22]

In an unprecedented "Double Click" photochemical cascade, an easily assembled photoprecursor undergoes sequential cycloadditions of photogenerated *o*-azaxylylenes to dramatically increase molecular complexity in a single experimental step (Figure 1.13).[30]

Photochemical cascade reactions like the one depicted in Figure 1.13 also represent an important strategy for accessing complex topology in small molecules, which is positively correlated to bioactivity.[31] Consequently, developing photochemical cascades which drastically increase molecular complexity in a single experimental step is a primary objective in the Kutateladze Group.

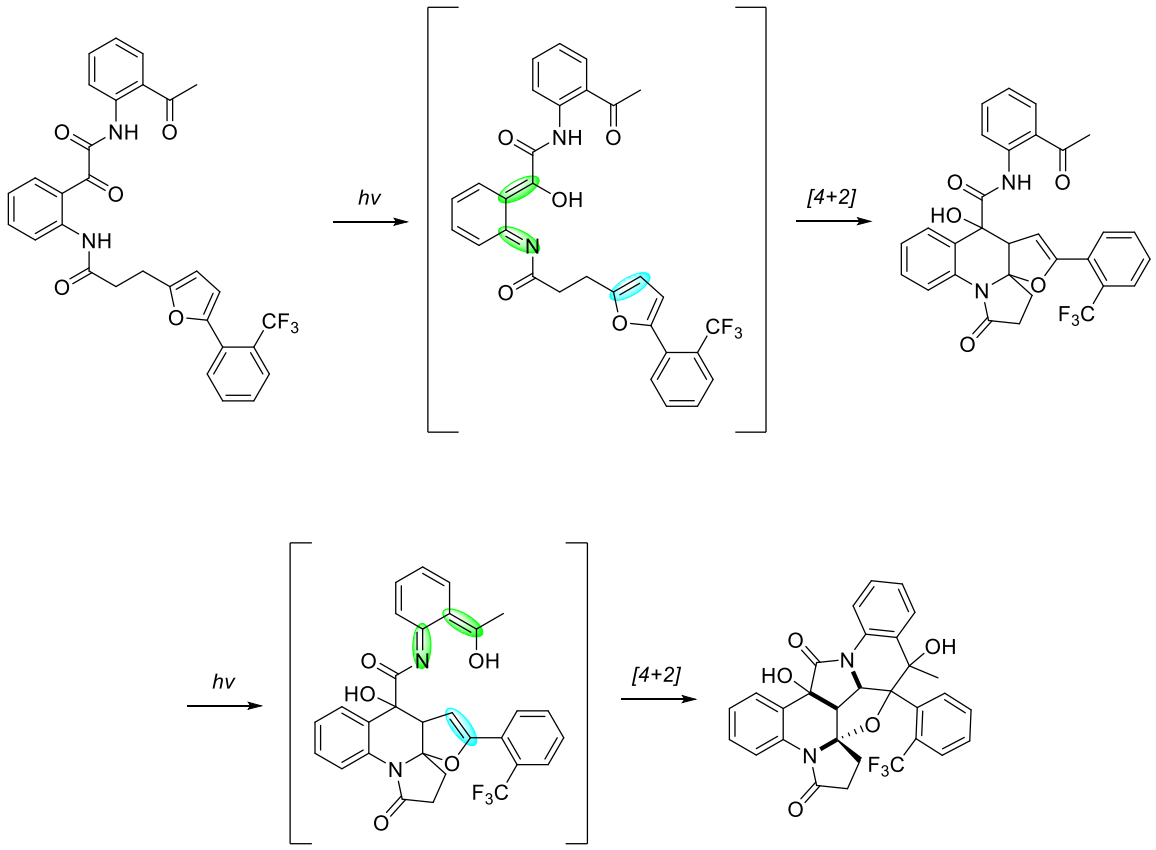

Figure 1.13. "Double Click" Reaction of photogenerated *o*-azaxylylenes.[30]

While the Kutateladze group has pioneered the use of ESIPT-generated *o*-azaxylylenes for the construction of complex scaffolds bearing privileged structures, ESIPT remains an underutilized tool in synthetic chemistry. Moreover, ESIPT-enabled reactions that do not involve a formal cycloaddition are lacking. Hence, there is an urgent need to develop ESIPT-enabled reactions outside the realm of cycloadditions that access privileged structures and pharmaceutically relevant scaffolds.

2. RESEARCH

2.1 RELEVANCE OF BENZOXAZINONES

2.1.1 STRUCTURAL CHARACTERISTICS OF BENZOXAZINONES

Oxazines are heterocycles containing one oxygen atom and one nitrogen atom in a singly or doubly unsaturated ring. (Figure 2.1). Benzoxazines are bicyclic heterocycles comprising of an oxazine moiety fused to a benzene ring. (Figure 2.1). Benzoxazinones are benzoxazines that also contain a carbonyl within the oxazine heterocycle. There are a variety of structural isomers of benzoxazinones, which are often referred to as benzoxazinoids. For the sake of simplicity, all benzoxazinoids and their derivatives herein will be referred to as benzoxazinones.

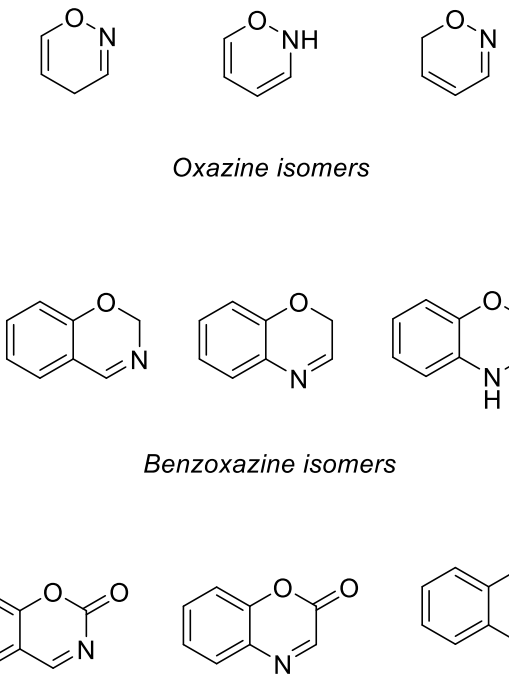

Figure 2.1. Oxazine, Benzoxazine and Benzoxazinone structures.

.

2.1.2 DISCOVERY AND AGROCHEMICAL SIGNIFICANCE

Benzoxazinones were first identified as natural pesticides in rye plants by Hietala and Virtanen in 1960, which prompted researchers in the agrochemical industry to understand its function more deeply.[32] Over the next thirty years, it was determined that this class of natural products was found in a variety of grasses and cereals in the family Poaceae and conferred resistance against fungi, bacteria and insects.[33] Given the potential use of benzoxazinoids as commercial pesticides and insecticides, significant industrial interest fueled research to elucidate their biosynthesis and mechanisms of bioactivity.

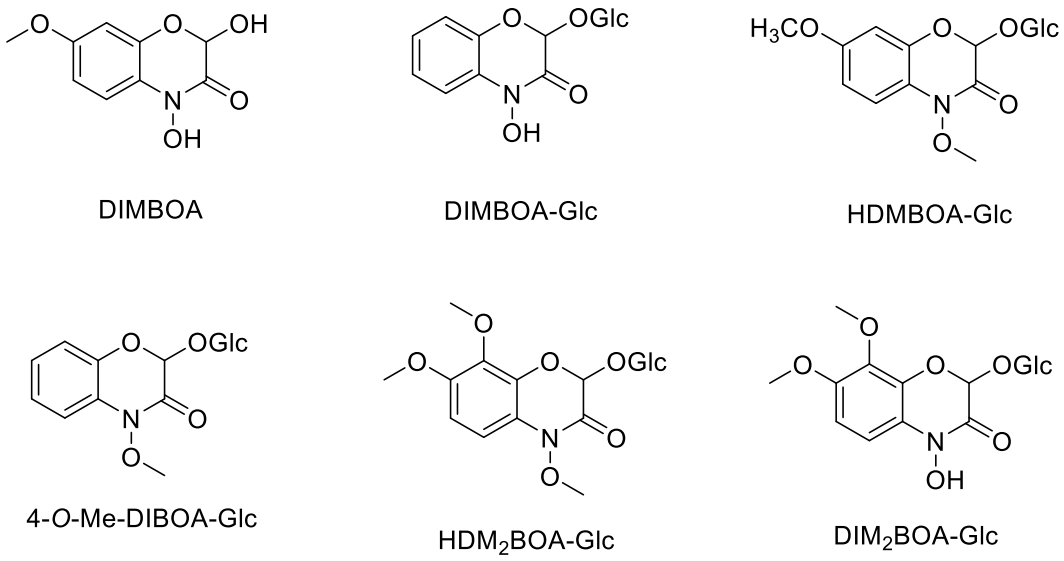

Figure 2.2. DIMBOA and its derivatives. 2,4-dihydroxy-7-methoxy-1,4-benzoxazin-3-one has been studied extensively as a plant defense chemical.

Benzoxazinones have been shown to act as a "general defense" in plants, exhibiting toxicity to a wide range of insects, bacteria, and fungi.[34] One particular benzoxazinone, 2,4-dihydroxy-7-methoxy-1,4-benzoxazin-3-one (DIMBOA) (Figure 2.2), has been the subject of several studies to elucidate molecular modes of bioactivity. DIMBOA acts as an enzyme inhibitor of ATPase and chloroplast coupling factor 1, which explains its widespread toxicity and negative allelopathy effects.[35] Cuevas and Niemeyer discovered DIMBOA's ability to inactivate acetylcholinesterase in *Rhopalosiphum padi*, an aphid that antagonizes wheat and cereal crop harvest around the world.[36] It was also found to inhibit function of α-chymotrypsin in insects, which is essential for digestive function.[37]

The biosynthesis of benzoxazininones is well understood and relatively short, making transgenesis of this pathway into other plants an attractive strategy for conferring general defense against insects, fungi and bacteria into more vulnerable crops.[38,39] The first successful transgenesis in *Arabidopsis thaliana* was reported by Abramov et. al in 2021, although concentrations of biosynthesized benzoxazinones were not high enough to confer general defense.[40] Further research to improve bioengineering of the benzoxazinone biosynthetic pathway is well underway.

2.1.3. MEDICINAL APPLICATIONS OF BENZOXAZINONES

There is growing interest in the medicinal properties of natural and synthetic benzoxazinones. An early study outlined the antibacterial properties of 2,4-dihydroxy-7-methoxy-1,4-benzoaxazin-3-one (DIMBOA) *in vitro* and found that it exhibited growth inhibitory properties against many bacterial strains that affect humans, including *Staphylococcus aureus* and *Escherichia coli*.[41] In addition to its antibacterial properties, DIMBOA acted as a strong antioxidant in DPPH assays, whereby the free-radical scavenging activity of a molecule can be measured.

Benzoxazinones have also been reported to confer anti-cancer, anti-platelet aggregation, antifungal, antidepressant, anti-inflammatory, and anti-viral effects.[42-45] In a study done by Jiang et al, four benzoxazinone derivatives were synthesized and their activity was screened using several c-Myc-overexpressed cancer cell lines (Figure 2.3).[46] Cell morphological analysis, wound healing assays, reverse-transcriptase-PCR (RT-PCR), electrophoretic mobility shift assays, and circular dichroism experiments were conducted to assess the effects of the synthesized benzoxazinones on the cancerous cells.

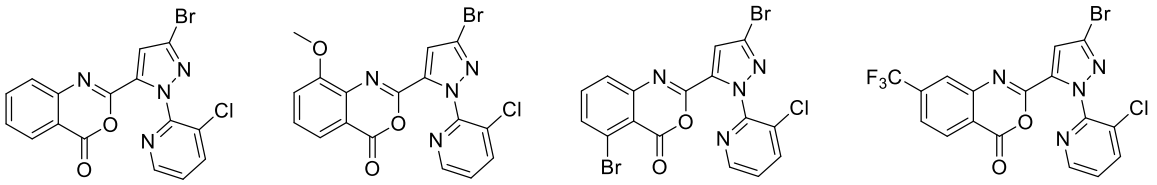

Figure 2.3. Synthetic benzoxazinones tested for anticancer activity.[46]

Morphological analysis revealed that these compounds inhibited proliferation of cancerous cells and, in some cells, induced apoptosis. Cell migration was significantly hindered, as indicated by wound healing assays. Remarkably, RT-PCR indicated that all four compounds downregulated expression of c-Myc mRNA, likely contributing to their ability to inhibit cell proliferation. EMSA experiments using GC-rich ds-DNA in the promoter of c-Myc promoter region indicated that the four compounds induced the formation of G-quadruplexes, potentially inhibiting oncogenic activity and proliferation.[47] Circular dichroism (CD) spectroscopy further validated the hypothesis that these compounds induced the formation of G-quadruplexes, as these structures exhibit characteristic peaks in CD spectra. While some benzoxazinones showed greater inhibitive properties than others in this study, all four compounds exhibited strong anti-cancer activity and have potential as pharmaceutical candidates.

Borate and coworkers showed that benzoxazinone derivatives containing a triazole moiety were effective antifungal agents, having inhibited growth of seven relevant fungal

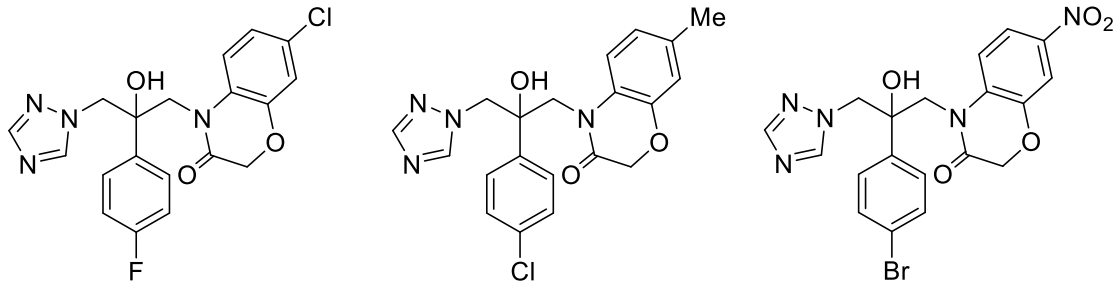

strains (Figure 2.4)[44]. Minimum inhibitory concentrations (MIC) of the benzoxazinones were comparable to commercially available antifungal medications, such as Amphotericin B and Fluconazole.

Figure 2.4. Benzoxazinones exhibiting antifungal activity.[44]

Ishizaki and coworkers were the first to hypothesize a mechanism for the antifungal activities of benzoxazinones, arguing their ability to covalently bind to guanine residues could induce mutations harmful to fungal strains.[45]

Atkinson and coworkers were the first to demonstrate the anti-depressant activities of benzoxazinones.[48] Aberrant levels of serotonin (5-HT) in the brain are linked to a variety of mood disorders, most notably anxiety and depression.[49] Synaptic serotonin levels are

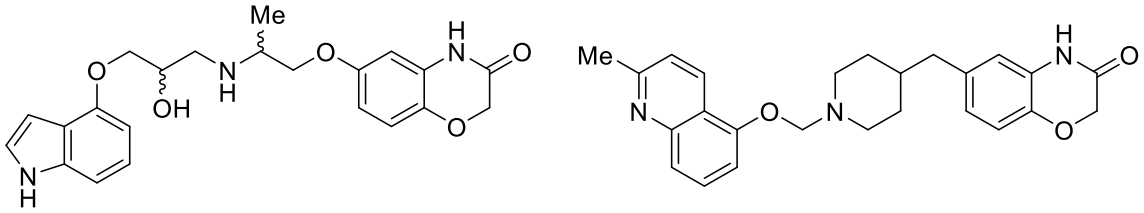

1 **2**

regulated by 5-HT transporters (SerT) and 5-HT receptors (5-HT_{1A}). In their study, a high-throughput screen identified benzoxazinone **1** (Figure 2.5) as having a high affinity to the 5-HT_{1A} receptor, signaling its potential as a serotonin regulator and potential therapeutic for anxiety and depression. Using **1** as a starting point, several analogues were synthesized and screened for affinity for the 5-HT_{1a} receptor and potency for SerT. It was found that benzoxazinone **2** (Figure 2.5) had high affinity for 5-HT_{1A} with potent inhibition of 5-HT reuptake, making it a strong therapeutic candidate for the treatment of anxiety and depression.

Figure 2.5. Benzoxazinones exhibiting anti-depressant activity.[48]

Benzoxazinones have long been known to exhibit anti-viral properties as well. Hedstrom et. al. were the first to demonstrate the ability of benzoxazinones to inhibit serine proteases of the chymotrypsin superfamily.[50] When it was discovered that the protein encoded by UL26, a gene associated with herpes simplex type 1 (HSV-1), was a protease, Jarvest and coworkers recognized the potential of benzoxazinones as inhibitors.[51] Two lead compounds, **3** and **4** (Figure 2.6) were synthesized and tested for inhibitory activity against HSV-1 protease. Both compounds were found to exhibit a half maximal inhibitory concentration (IC_{50}) of 90 μM. After optimization and introduction of a CBz-alaninyl-amino group to synthesize compound **5** (Figure 2.6), IC_{50} decreased to 12 μM, making it a potent inhibitor of HSV-1 protease.

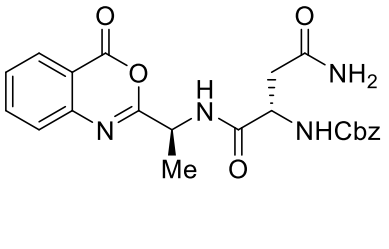

3

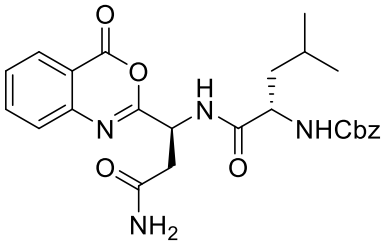

4

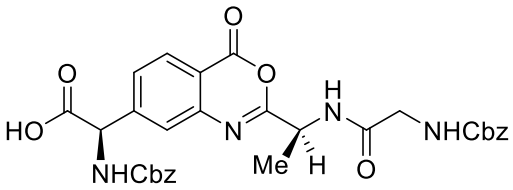

5

Figure 2.6. Benzoxazinone HSV-1 Protease Inhibitors.[51]

In addition to the anti-cancer, antifungal, antidepressant and antiviral properties of benzoxazinones, they have also been shown to confer anti-inflammatory and anti-platelet aggregation properties.[52] Hsieh and coworkers were interested in the small molecule regulation of neutrophils, which secrete cytotoxins in response to a variety of stimuli. One such cytotoxin, superoxide anion, is a precursor to several reactive oxygen species (ROS) and bioactive lipids, which are known to further antagonize inflammation. Neutrophil elastase (NE), a serine protease in the same family as chymotrypsin, is secreted by activated neutrophils, and is known to deteriorate tissue in inflammatory diseases. Given the reports by Hedstrom and coworkers[50] that 2-substituted benzoxazinones could inhibit serine proteases in the chymotrypsin family, it was hypothesized that synthetic analogues could also inhibit activity of NE. A series of 2,8-disubstituted benzoxazinones were synthesized and subjected to anti-platelet aggregation, inhibition of superoxide anion generation, and inhibition of neutrophil elastase release assays. While a library of 21 analogues was synthesized, three molecules (Figure 2.7) showed strong inhibition of arachidonic acid-induced platelet aggregation, inhibition of superoxide anion generation and inhibition of neutrophil elastase release. These results indicate that 2,8-disubstituted benzoxazinones confer therapeutic potential as anti-inflammatory and anti-plate aggregation agents.

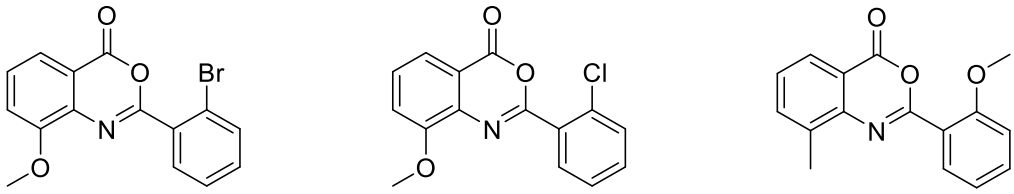

Figure 2.7. Benzoxazinones conferring anti-inflammatory and anti-plate aggregation activity.[52]

After the 2003 outbreak of severe acute respiratory syndrome (SARS), much attention was drawn to human coronaviruses (HCoVs). One attractive target for a potential HCoV anti-viral agent is HCoV protease, which cleaves viral polypeptide chains into functional viral proteins after translation of viral mRNA by host ribosomes. Hsieh and coworkers had already reported the anti-inflammatory and anti-platelet aggregation effects of 2-substituted benzoxazinones[52], and therefore screened these molecules for inhibitory activity of HCoV protease. They found that three 2-substituted benzoxazinones exhibited strong inhibitory activity against HCoV protease (Figure 2.8), which could then be considered lead compounds for further pharmacological efforts.

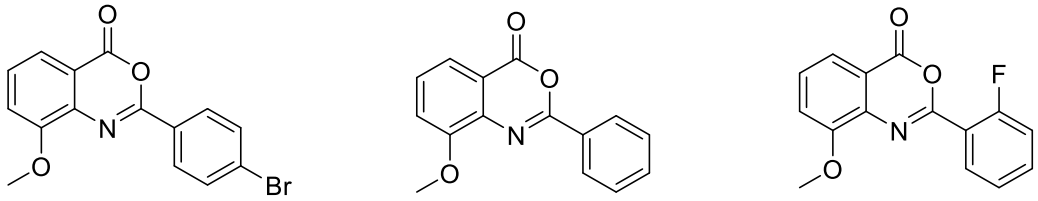

Figure 2.8. Benzoxazinones conferring anti-human coronavirus activity.

Perhaps the most impactful benzoxazinone-based pharmaceutical on the market is Efavirenz (Figure 2.9), a nonnucleoside reverse transcriptase inhibitor (NNRTI) that has been a leading treatment for human immunodeficiency virus (HIV) since 1998.[53]

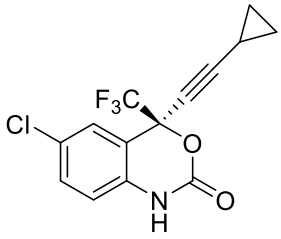

Efavirenz

Figure 2.9. Efavirenz, a benzoxazinone-based HIV-antiviral.

Acquired immunodeficiency syndrome (AIDS) is a deadly disease that begins with infection by HIV, a virus that causes severe immunosuppression and affects approximately 37 million people worldwide. Therapeutic approaches to HIV typically aim to interrupt the HIV life-cycle, and often consist of protease inhibition and inhibition of reverse-transcriptase activity.[53] Two main classes of drugs aim to inhibit reverse-transcriptase (RT) activity: nucleotide RT inhibitors (NRTI) and nonnucelotide RT inhibitors (NNRTI). While NRTIs are metabolized into the active drug, NNRTIs are noncompetitive inhibitors that bind to an allosteric site on the enzyme, thus reducing enzyme activity. Efavirenz is a potent NNRTI and significantly reduces the symptoms and transmission of HIV-1.[54, 55] However, efavirnenz has important limitations and drawbacks. One notable drawback is congenital malformation of the neural tube when efavirenz in administered during pregnancy, severely limiting its use in pregnant women.[56-58] Efavirenz also confers adverse effects on the patient's central nervous system, which are sporadic and difficult to treat.[59] Like most drugs administered as a "monotherapy", resistance to efavirenz is also an issue in the treatment of HIV-1. Therefore, it is imperative that new analogues of efavirenz are tested for anti-retroviral activity. It follows that improved methods to synthesize benzoxazinones like efavirenz are crucial to the pursuit of effective therapeutic treatment against viral infections like HIV-1.

2.1.4 SYNTHESIS OF BENZOXAZINONES

While there are a variety of synthetic strategies to access benzoxazinones and their derivatives, ring-closing strategies are typically the most common. An early report by

Shridhar and coworkers describes the reaction of *o*-aminophenol with chloroethanoyl chloride in the presence of sodium bicarbonate and methyl isobutyl ketone (Figure 2.10).[60]

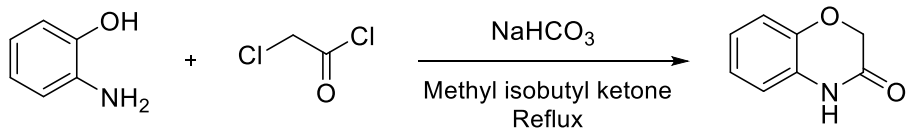

Figure 2.10. Synthesis of 2H-1,4-benzoxazin-3-one by Shridhar et. al.[60]

Although a facile synthesis that is high yielding, this reaction was limited in its scope. Notably, synthesizing more complex benzoxazinones was difficult, and required more functionalized starting materials to yield more complex benzoxazinones that would be of agrochemical or pharmaceutical interest.

Another report by Frechette and Beach[61] also employed *o*-aminophenol, this time with a bis-electrophile, α-bromo-γ-butyrolactone to react in a two-step sequence providing a more functionalized benzoxazinone (Figure 2.11). This reaction worked with several substituted *o*-aminophenols with yields up to 86%.

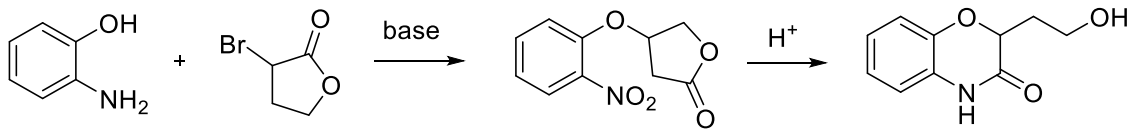

Figure 2.11. Synthesis of 1,4-benzoxazin-3-ones by Frechette & Beach.[61]

Interest in the synthesis of 1,3-benzoxazin-2-ones increased dramatically after FDA approval of efavirenz as a NNRTI for the treatment of HIV-1. On a laboratory scale, these

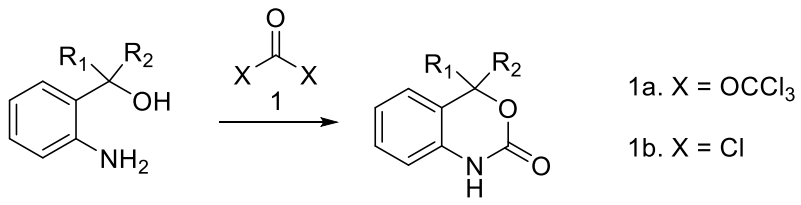

benzoxazinones are typically synthesized using amino benzyl alcohols and phosgene derivatives such as triphosgene **1a** (Figure 2.12).[62] However, for the kilogram-scale synthesis of efavirenz, phosgene **1b** is generally required.[63]

Figure 2.12. Benzoxazinone synthesis requiring phosgene or phosgene derivatives.

Phosgene, which was used as the first poisonous gas during World War 1, is extremely toxic and induces severe respiratory effects in humans.[64] There is a growing community of chemists looking to remove phosgene from their syntheses because of the risk it poses to those using it. Considering the necessary use of phosgene in the kilogram-scale synthesis of 1,3-benzoxazin-2-ones, Hernandez and coworkers developed a phosgene-free alternative (Figure 2.13).[62] Phthalide **2** was reacted with an aluminum amide reagent, which underwent aminolysis to provide **3**. A Hoffman rearrangement then provided the 1,3-benzoxazin-3-one **4**.

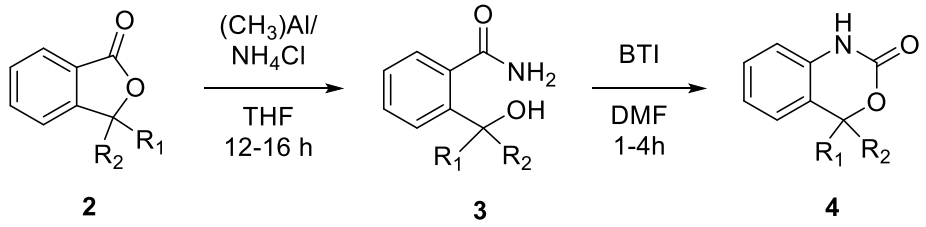

Figure 2.13. Phosgene-free synthesis of 1,3-benzoxazin-3-ones.[62]

The synthesis of alkynylbenzoxazinones has also gained much attention, both for their relation to efavirenz, and because of their synthetic potential for transition-metal mediated transformations. A common synthetic strategy to access alkynyl-1,3-benzoxazin-2-ones is depicted in Figure 2.14.[65] A terminal alkyne, such as trimethylsilylacetylene, undergoes proton abstraction by *n*-BuLi, afterwhich a tosyl-protected amine **5** is added. Addition of triethylamine and triphosgene then generates the TMS-protected alkynyl-1,3-benzoxazin-2-one **6**, which after deprotection with tetra-n-butylammonium fluoride (TBAF) yields the benzoxazinone **7**.

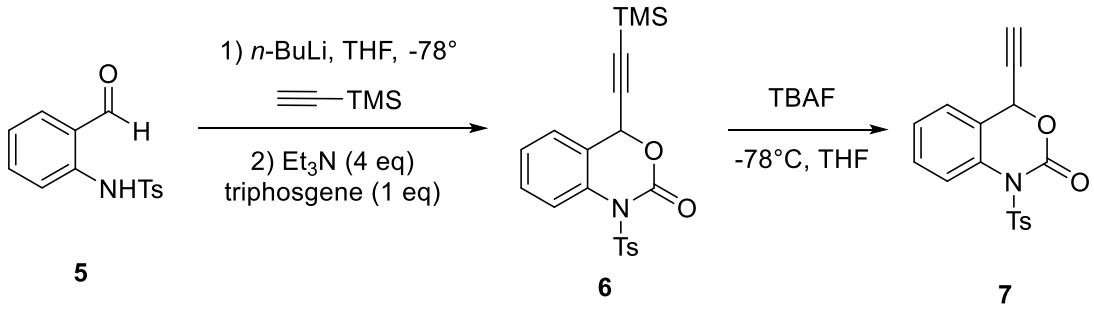

Figure 2.14. Synthesis of alkynyl-1,3-benzoxazin-2-one.[65]

While this method is relatively high yielding, its use of strong bases such as *n*-butyllithium limit its scope when sensitive functional groups are involved. Ideally, a method for the synthesis of alkynyl-1,3-benzoxazin-2-ones would tolerate sensitive functional groups and avoid the use of acutely toxic reagents like triphosgene.

2.1.5 SYNTHETIC POTENTIAL OF BENZOXAZINONES

Interest in 4-alkynyl-1,3-benzoxazin-2-ones has surged in the past decade, as transition-metal mediated reactions of aniline-bearing propargyl alcohols have proven useful for the synthesis of functionalized indoles (Figure 2.15).[66-70]

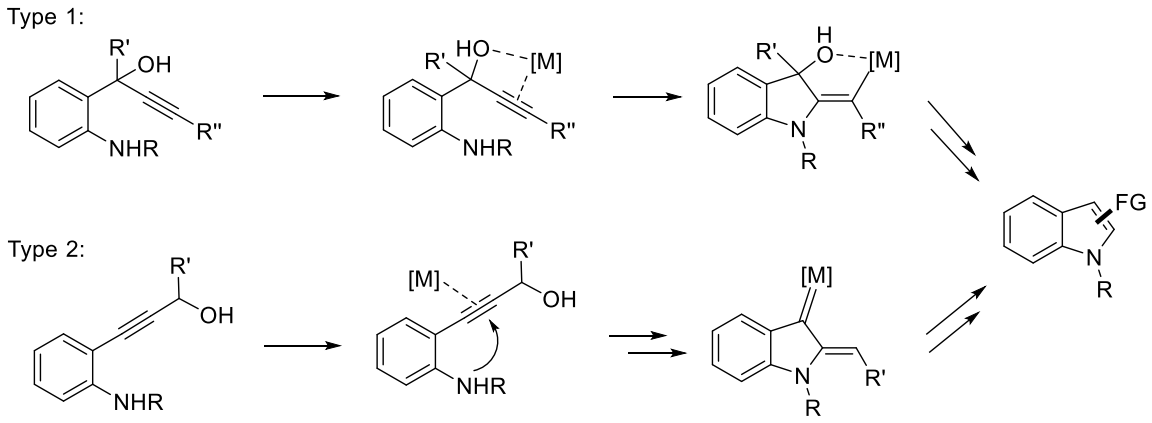

Figure 2.15. Transition-metal-mediated reactions for the synthesis of indoles.[66-70]

Inspired by the reactivity depicted in Figure 2.15, Li and coworkers developed the first copper-catalyzed decarboxylative amination of 4-alkynyl-1,3-benzoxazinones to access functionalized indoles (Figure 2.16).[71] Beginning with 4-alkynyl-1,3-benzoxazinone **1**, a copper-catalyzed decarboxylative amination with **2** provided a propargylamine *in-situ*. Subsequent intramolecular hydroamination would provide the key intermediate **3**, after which two indole derivatives were accessible, either through an acid-catalyzed Cope rearrangement to provide **4**, or through a base-mediated proton transfer to provide **5**. The strategy proved to be effective, with yields as high as 99% and 16 examples of both the Cope-rearranged indoles and the 1,3-proton transfer products.

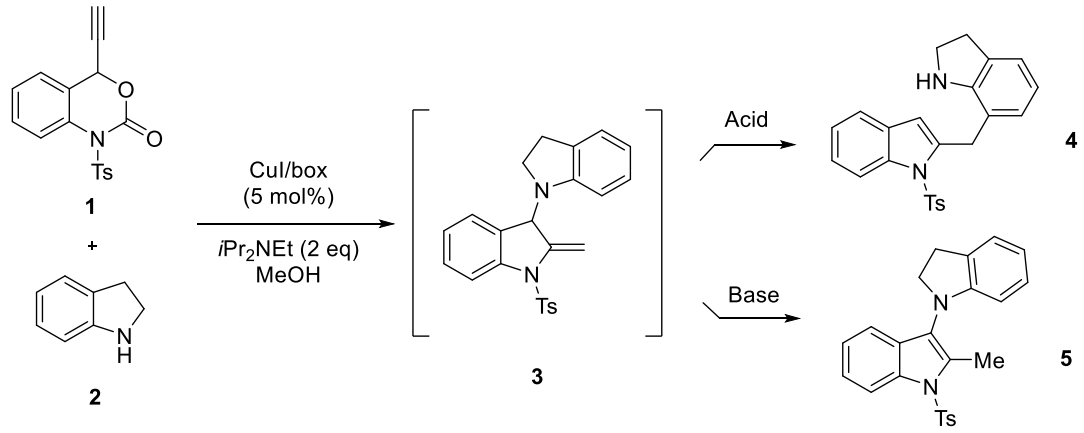

Figure 2.16. Copper-catalyzed decarboxylative amination to access indoles.[71]

With continued interest in decarboxylative coupling reactions, Wang and coworkers developed a copper-catalyzed decarboxylation and hydroamination between 4-alkynylbenzoxazinones and β-ketoesters to access β-ketoester-functionalized indoles.[72] Similar to the work done by Li et al.[71], this strategy relied on nucleophilic attack onto a key copper-allenylidene intermediate, followed by intramolecular amination to access the functionalized indoles.

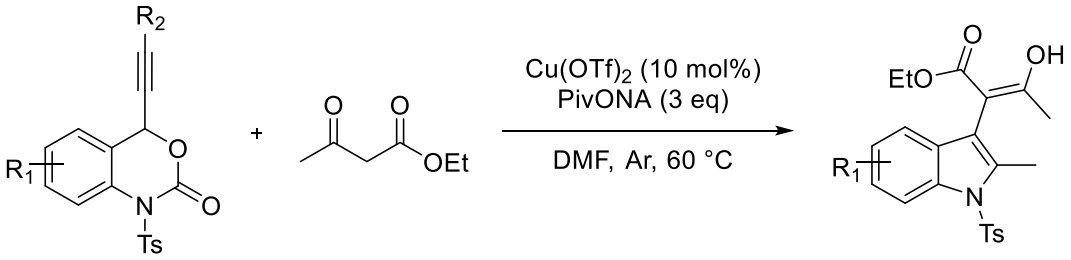

Figure 2.17. Copper-catalyzed decarboxylative amination with β-ketoesters.[72]

In the interest of synthesizing biindoles, Xiao and coworkers employed a similar strategy involving copper-catalyzed decarboxylation, propargylation, and hydroamination of 4-alkynylbenzoxazinones, this time using indoles as a nucleophile (Figure 2.18).[73]

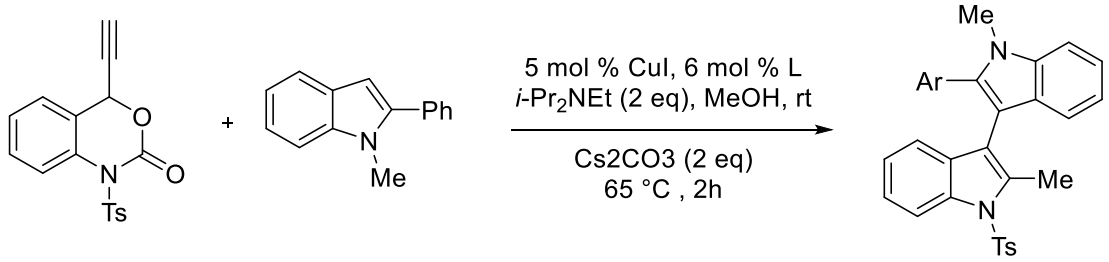

Figure 2.18. Synthesis of biindoles from 4-alkynylbenzoxazinones.[73]

In 2019, Yuan and coworkers discovered that high temperature (100 °C) reactions of 4-alkynylbenzoxazinones and acylhydroxamates provided access to 4-alkynylquinazolines (Figure 2.19).[74] The reaction proceeded via intermolecular [4+2] annulation of an *in-situ* generated *o*-aza-xylylene and without transition-metal-catalysts.

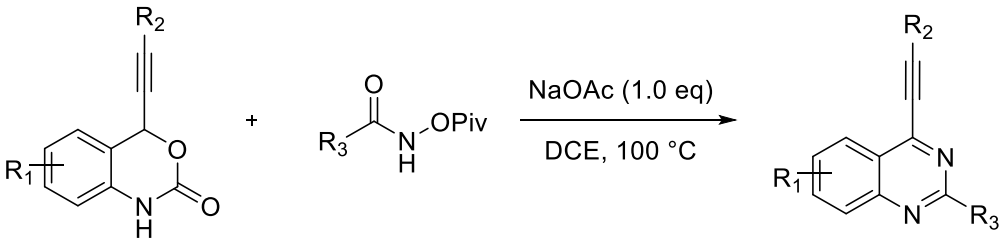

Figure 2.19. Synthesis of 4-alkynylquinazolines from 4-alkynylbenzoxaiznones.[74]

2.2 REACTION DEVELOPMENT

We report herein the discovery and development of a photochemical reaction to access 4-alkynylbenzoxazinones from simple precursors.

2.2.1 REACTION DISCOVERY

While our group has published extensively on the use of ESIPT-generated *o*-azaxylylenes as 1,4-biradicals in formal cycloadditions (Figure 2.20), this key intermediate remains underutilized as a synthetic tool. It was my task to explore the reactivity of ESIPT-generated *o*-azaxylylenes outside the realm of formal cycloadditions.

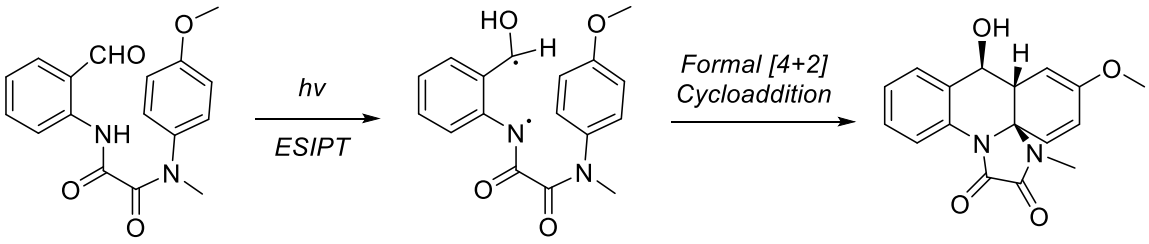

Figure 2.20. Formal [4+2]-cycloaddition of ESIPT-generated 1,4-biradical.[75]

The approach taken to explore new reactivity was simple: an *o*-aminoketone was linked to an unsaturated moiety. The *o*-aminoketone acts as a photoactive core, which should undergo ESIPT when irradiated, producing the 1,4-biradical. The scaffold linking the *o*-aminoketone to the unsaturated moiety, however, needed to be short enough that an intramolecular cycloaddition was unfavorable (Figure 2.21).

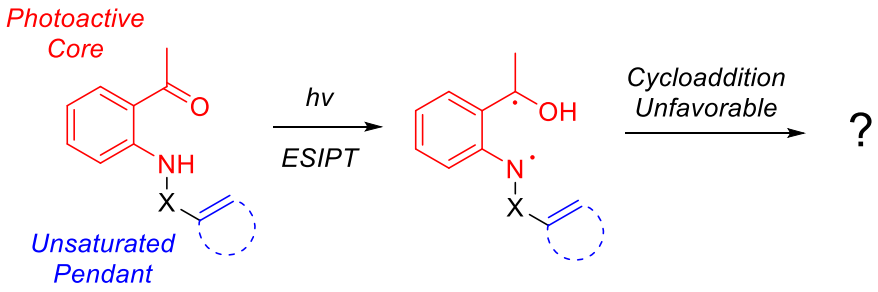

Figure 2.21. Strategy to explore reactivity of ESIPT-generated biradical.

In this regard, it was experimentally simple to append an *o*-aminoketone, 2-aminoacetophenone, to 2-butynoic acid using N,N'-dicyclohexylcarbodiimide (DCC) as a coupling reagent to make *N*-(2-Acetylphenyl)-2-butynamide **1a** (Figure 2.22). Both starting materials are readily available and inexpensive. The reaction is also high yielding, making it ideal for experimentation with photochemistry.

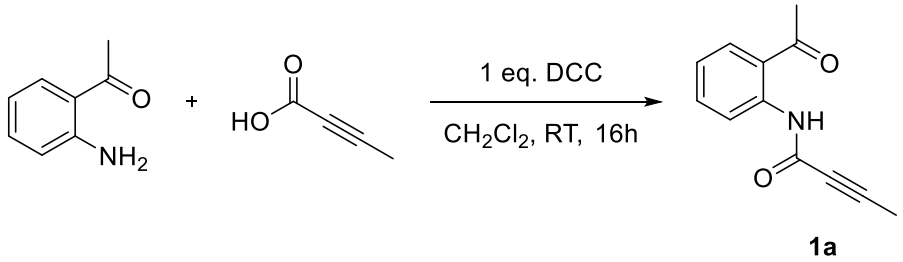

Figure 2.22. Facile synthesis of experimental photoprecursor.

It was hypothesized that irradiation of **1a** would initiate ESIPT, producing the 1,4-biradical. However, it was not clear what would happen next, as a formal cycloaddition to the alkyne was unlikely to occur. Initial NMR-scale irradiations with 365 nm light in deuterated solvents indicated **1a** was photoactive, however the structure of the photoproduct was unclear. A larger-scale photoreaction was performed in degassed DMSO, after which flash-column chromatography was used to separate the photoprecursor **1a** from the photoproduct. To our surprise, a photo-induced alkyne migration and photorearrangement occurred, producing benzoxazinone **2a** (Figure 2.23).

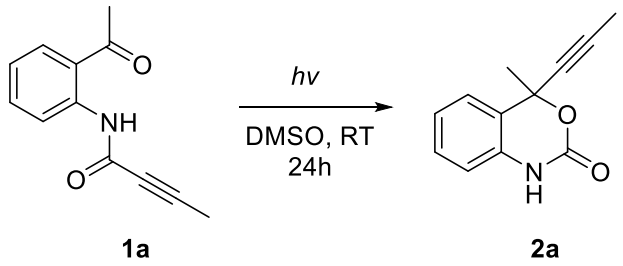

1a 2a

Figure 2.23. Serendipitous discovery yielding a photogenerated benzoxazinone.

To ensure the rearrangement was not thermally driven, an NMR sample of **1a** in deuterated DMSO was heated at 100°C for twelve hours. Heating induced no changes in the starting material.

While the initial photoreaction was moderately low yielding (26%), the photogenerated benzoxazinone appeared to be stable. Further heat tests on the benzoxazinone were conducted, whereby **2a** was dissolved in toluene and DMSO and heated at 100°C for six hours. Again, heating did not induce any changes or decomposition. Continued irradiation of **2a** using 365 nm light for 24 hours again showed no changes when done on an NMR-scale in deuterated DMSO, methylene chloride and acetonitrile.

With validation that the reaction was proceeding photochemically, we proceeded to optimize reaction conditions and evaluate the scope of the reaction.

2.2.2 REACTION OPTIMIZATION

Initial NMR-scale solvent screens indicated that DMSO, acetonitrile, and methylene chloride were the most promising in converting photoprecursor **1a** into benzoxazinone **2a**. Further solvent and light source screens were conducted, with or without the addition of 4,4’-dimethoxybenzophenone **4** as a triplet-sensitizer. While no internal standard was added to quantitatively measure yield on an NMR-scale, percent

conversion (% C) was roughly estimated by integrating the ratio of photoprecursor to photoproduct. No side products were apparent on NMR, so while % C was a rough estimation, we felt comfortable using this metric for further optimize reaction conditions.

NMR-scale irradiations were conducted using deuterated methylene chloride, deuterated acetonitrile and deuterated DMSO. Initial trials without triplet-sensitizer **4** quickly indicated that the photoprecursor **1a** was more reactive under 365 nm light. While **4** has peak UV-Vis absorption near 300 nm, addition of this sensitizer at 0.2 eq and 1.0 eq appeared to have little to no effect in any solvent. Of the three solvents, deuterated methylene chloride yielded the lowest conversion (Table 2.1, entries 1-6). Deuterated acetonitrile also yielded relatively low conversion, although its average conversion was greater than deuterated methylene chloride (Table 2.1, entries 7-12). Finally, deuterated DMSO yielded the highest percent conversion (Table 2.1, entries 13-18). While the highest percent conversion was observed using 0.2 eq of triplet sensitizer **4** (Table 2.1, entry 14), it was not significantly different from the reaction that lacked **4** altogether. For this reason, we proceeded using the conditions of entry 13 for the sake of simplifying purification.

Degassing solvents is also critical to photochemistry, as triplet oxygen can often interfere with desired transformations.[76] Further trials using DMSO were done using solvent degassed by two methods: the first trial was degassed using three cycles of freeze-pump-thaw, while the second was degassed by bubbling nitrogen through the solvent for twenty minutes. While the freeze-pump-thaw method is far more rigorous, both trials yielded the same percent conversion. For the sake of time, the latter method was used for all scope reactions.

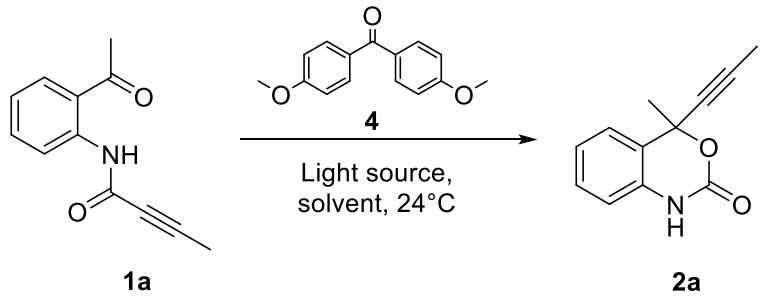

1a **2a**

entry	**4** (eq)	lamp (nm)	solvent	% Conversion
1	0.0	365	CD_2Cl_2	8
2	0.2	365	CD_2Cl_2	6
3	1.0	365	CD_2Cl_2	6
4	0.0	300	CD_2Cl_2	1
5	0.2	300	CD_2Cl_2	0
6	1.0	300	CD_2Cl_2	0
7	0.0	365	CD_3CN	11
8	0.2	365	CD_3CN	9
9	1.0	365	CD_3CN	12
10	0.0	300	CD_3CN	2
11	0.2	300	CD_3CN	3
12	1.0	300	CD_3CN	3
13	0.0	365	DMSO	25
14	0.2	365	DMSO	27
15	1.0	365	DMSO	26
16	0.0	300	DMSO	4
17	0.2	300	DMSO	3
18	1.0	300	DMSO	4

Table 2.1 Reaction Optimization.

2.2.3 SCOPE OF REACTIVITY

With optimal conditions determined, the scope of the photoreaction was examined (Table 2.2). Considering the model precursor **1a** was synthesized from 2-butynoic acid, a simple synthesis of photoprecursor **1b** from propiolic acid and 2-aminoacetophenone followed logically. As predicted, bezonxazinone **2b** was isolated in similar yield.

While alkyne migration appeared to occur smoothly, we considered the possibility of sp^2-hybridized carbon migration as well. To our delight, photoprecursor **1c** converted smoothly to photoproduct **2c** in 36% yield under standard reaction conditions. Its thiophene analogue, **1h**, also converted smoothly to benzoxazinone **2h** under standard reaction conditions.

Interestingly, irradiation of **1h** in methylene chloride yielded a different photoproduct, depicted in Figure 2.24. In this reaction, an apparent electrocyclization and subsequent rearomatization occurred, producing **3a**.

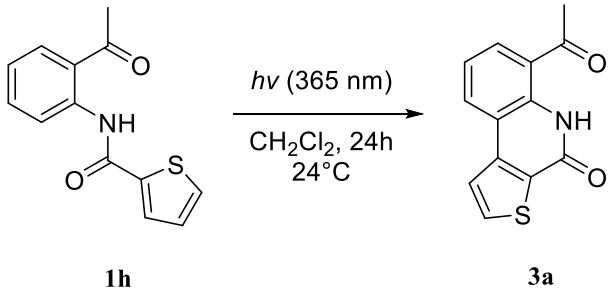

1h **3a**

Figure 2.24. Electrocyclization and rearomatization of 1h to produce 3a.

Unfortunately, photoprecursors **1c** and **1h** demonstrated the only successful migrations of sp^2 centers. Further attempts involving alkenes and sp^2-hybridized heterocycles failed to yield any benzoxazinone photoproducts.

Focusing again on alkyne migrations, an aminotetralone was employed as a photoactive core to synthesize **1d** and **1e**, both of which converted to their respective benzoxazinone photoproducts in similar yields to their 2-aminoacetophenone analogues. A significant increase in yield was observed in the conversion of **1f** to benzoxazinone **2f**, after which it was hypothesized that a greater amount of molecular weight on the end of the

alkyne could stabilize any radical intermediates involved in the photoreaction. This hypothesis was further validated by the photogenerated benzoxazinone **2g**, the tetralone analogue of **2f**. Given this newfound evidence of improved reactivity, **1i** was synthesized from phenylpropiolic acid. To our delight, **1i** reacted efficiently under standard conditions to provide benzoxazinone **2i** in 80% yield. Finally, a tetralone analogue **1j** was synthesized, which underwent the desired photochemical transformation in 88% yield.

Photoprecursor	Photoproduct	Photoprecursor	Photoproduct
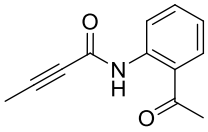	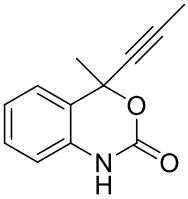	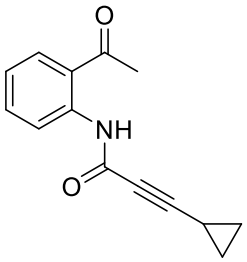	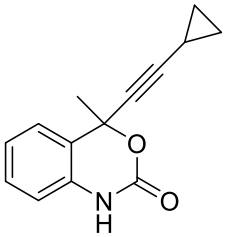
1**a**	**2a** (26%)	**1f**	**2f** (38%)
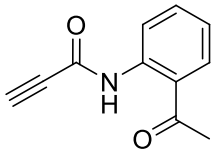	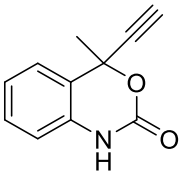	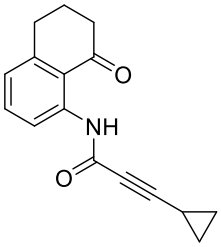	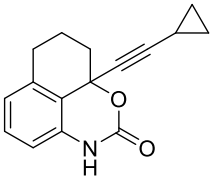
1b	**2b** (31%)	**1g**	**2g** (41%)
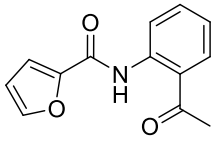	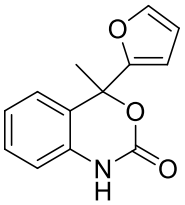	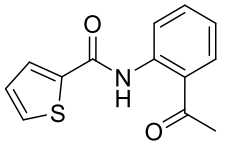	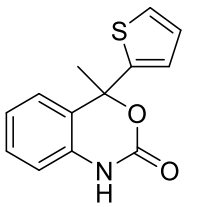
1c	**2c** (36%)	**1h**	**2h** (24%)
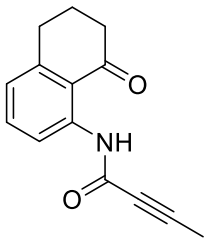	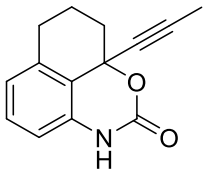	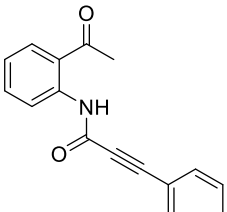	
1d	**2d** (29%)	**1i**	**2i** (80%)

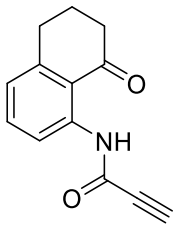

1e

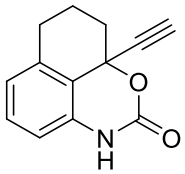

2e (26%)

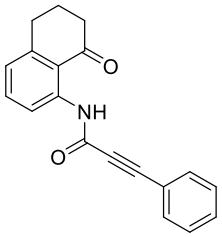

1j

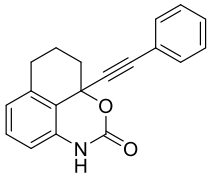

2j (88%)

Table 2.2. Scope of Reactivity

2.2.4 MECHANISTIC RATIONALE

A proposed mechanism for the photoreaction of **1a** is depicted in Figure 2.25. Beginning with photoprecursor **1a**, irradiation with 365 nm light initiates ESIPT and ISC, resulting in a triplet 1,4-biradical **1aa**. Combination of the benzyl radical with an alkynyl radical closes a six-membered ring, producing intermediate **1ab**. Subsequent alkyne migration and ring-opening produces isocyanate **1ac**, which is attacked by the alcohol to close a six-membered ring, providing intermediate **1ad**. Two proton transfers then provide the photoproduct, benzoxazinone **2a**.

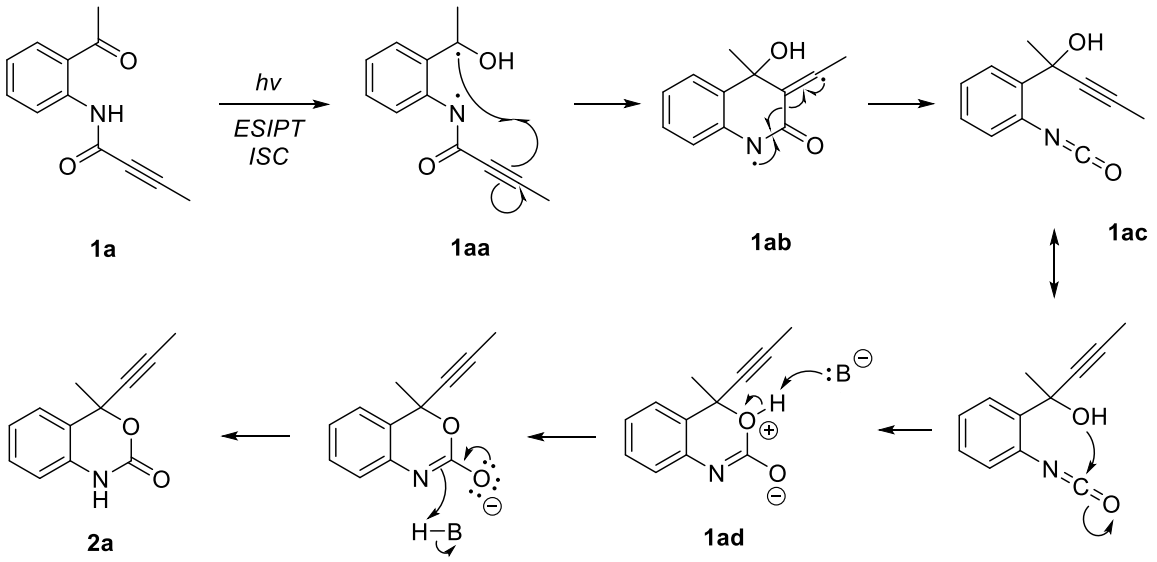

Figure 2.25. Mechanistic rationale for photochemical alkyne migration.

2.3 DISCUSSION

Given the straightforward approach to photoprecursor synthesis and the experimentally simple photoirradiation, we consider this method for the synthesis of 4-alkynyl-1,3-benzoxazin-2-ones competitive with other methods. One advantage of this method to those described in Chapter 2.1.4 is the lack of hazardous or acutely toxic reagents. In fact, all but two photoprecursors were synthesized using DCC as a coupling agent, which is inexpensive and easy to use. Further, this method does not require any precious transition-metal catalysts. Finally, assuming the appropriate starting materials are commercially available, this method provides access to 4-alkynyl-1,3-benzoxazinones in as little two synthetic steps (Figure 2.26).

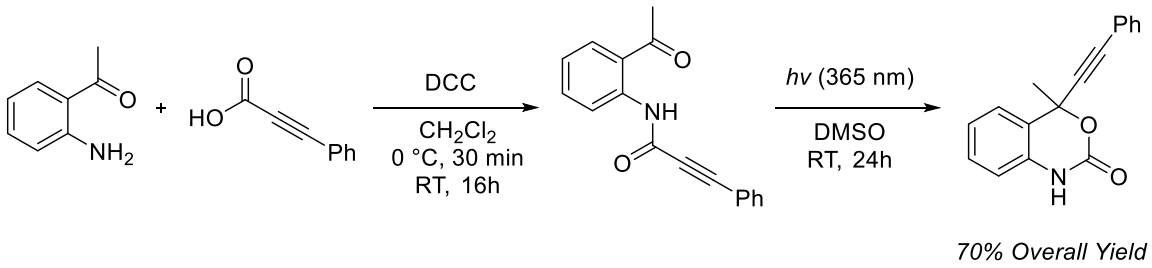

Figure 2.26. Concise photochemical synthesis of 4-alkynyl-1,3-benzoxazin-2-one.

Of course, this method is not without its limitations. Notably, terminal alkynes and alkynes lacking a neighboring π-system do not migrate with high efficiency. This observation is most likely caused by the stability, or lack thereof, of the vinyl intermediate (Figure 2.27, intermediate **1ab**). Indeed, when this vinyl intermediate is conjugated by a neighboring π-system, yields significantly increased. The most obvious examples of this are the photochemical transformations of **1i** and **1j** to **2i** and **2j**, respectively. As depicted in Figure 2.27, the vinyl intermediate produced *in-situ* is conjugated to a benzene ring (Figure 2.27, **1ib**) and is therefore significantly more stable than a vinyl group with no conjugation (Figure 2.27, **1ab**). We hypothesize that this additional stability is what led to dramatically higher yields in photoproducts **2i** and **2j**.

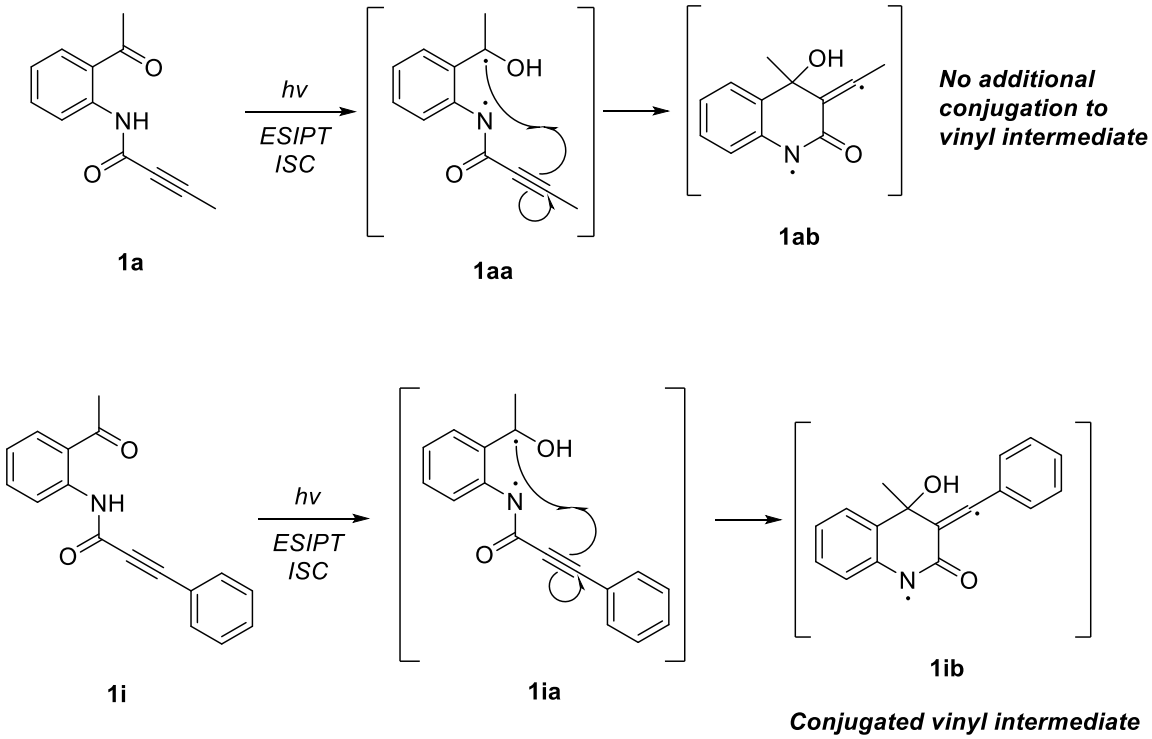

Figure 2.27. Additional conjugation stabilizes vinyl intermediate.

Another limitation of this method is the need for *o*-amidoketones for alkyne migration to occur. While ESIPT can occur with *o*-alkylketones, *o*-acylphenols, and *o*-amidoimines (Figure 2.28), we hypothesize that only *o*-amidoketones possess properties favorable for an alkyne migration to follow. As depicted in Figure 2.25, a key intermediate for successful alkyne migration is formation of the isocyanate **1ac.** Formation of the

isocyanate requires an *N*-centered radical, thereby eliminating *o*-alkyketones and *o*-acylphenols as possible photoactive cores to undergo ESIPT and subsequent alkyne migration.

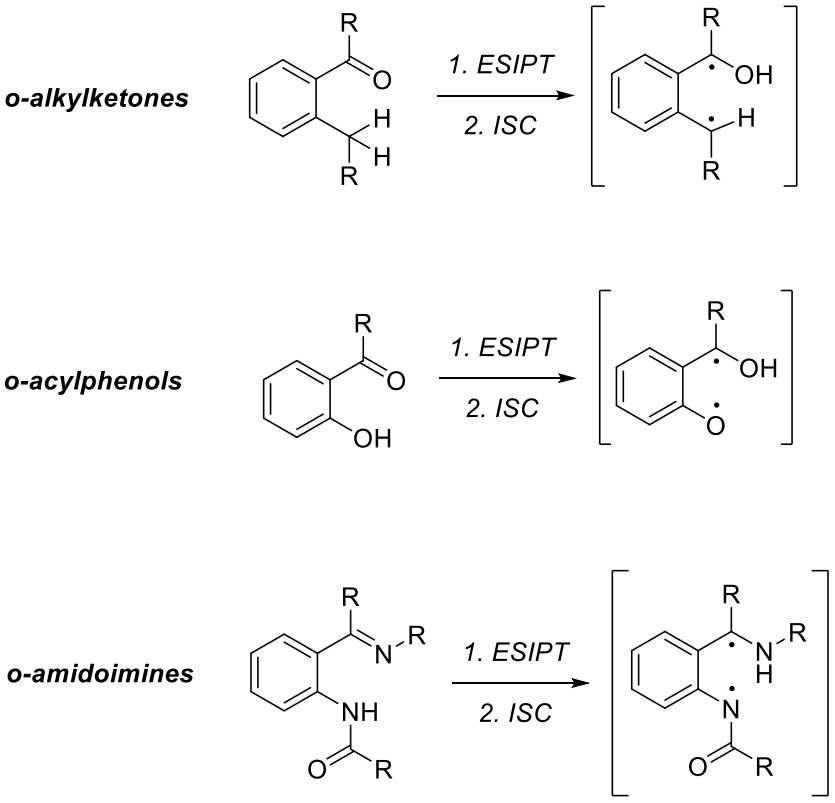

Figure 2.28. Photoactive cores capable of undergoing ESIPT.

Another consideration is nucleophilic attack of the isocyanate **1ac** by the hydroxyl group to close a ring and produce intermediate **1ad** (Figure 2.25). After failing to obtain the desired product with an *o*-amidoimine (Figure 2.29), we hypothesized that a nitrogen atom possessing a full octet of electrons may not be nucleophilic enough to complete this key step in the reaction. It is possible that using an oxazoline as the imine introduced unanticipated steric hindrance, causing the reaction to fail. However, we were not able to attempt the reaction with a free imine to test this hypothesis.

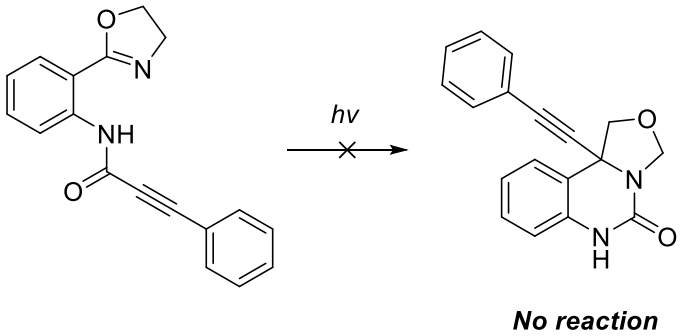

Figure 2.29. Attempted alkyne migration using *o*-amidoimine.

While terminal alkynes and lower molecular-weight alkynes migrated with lower yields, higher yielding 1,3-benzoxazin-2-ones bearing a phenyl alkyne at the 4 position is still of interest to researchers exploring decarboxylative and Cu-catalyzed amination reactions in the pursuit of functionalized indoles, as detailed in Chapter 2.1.5. We hope this method provides an experimentally simple alternative for constructing the starting materials necessary for this exploration.

To our knowledge, the reaction described herein is the first reported photochemical alkyne migration. Furthermore, this reaction represents one of few, if any, uses of ESIPT as a synthetic tool outside the realm of formal cycloadditions. It is our hope that more researchers will explore the potential of ESIPT as a tool to access privileged scaffolds, structures, and pharmacophores.

The photoproducts synthesized for this thesis are also similar in structure to efavirenz (Figure 2.30), a benzoxazinone-based non-nucleotide reverse transcriptase inhibitor (NNRTI) widely used as an antiviral agent in the treatment of HIV-1. This method, therefore, is an attractive one for the synthesis of efavirenz analogues, which are in high demand for biological testing.

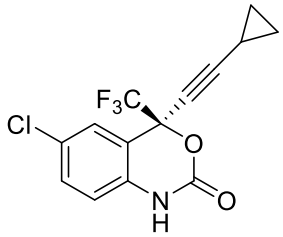

Efavirenz

Figure 2.30. Efavirenz, a benzoxazinone-based NNRTI.

The reported photoproducts in Table 2.2 will be sent to the National Cancer Center NCI-60 Program, where they will be screened for bioactivity as anti-cancer agents. This endeavor supports our mission to develop photochemical methodologies which provide access to pharmaceutically relevant scaffolds and molecules.

2.4 FUTURE WORK

While we made considerable progress in the discovery and development of ESIPT-enabled alkyne migrations to access 4-alkynyl-1,3-benzoxazin-2-ones, there remains a significant amount of work to further expand the scope of the reaction and its underlying mechanism.

As discussed in chapter 2.3, we hypothesized that *o*-amidoketones are the most favorable photoactive core to undergo ESIPT and subsequent alkyne migration. However, additional experimentation is required to test this hypothesis, as there are many more scaffolds that will undergo ESIPT than the ones depicted in Figure 2.28.

Another question that was not addressed in the course of this work is the possibility of an enantioselective reaction by way of a chiral organocatalyst. While it was proposed that a chiral organocatalyst could potentially bond non-covalently to the oxygen and

nitrogen atoms of the *o*-amidoketone, we were skeptical of the strategy, as both atoms are active in the ESIPT process. Further strategizing and experimentation will be required to explore the question of enantioselectivity.

Additionally, potential of this reaction to participate in photochemical cascades is strong. Figure 2.31 depicts one example, whereby an *o*-amidobenzaldehyde **A** is coupled with hydrazide **B** to form photoprecursor **C**. If photoirradiation induces ESIPT and a subsequent alkyne migration, it would theoretically be possible for the alkyne to undergo a [4+2] reaction with the tethered furan, resulting in photoproduct **D**. This reaction would demonstrate the ability of photochemical cascades induce a dramatic rise in complexity in a single experimental step.

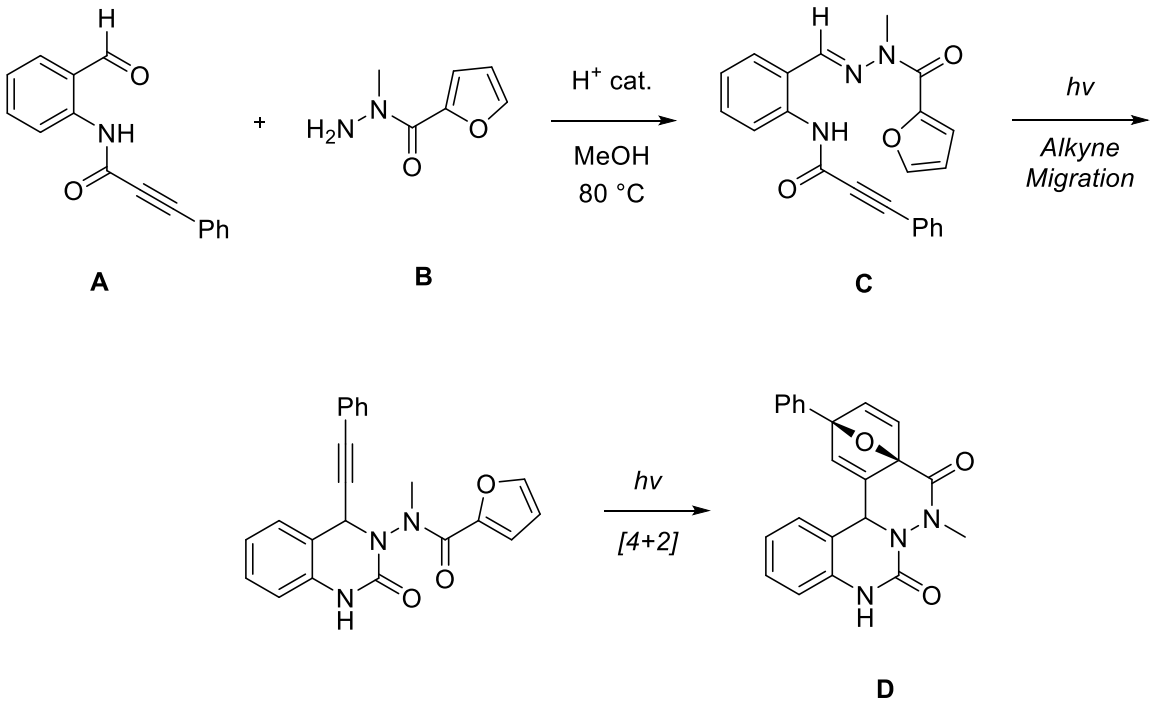

Figure 2.31. Possible photochemical cascade involving benzoxazinone.

Finally, there is great potential use of this method in diversity-oriented synthesis (DOS), which aims to build the greatest amount structural and appendage diversity in a small molecule library.[77-79] Photochemistry is conducive to DOS, as it allows for the construction of a variety of scaffolds, often complex and drug-like in nature. Expansion of this reaction's scope would make it a valuable tool for researchers building DOS libraries for biological screening.

2.5 CONCLUSION

In conclusion, we have developed a novel photochemical method for the facile construction of 4-alkynyl-1,3-benzoxazin-2-ones. To our knowledge, this reaction is the first photochemical alkyne migration to be reported. While the scope of the reaction needs expansion, the desired products yielded thus far are of great utility to synthetic chemists

exploring the reactivity of alkynylbenzoxazinones to access functionalized heterocycles, and to medicinal chemists exploring bioactivity of alkynylbenzoxazinones.

3. EXPERIMENTAL

GENERAL

All ground-state reactions were done using oven-dried glassware and stir bars. When inert atmosphere was required, reactions were done using a nitrogen-filled balloon. Dry solvents were obtained from Fisher Scientific. All photoreactions were done using pyrex square bottles, which were placed in a water bath for temperature control. Solvents for irradiation were degassed by bubbling nitrogen through an airtight septum that contained a venting needle. All irradiations were done using 365 nm LEDs that were built in-lab. All commercial reagents were purchased from Oakwood Chemical, TCI Chemical, Sigma, and AK Scientific, and were used without further purification unless otherwise stated. Silica gel was used for flash column chromatography.

^{1}H and ^{13}C NMR spectra for characterization of novel compounds were collected in CDCl3 using residual solvent peaks as an internal standard (δH 7.26 ppm; δC 77.16 ppm) at 25 °C at the NMR Facility at the University of Denver (500 MHz Bruker Avance III Spectrometer). All chemical shifts are reported in parts per million (ppm). Splitting patterns are indicated as follows: br, broad; s, singlet; d, doublet; t, triplet; q, quartet; m, multiplet; dd, doublet of doublets; dt, doublet of triplets.

3.1 SYNTHESIS OF PHOTOPRECURSORS

8-amino-3,4-dihydronaphthalen-1(2H)-one:

Prepared by a reported procedure[80]:

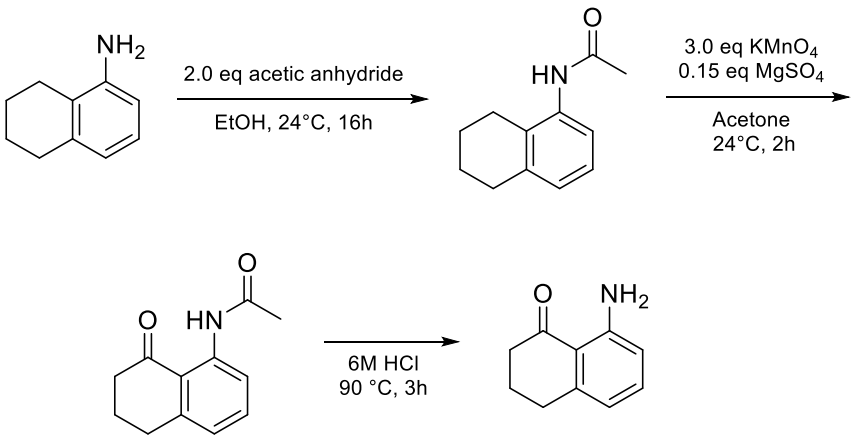

N-(2-acetylphenyl)but-2-ynamide (1a):

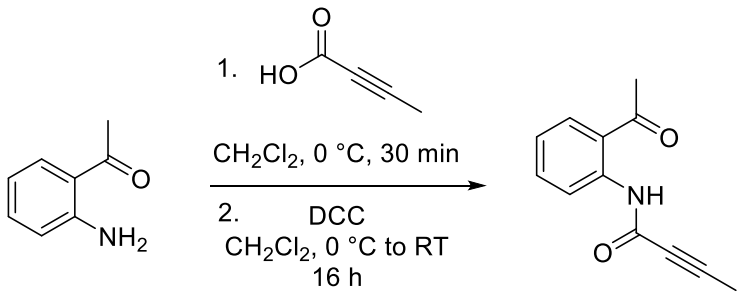

1a

An oven-dried 100 mL round bottom flask was charged with an oven-dried stir bar. To this flask was added 2-aminoacetophenone (0.675 g, 5 mmol, 1 eq) and 20 mL methylene chloride. The flask was cooled to 0 °C and stirred. 2-butynoic acid (0.420 g, 5 mmol, 1 eq) was then added to the flask and the reaction was stirred at 0 °C for 30 minutes. After 30 minutes, DCC (1.032 g, 5 mmol, 1 eq) was added at 0 °C and the reaction was slowly allowed to warm to room temperature, then stirred for 16 hours. Reaction progress was

measured by TLC. Upon reaction completion, the mixture was concentrated, then the residue was dissolved in a minimal amount of ethyl acetate and filtered through a pad of celite to remove dicyclohexylurea (DCU). Filtrate was concentrated onto silica and purified using automated flash chromatography to provide **1a** (0.683 g, 3.4 mmol, 68% yield).

^{1}H NMR (500 MHz, CDCl3) δ 11.92 (s, 1H), 8.71 (d, J = 8.5 Hz, 1H), 7.93 (dd, J = 8.1, 1.5 Hz, 1H), 7.58 (ddd, J = 8.8, 7.2, 1.6 Hz, 1H), 7.20 – 7.13 (m, 1H), 2.70 (s, 3H), 2.05 (s, 3H).

N-(2-acetylphenyl)propiolamide (1b):

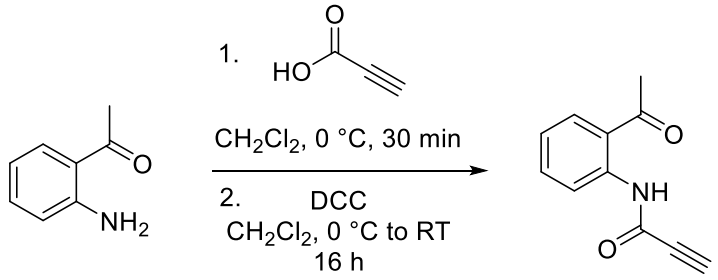

1b

An oven-dried 100 mL round bottom flask was charged with an oven-dried stir bar. To this flask was added 2-aminoacetophenone (0.675 g, 5 mmol, 1 eq) and 20 mL methylene chloride. The flask was cooled to 0 °C and stirred. Propiolic acid (0.350 g, 5 mmol, 1 eq) was then added to the flask and the reaction was stirred at 0 °C for 30 minutes. After 30 minutes, DCC (1.032 g, 5 mmol, 1 eq) was added at 0 °C and the reaction was slowly allowed to warm to room temperature, then stirred for 16 hours. Reaction progress was measured by TLC. Upon reaction completion, the mixture was concentrated, then the residue was dissolved in a minimal amount of ethyl acetate and filtered through a pad of

celite to remove dicyclohexylurea (DCU). Filtrate was concentrated onto silica and purified using automated flash chromatography to provide **1b** (0.579 g, 3.1 mmol, 62% yield).

^{1}H NMR (500 MHz, CDCl3) δ 12.15 (s, 1H), 8.70 (d, J = 8.5 Hz, 1H), 7.95 (dd, J = 7.9, 1.6 Hz, 1H), 7.64 – 7.57 (m, 1H), 7.24 – 7.18 (m, 1H), 2.97 (s, 1H), 2.71 (s, 3H).

N-(2-acetylphenyl)furan-2-carboxamide (1c):

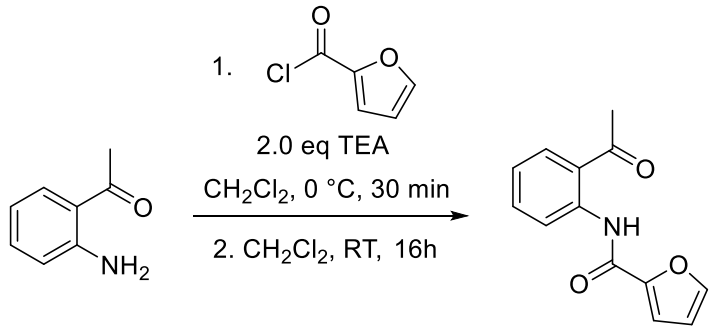

1c

An oven-dried 100 mL round bottom flask was charged with an oven-dried stir bar. To this flask, 20 mL methylene chloride and 2-furoyl chloride (0.788 mL, 1.04 g, 8 mmol, 1 eq) were added. The reaction was cooled to 0 °C, then 2-aminoacetophenone (1.08 g, 8 mmol, 1 eq) and triethylamine (2.232 mL, 16 mmol, 2 eq) in methylene chloride (15 mL) were added dropwise using an addition funnel. The reaction was stirred at 0 °C to RT for 16 hours. Once the reaction was complete by TLC, the resulting mixture was extracted three times with DCM, organic layers were combined and washed with brine, dried over anhydrous sodium sulfate and concentrated in vacuo. Crude product was purified on using automated flash chromatography to provide **1c**. (1.265 g, 5.52 mmol, 69%)

^{1}H NMR (500 MHz, $CDCl_3$) δ 12.71 (s, 1H), 8.96 – 8.90 (m, 1H), 7.97 (dd, *J* = 8.1, 1.6 Hz, 1H), 7.67 – 7.59 (m, 2H), 7.22 – 7.15 (m, 1H), 6.58 (dd, *J* = 3.6, 1.8 Hz, 1H), 2.74 (s, 3H).

N-(8-oxo-5,6,7,8-tetrahydronaphthalen-1-yl)but-2-ynamide (1d):

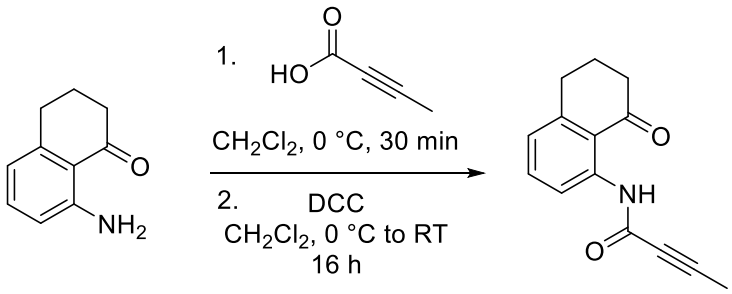

1d

An oven-dried 100 mL round bottom flask was charged with an oven-dried stir bar. To this flask was added aminotetralone (0.805 g, 5 mmol, 1 eq) and 20 mL methylene chloride. The flask was cooled to 0 °C and stirred. 2-butynoic acid (0.420 g, 5 mmol, 1 eq) was then added to the flask and the reaction was stirred at 0 °C for 30 minutes. After 30 minutes, DCC (1.032 g, 5 mmol, 1 eq) was added at 0 °C and the reaction was slowly allowed to warm to room temperature, then stirred for 16 hours. Reaction progress was measured by TLC. Upon reaction completion, the mixture was concentrated, then the residue was dissolved in a minimal amount of ethyl acetate and filtered through a pad of celite to remove dicyclohexylurea (DCU). Filtrate was concentrated onto silica and purified using automated flash chromatography with hexanes and ethyl acetate as elution solvents to provide **1d**. (0.658 g, 2.9 mmol, 58% yield)

^{1}H NMR (500 MHz, $CDCl_3$) δ 12.39 (s, 1H), 8.56 (d, *J* = 8.4 Hz, 1H), 7.47 (t, *J* = 8.0 Hz, 1H), 6.98 (d, *J* = 7.6 Hz, 1H), 3.00 (t, *J* = 6.1 Hz, 2H), 2.76 – 2.70 (m, 2H), 2.12 (p, *J* = 6.4 Hz, 2H), 2.04 (s, 3H).

^{13}C NMR (126 MHz, $CDCl_3$) δ 203.18, 151.76, 146.08, 141.24, 135.07, 123.61, 118.80, 118.25, 84.17, 77.32, 77.07, 76.81, 76.05, 40.69, 30.90, 22.68, 3.88.

N-(8-oxo-5,6,7,8-tetrahydronaphthalen-1-yl)propiolamide (ie):

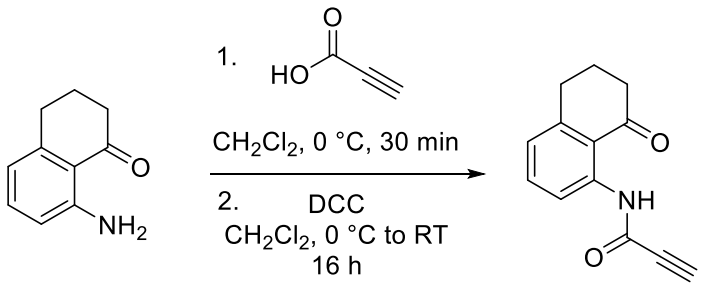

1e

An oven-dried 100 mL round bottom flask was charged with an oven-dried stir bar. To this flask was added aminotetralone (0.805 g, 5 mmol, 1 eq) and 20 mL methylene chloride. The flask was cooled to 0 °C and stirred. Propiolic acid (0.350 g, 5 mmol, 1 eq) was then added to the flask and the reaction was stirred at 0 °C for 30 minutes. After 30 minutes, DCC (1.032 g, 5 mmol, 1 eq) was added at 0 °C and the reaction was slowly allowed to warm to room temperature, then stirred for 16 hours. Reaction progress was measured by TLC. Upon reaction completion, the mixture was concentrated, then the residue was dissolved in a minimal amount of ethyl acetate and filtered through a pad of celite to remove dicyclohexylurea (DCU). Filtrate was concentrated onto silica and purified using automated flash chromatography with hexanes and ethyl acetate as elution solvents to provide **1e**. (0.658 g, 2.9 mmol, 36% yield)

^{1}H NMR (500 MHz, $CDCl_3$) δ 12.62 (s, 1H), 8.55 (d, *J* = 8.5 Hz, 1H), 7.49 (t, *J* = 8.0 Hz, 1H), 7.05 – 6.99 (m, 1H), 3.01 (t, *J* = 6.1 Hz, 2H), 2.96 (s, 1H), 2.77 – 2.71 (m, 2H), 2.13 (p, *J* = 6.4 Hz, 2H).

^{13}C NMR (126 MHz, $CDCl_3$) δ 203.30, 150.35, 146.21, 140.77, 135.12, 124.15, 118.91, 118.37, 78.17, 77.33, 77.07, 76.82, 73.63, 40.63, 30.84, 22.65.

N-(2-acetylphenyl)-3-cyclopropylpropiolamide (1f):

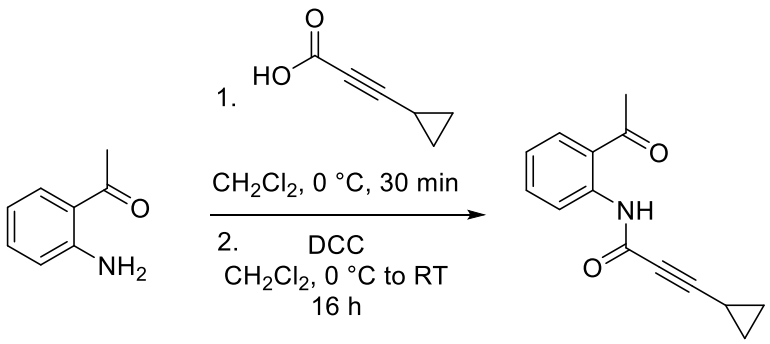

1f

An oven-dried 25 mL round bottom flask was charged with an oven-dried stir bar. To this flask was added 2-aminoacetophenone (0.270 g, 2 mmol, 1 eq) and 10 mL methylene chloride. The flask was cooled to 0 °C and stirred. 3-cyclopropylpropiolic acid (0.220 g, 2 mmol, 1 eq) was then added to the flask and the reaction was stirred at 0 °C for 30 minutes. After 30 minutes, DCC (0.412 g, 2 mmol, 1 eq) was added at 0 °C and the reaction was slowly allowed to warm to room temperature, then stirred for 16 hours. Reaction progress was measured by TLC. Upon reaction completion, the mixture was concentrated, then the residue was dissolved in a minimal amount of ethyl acetate and filtered through a pad of celite to remove dicyclohexylurea (DCU). Filtrate was concentrated onto silica and purified using automated flash chromatography to provide **1f** (0.189 g, 0.82 mmol, 41% yield)

^{1}H NMR (500 MHz, $CDCl_3$) δ 11.77 (s, 1H), 8.59 (d, *J* = 8.5 Hz, 1H), 7.82 (dd, *J* = 8.0, 1.6 Hz, 1H), 7.47 (ddd, *J* = 8.6, 7.2, 1.6 Hz, 1H), 7.09 – 7.02 (m, 1H), 2.60 (s, 3H), 1.34 (tt, *J* = 7.5, 5.6 Hz, 1H), 0.87 (dt, *J* = 8.3, 2.0 Hz, 4H).

^{13}C NMR (126 MHz, $CDCl_3$) δ 203.07, 152.31, 140.91, 135.62, 132.10, 123.28, 122.19, 121.79, 92.59, 77.79, 77.54, 77.29, 72.36, 29.03, 9.61, -0.00.

3-cyclopropyl-N-(8-oxo-5,6,7,8-tetrahydronaphthalen-1-yl)propiolamide (1g):

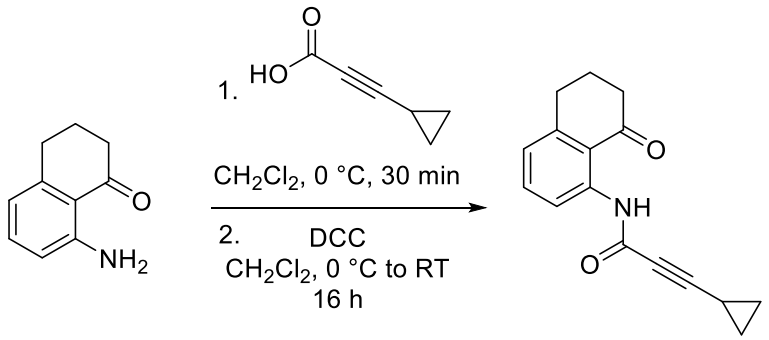

1g

An oven-dried 25 mL round bottom flask was charged with an oven-dried stir bar. To this flask was added aminotetralone (0.322 g, 2 mmol, 1 eq) and 10 mL methylene chloride. The flask was cooled to 0 °C and stirred. 3-cyclopropylpropiolic acid (0.220 g, 2 mmol, 1 eq) was then added to the flask and the reaction was stirred at 0 °C for 30 minutes. After 30 minutes, DCC (0.412 g, 2 mmol, 1 eq) was added at 0 °C and the reaction was slowly allowed to warm to room temperature, then stirred for 16 hours. Reaction progress was measured by TLC. Upon reaction completion, the mixture was concentrated, then the residue was dissolved in a minimal amount of ethyl acetate and filtered through a pad of celite to remove dicyclohexylurea (DCU). Filtrate was concentrated onto silica and purified using automated flash chromatography to provide **1g** (0.192 g, 0.76 mmol, 38% yield).

^{1}H NMR (500 MHz, $CDCl_3$) δ 12.34 (s, 1H), 8.55 (d, *J* = 8.4 Hz, 1H), 7.46 (t, *J* = 8.0 Hz, 1H), 6.99 – 6.94 (m, 1H), 3.00 (t, *J* = 6.1 Hz, 2H), 2.76 – 2.70 (m, 2H), 2.12 (p, *J* = 6.5 Hz, 2H), 1.44 (tt, *J* = 7.8, 5.7 Hz, 1H), 1.01 – 0.92 (m, 4H).

^{13}C NMR (126 MHz, $CDCl_3$) δ 203.60, 152.20, 146.58, 141.76, 135.49, 124.02, 119.14, 118.59, 92.30, 77.96, 77.71, 77.45, 72.48, 41.14, 31.36, 23.17, 9.63, 0.00.

N-(2-acetylphenyl)thiophene-2-carboxamide (1h):

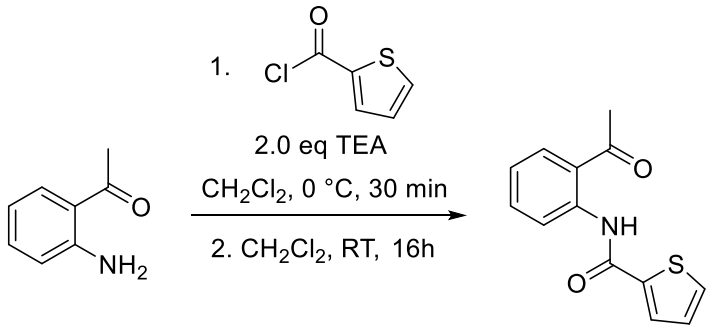

1h

An oven-dried 100 mL round bottom flask was charged with an oven-dried stir bar. To this flask, 20 mL methylene chloride and 2-thiophenecarbonyl chloride (0.855 mL, 1.17 g, 8 mmol, 1 eq) were added. The reaction was cooled to 0 °C, then 2-aminoacetophenone (1.08 g, 8 mmol, 1 eq) and triethylamine (2.232 mL, 16 mmol, 2 eq) in methylene chloride (15 mL) were added dropwise using an addition funnel. The reaction was stirred at 0 °C to RT for 16 hours. Once the reaction was complete by TLC, the resulting mixture was extracted three times with DCM, organic layers were combined and washed with brine, dried over anhydrous sodium sulfate and concentrated in vacuo. Crude product was purified on using automated flash chromatography to provide **1h**. (1.45 g, 5.92 mmol, 74% yield)

^{1}H NMR (500 MHz, $CDCl_3$) δ 12.73 (s, 1H), 8.93 – 8.87 (m, 1H), 7.97 (dd, *J* = 8.0, 1.6 Hz, 1H), 7.86 (dd, *J* = 3.8, 1.2 Hz, 1H), 7.66 – 7.57 (m, 2H), 7.21 – 7.13 (m, 2H), 2.74 (s, 3H).

N-(2-acetylphenyl)-3-phenylpropiolamide (1i):

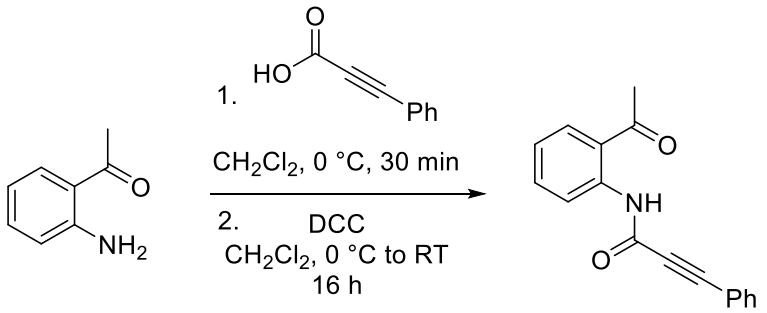

1i

An oven-dried 100 mL round bottom flask was charged with an oven-dried stir bar. To this flask was added 2-aminoacetophenone (0.675 g, 5 mmol, 1 eq) and 20 mL methylene chloride. The flask was cooled to 0 °C and stirred. Phenylpropiolic acid (0.730 g, 5 mmol, 1 eq) was then added to the flask and the reaction was stirred at 0 °C for 30 minutes. After 30 minutes, DCC (1.032 g, 5 mmol, 1 eq) was added at 0 °C and the reaction was slowly allowed to warm to room temperature, then stirred for 16 hours. Reaction progress was measured by TLC. Upon reaction completion, the mixture was concentrated, then the residue was dissolved in a minimal amount of ethyl acetate and filtered through a pad of celite to remove dicyclohexylurea (DCU). Filtrate was concentrated onto silica and purified using automated flash chromatography to provide **1i** (1.15 g, 4.4 mmol, 88% yield).

^{1}H NMR (500 MHz, $CDCl_3$) δ 12.02 (s, 1H), 8.62 (d, *J* = 8.5 Hz, 1H), 7.80 (dd, *J* = 8.0, 1.6 Hz, 1H), 7.51 (dt, *J* = 6.9, 1.5 Hz, 2H), 7.45 (ddd, *J* = 8.7, 7.2, 1.6 Hz, 1H), 7.37 – 7.30 (m, 1H), 7.27 (dd, *J* = 8.2, 6.6 Hz, 2H), 7.05 (td, *J* = 7.7, 1.2 Hz, 1H), 2.57 (s, 3H).

^{13}C NMR (126 MHz, $CDCl_3$) δ 202.71, 151.65, 140.27, 135.18, 132.83, 131.75, 130.34, 128.56, 123.15, 121.75, 121.23, 120.05, 85.56, 84.07, 77.43, 77.17, 76.92, 28.53.

N-(8-oxo-5,6,7,8-tetrahydronaphthalen-1-yl)-3-phenylpropiolamide (1j):

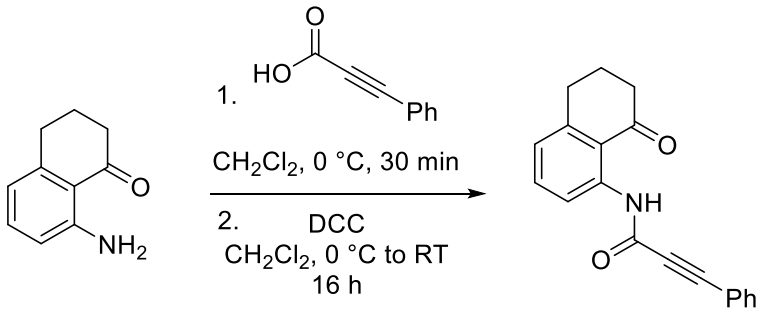

1j

An oven-dried 100 mL round bottom flask was charged with an oven-dried stir bar. To this flask was added aminotetralone (0.805 g, 5 mmol, 1 eq) and 20 mL methylene chloride. The flask was cooled to 0 °C and stirred. Phenylpropiolic acid (0.730 g, 5 mmol, 1 eq) was then added to the flask and the reaction was stirred at 0 °C for 30 minutes. After 30 minutes, DCC (1.032 g, 5 mmol, 1 eq) was added at 0 °C and the reaction was slowly allowed to warm to room temperature, then stirred for 16 hours. Reaction progress was measured by TLC. Upon reaction completion, the mixture was concentrated, then the residue was dissolved in a minimal amount of ethyl acetate and filtered through a pad of celite to remove dicyclohexylurea (DCU). Filtrate was concentrated onto silica and purified using automated flash chromatography to provide **1j** (1.18 g, 4.1 mmol, 82% yield).

^{1}H NMR (500 MHz, $CDCl_3$) δ 12.61 (s, 1H), 8.60 (d, *J* = 8.4 Hz, 1H), 7.67 – 7.61 (m, 2H), 7.53 – 7.42 (m, 2H), 7.39 (dd, *J* = 8.2, 6.6 Hz, 2H), 6.99 (d, *J* = 7.5 Hz, 1H), 3.00 (t, *J* = 6.1 Hz, 2H), 2.73 (t, *J* = 6.5 Hz, 2H), 2.12 (p, *J* = 6.4 Hz, 2H).

^{13}C NMR (126 MHz, $CDCl_3$) δ 203.25, 151.68, 146.19, 141.20, 135.12, 132.83, 130.27, 128.53, 123.86, 120.16, 118.81, 118.30, 85.37, 84.22, 77.38, 77.13, 76.87, 40.67, 30.89, 22.69.

3.2 Synthesis Of Photoproducts

4-methyl-4-(prop-1-yn-1-yl)-1,4-dihydro-2H-benzo[d][1,3]oxazin-2-one (2a):

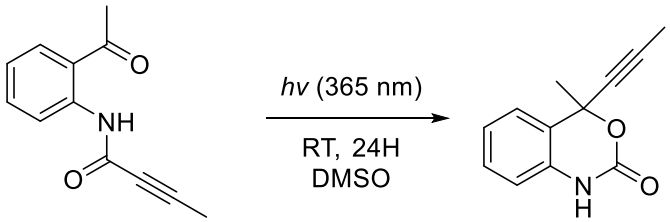

1a **2a**

To a 100 mL Pyrex square bottle, 0.150 g **1a** (0.745 mmol, 1 eq) and 50 mL DMSO was added. The bottle was sealed with a Teflon septum, the septum was punctured with a venting need and solvent was degassed by bubbling nitrogen through the solution with a needle for twenty minutes. After degassing, the bottle was placed in a water bath at room temperature and irradiated with 365 nm LEDs for 24 hours. After 24 hours, the mixture was concentrated on a high vacuum, suspended in methylene chloride, then reconcentrated onto silica for purification using automated flash chromatography using ethyl acetate and hexanes as elution solvents to provide **2a**. (0.038 g, 0.193 mmol, 26% yield)

^{1}H NMR (500 MHz, $CDCl_3$) δ 9.80 (s, 1H), 7.35 – 7.30 (m, 1H), 7.31 – 7.24 (m, 1H), 7.13 – 7.06 (m, 1H), 6.96 (d, *J* = 7.9 Hz, 1H), 1.98 (s, 3H), 1.87 (s, 3H).

^{13}C NMR (126 MHz, $CDCl_3$) δ 152.98, 134.02, 129.46, 124.11, 123.79, 123.59, 114.99, 83.90, 78.08, 77.34, 77.09, 76.83, 28.35, 3.73.

4-ethynyl-4-methyl-1,4-dihydro-2H-benzo[d][1,3]oxazin-2-one (2b):

1b **2b**

To a 100 mL Pyrex square bottle, 0.150 g **1b** (0.801 mmol, 1 eq) and 50 mL DMSO was added. The bottle was sealed with a Teflon septum, the septum was punctured with a venting need and solvent was degassed by bubbling nitrogen through the solution with a needle for twenty minutes. After degassing, the bottle was placed in a water bath at room temperature and irradiated with 365 nm LEDs for 24 hours. After 24 hours, the mixture was concentrated on a high vacuum, suspended in methylene chloride, then reconcentrated onto silica for purification using automated flash chromatography using ethyl acetate and hexanes as elution solvents to provide **2b**. (0.046 g, 0.248 mmol, 31% yield)

^{1}H NMR (500 MHz, $CDCl_3$) δ 9.49 (s, 1H), 7.37 (s, 1H), 7.35 – 7.28 (m, 1H), 7.13 (t, *J* = 7.6 Hz, 1H), 6.96 (d, *J* = 7.9 Hz, 1H), 2.77 (d, *J* = 3.1 Hz, 1H), 2.04 (s, 3H).

^{13}C NMR (126 MHz, $CDCl_3$) δ 152.24, 133.98, 129.87, 123.88, 123.84, 123.07, 114.99, 82.00, 77.29, 77.03, 76.78, 76.64, 75.27, 28.05.

4-(furan-2-yl)-4-methyl-1,4-dihydro-2H-benzo[d][1,3]oxazin-2-one (2c):

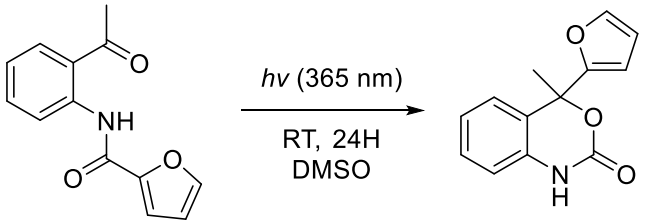

1c **2c**

To a 100 mL Pyrex square bottle, 0.150 g **1c** (0.654 mmol, 1 eq) and 50 mL DMSO was added. The bottle was sealed with a Teflon septum, the septum was punctured with a venting need and solvent was degassed by bubbling nitrogen through the solution with a needle for twenty minutes. After degassing, the bottle was placed in a water bath at room temperature and irradiated with 365 nm LEDs for 24 hours. After 24 hours, the mixture was concentrated on a high vacuum, suspended in methylene chloride, then reconcentrated onto silica for purification using automated flash chromatography using ethyl acetate and hexanes as elution solvents to provide **2c**. (0.054 g, 0.236 mmol, 36% yield)

^{1}H NMR (500 MHz, $CDCl_3$) δ 9.14 (s, 1H), 7.43 – 7.39 (m, 1H), 7.34 – 7.27 (m, 1H), 7.14 – 7.05 (m, 2H), 6.93 (d, *J* = 8.0 Hz, 1H), 6.32 (dd, *J* = 3.4, 1.8 Hz, 1H), 6.17 (d, *J* = 3.3 Hz, 1H), 2.12 (s, 3H).

^{13}C NMR (126 MHz, $CDCl_3$) δ 153.76, 152.33, 143.42, 134.62, 129.61, 124.80, 123.46, 122.93, 114.73, 110.21, 108.43, 80.95, 77.27, 77.02, 76.77, 25.29.

9a-(prop-1-yn-1-yl)-7,8,9,9a-tetrahydronaphtho[1,8-de][1,3]oxazin-2(3H)-one (2d):

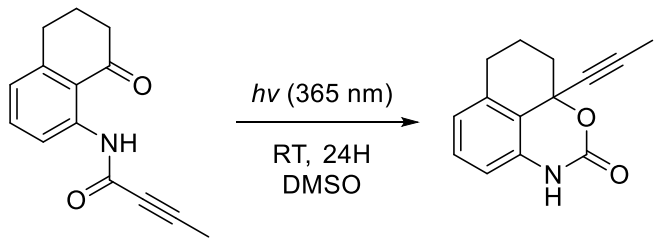

1d **2d**

To a 100 mL Pyrex square bottle, 0.150 g **1d** (0.660 mmol, 1 eq) and 50 mL DMSO was added. The bottle was sealed with a Teflon septum, the septum was punctured with a venting need and solvent was degassed by bubbling nitrogen through the solution with a needle for twenty minutes. After degassing, the bottle was placed in a water bath at room temperature and irradiated with 365 nm LEDs for 24 hours. After 24 hours, the mixture was concentrated on a high vacuum, suspended in methylene chloride, then reconcentrated onto silica for purification using automated flash chromatography using ethyl acetate and hexanes as elution solvents to provide **2d**. (0.043 g, 0.191 mmol, 29% yield)

^{1}H NMR (500 MHz, $CDCl_3$) δ 8.05 (s, 1H), 7.19 (t, *J* = 7.8 Hz, 1H), 6.87 (d, *J* = 7.7 Hz, 1H), 6.69 (d, *J* = 7.8 Hz, 1H), 2.93 – 2.74 (m, 2H), 2.49 (dt, *J* = 11.2, 2.9 Hz, 1H), 2.27 – 2.13 (m, 1H), 2.10 (ddd, *J* = 14.0, 11.4, 2.8 Hz, 2H), 1.83 (s, 3H).

^{13}C NMR (126 MHz, $CDCl_3$) δ 152.72, 135.22, 134.50, 129.11, 123.68, 120.31, 111.60, 84.04, 77.74, 77.27, 77.02, 76.77, 75.29, 34.96, 27.04, 19.99, 3.86.

9a-ethynyl-7,8,9,9a-tetrahydronaphtho[1,8-de][1,3]oxazin-2(3H)-one (2e):

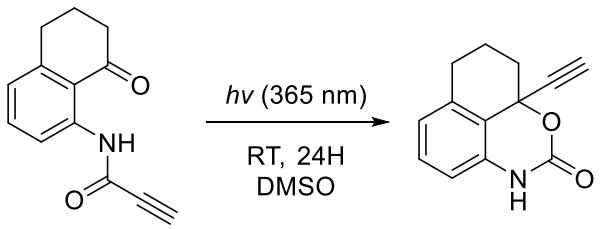

1e **2e**

To a 100 mL Pyrex square bottle, 0.150 g **1e** (0.703 mmol, 1 eq) and 50 mL DMSO was added. The bottle was sealed with a Teflon septum, the septum was punctured with a venting need and solvent was degassed by bubbling nitrogen through the solution with a needle for twenty minutes. After degassing, the bottle was placed in a water bath at room temperature and irradiated with 365 nm LEDs for 24 hours. After 24 hours, the mixture was concentrated on a high vacuum, suspended in methylene chloride, then reconcentrated onto silica for purification using automated flash chromatography using ethyl acetate and hexanes as elution solvents to provide **2e**. (0.039 g, 0.183 mmol, 26% yield)

^{1}H NMR (500 MHz, $CDCl_3$) δ 8.37 (s, 1H), 7.22 (t, *J* = 7.8 Hz, 1H), 6.89 (d, *J* = 7.8 Hz, 1H), 6.73 (d, *J* = 7.8 Hz, 1H), 2.95 – 2.86 (m, 1H), 2.81 (ddd, *J* = 17.6, 11.2, 6.4 Hz, 1H), 2.69 (s, 1H), 2.59 – 2.52 (m, 1H), 2.28 – 2.09 (m, 3H).

^{13}C NMR (126 MHz, $CDCl_3$) δ 152.49, 135.42, 134.59, 129.58, 123.84, 119.18, 111.83, 81.88, 77.27, 77.02, 76.77, 75.50, 74.65, 34.55, 26.94, 19.86.

4-(cyclopropylethynyl)-4-methyl-1,4-dihydro-2H-benzo[d][1,3]oxazin-2-one (2f):

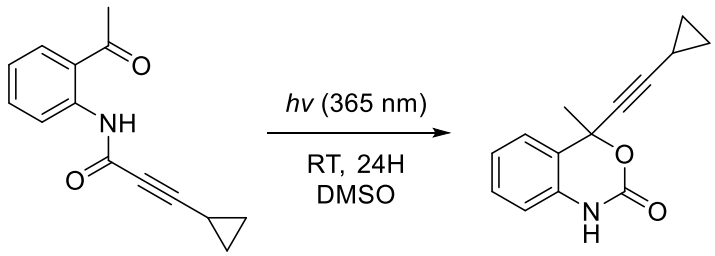

1f **2f**

To a 100 mL Pyrex square bottle, 0.150 g **1f** (0.660 mmol, 1 eq) and 50 mL DMSO was added. The bottle was sealed with a Teflon septum, the septum was punctured with a venting need and solvent was degassed by bubbling nitrogen through the solution with a needle for twenty minutes. After degassing, the bottle was placed in a water bath at room temperature and irradiated with 365 nm LEDs for 24 hours. After 24 hours, the mixture was concentrated on a high vacuum, suspended in methylene chloride, then reconcentrated onto silica for purification using automated flash chromatography using ethyl acetate and hexanes as elution solvents to provide **2f**. (0.057 g, 0.251 mmol, 38% yield)

^{1}H NMR (500 MHz, $CDCl_3$) δ 9.42 (s, 1H), 7.33 (dd, *J* = 7.6, 1.3 Hz, 1H), 7.28 (td, *J* = 7.7, 1.4 Hz, 1H), 7.10 (td, *J* = 7.5, 1.1 Hz, 1H), 6.92 (dd, *J* = 8.0, 1.1 Hz, 1H), 1.96 (s, 3H), 1.28 (tt, *J* = 8.2, 5.0 Hz, 1H), 0.85 – 0.77 (m, 2H), 0.72 (ddd, *J* = 6.9, 5.2, 3.3 Hz, 2H).

^{13}C NMR (126 MHz, $CDCl_3$) δ 153.13, 134.48, 129.97, 124.71, 124.52, 124.14, 115.34, 91.94, 78.11, 77.83, 77.58, 77.32, 74.37, 29.20, 9.05, 9.03, 0.00.

9a-(cyclopropylethynyl)-7,8,9,9a-tetrahydronaphtho[1,8-de][1,3]oxazin-2(3H)-one (2g):

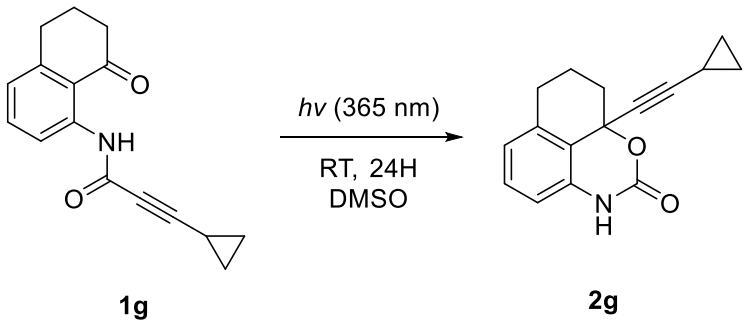

1g **2g**

To a 100 mL Pyrex square bottle, 0.150 g **1g** (0.592 mmol, 1 eq) and 50 mL DMSO was added. The bottle was sealed with a Teflon septum, the septum was punctured with a venting need and solvent was degassed by bubbling nitrogen through the solution with a needle for twenty minutes. After degassing, the bottle was placed in a water bath at room temperature and irradiated with 365 nm LEDs for 24 hours. After 24 hours, the mixture was concentrated on a high vacuum, suspended in methylene chloride, then reconcentrated onto silica for purification using automated flash chromatography using ethyl acetate and hexanes as elution solvents to provide **2g**. (0.061 g, 0.242 mmol, 41% yield)

^{1}H NMR (500 MHz, $CDCl_3$) δ 8.44 (s, 1H), 7.18 (t, *J* = 7.7 Hz, 1H), 6.86 (d, *J* = 7.7 Hz, 1H), 6.71 (d, *J* = 7.8 Hz, 1H), 2.88 (dd, *J* = 17.2, 5.7 Hz, 1H), 2.78 (ddd, *J* = 17.7, 11.4, 6.3 Hz, 1H), 2.49 – 2.42 (m, 1H), 2.24 – 2.04 (m, 3H), 1.30 – 1.18 (m, 1H), 0.80 – 0.60 (m, 4H).

^{13}C NMR (126 MHz, $CDCl_3$) δ 153.47, 135.56, 135.00, 129.49, 124.06, 120.74, 112.17, 91.98, 77.72, 77.46, 77.21, 75.81, 74.02, 35.52, 27.48, 20.48, 9.02, 8.98, 0.00.

4-methyl-4-(thiophen-2-yl)-1,4-dihydro-2H-benzo[d][1,3]oxazin-2-one (2h):

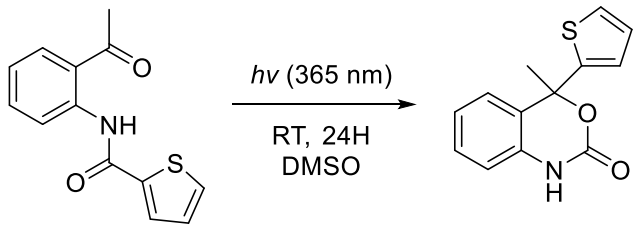

1h **2h**

To a 100 mL Pyrex square bottle, 0.150 g **1h** (0.612 mmol, 1 eq) and 50 mL DMSO was added. The bottle was sealed with a Teflon septum, the septum was punctured with a venting need and solvent was degassed by bubbling nitrogen through the solution with a needle for twenty minutes. After degassing, the bottle was placed in a water bath at room temperature and irradiated with 365 nm LEDs for 24 hours. After 24 hours, the mixture was concentrated on a high vacuum, suspended in methylene chloride, then reconcentrated onto silica for purification using automated flash chromatography using ethyl acetate and hexanes as elution solvents to provide **2h**. (0.036 g, 0.146 mmol, 24 % yield)

^{1}H NMR (500 MHz, $CDCl_3$) δ 8.20 (s, 1H), 7.33 (d, *J* = 7.7 Hz, 1H), 7.30 (d, *J* = 5.1 Hz, 1H), 7.25 (d, *J* = 7.8 Hz, 1H), 7.14 (t, *J* = 7.6 Hz, 1H), 6.94 – 6.85 (m, 2H), 6.82 (d, *J* = 3.7 Hz, 1H), 2.18 (s, 3H).

^{13}C NMR (126 MHz, $CDCl_3$) δ 151.81, 147.24, 134.56, 129.74, 126.56, 126.38, 125.55, 124.94, 124.69, 123.53, 114.58, 83.00, 77.27, 77.02, 76.76, 53.43, 28.82.

4-methyl-4-(phenylethynyl)-1,4-dihydro-2H-benzo[d][1,3]oxazin-2-one (2i):

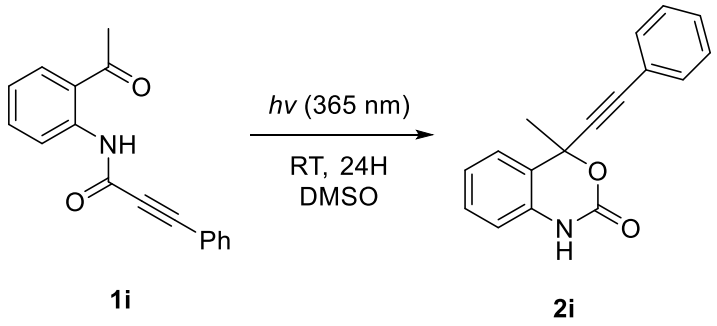

1i **2i**

To a 100 mL Pyrex square bottle, 0.150 g **1i** (0.570 mmol, 1 eq) and 50 mL DMSO was added. The bottle was sealed with a Teflon septum, the septum was punctured with a venting need and solvent was degassed by bubbling nitrogen through the solution with a needle for twenty minutes. After degassing, the bottle was placed in a water bath at room temperature and irradiated with 365 nm LEDs for 24 hours. After 24 hours, the mixture was concentrated on a high vacuum, suspended in methylene chloride, then reconcentrated onto silica for purification using automated flash chromatography using ethyl acetate and hexanes as elution solvents to provide **2i**. (0.120 g, 0.456 mmol, 80% yield)

^{1}H NMR (500 MHz, $CDCl_3$) δ 9.99 (s, 1H), 7.41 (t, *J* = 8.5 Hz, 3H), 7.29 (dt, *J* = 14.7, 7.0 Hz, 4H), 7.10 (t, *J* = 7.6 Hz, 1H), 7.01 (d, *J* = 8.0 Hz, 1H), 2.09 (s, 3H).

^{13}C NMR (126 MHz, $CDCl_3$) δ 152.47, 134.31, 131.90, 129.66, 128.99, 128.29, 123.97, 123.63, 123.61, 121.66, 115.07, 87.38, 86.82, 77.44, 77.43, 77.18, 76.92, 40.77, 28.49.

9a-(phenylethynyl)-7,8,9,9a-tetrahydronaphtho[1,8-de][1,3]oxazin-2(3H)-one (2j):

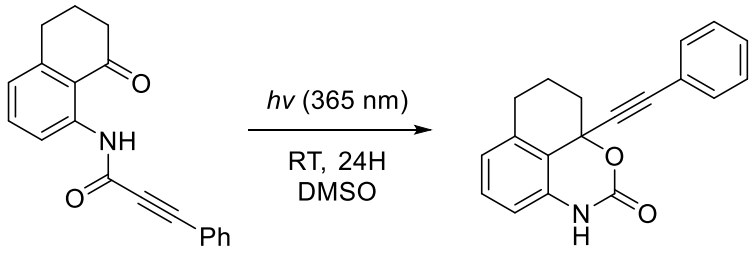

1j **2j**

To a 100 mL Pyrex square bottle, 0.150 g **1j** (0.518 mmol, 1 eq) and 50 mL DMSO was added. The bottle was sealed with a Teflon septum, the septum was punctured with a venting need and solvent was degassed by bubbling nitrogen through the solution with a needle for twenty minutes. After degassing, the bottle was placed in a water bath at room temperature and irradiated with 365 nm LEDs for 24 hours. After 24 hours, the mixture was concentrated on a high vacuum, suspended in methylene chloride, then reconcentrated onto silica for purification using automated flash chromatography using ethyl acetate and hexanes as elution solvents to provide **2j** (0.132 g, 0.456 mmol, 88% yield)

^{1}H NMR (500 MHz, $CDCl_3$) δ 9.99 (s, 1H), 7.41 (t, *J* = 8.5 Hz, 3H), 7.29 (dt, *J* = 14.7, 7.0 Hz, 4H), 7.10 (t, *J* = 7.6 Hz, 1H), 7.01 (d, *J* = 8.0 Hz, 1H), 2.09 (s, 3H).

^{13}C NMR (126 MHz, $CDCl_3$) δ 152.47, 134.31, 131.90, 129.66, 128.99, 128.29, 123.97, 123.63, 123.61, 121.66, 115.07, 87.38, 86.82, 77.44, 77.43, 77.18, 76.92, 40.77, 28.49.

4. REFERENCES

1. Ciamician, G. S., P., Chemische Lichtwirkungen. *Berichte der deutschen chemischen Gesellschaft* **1908,** *41* (1), 1071-1080.

2. Nicolaou, K. C.; Sarlah, D.; Shaw, D. M., Total synthesis and revised structure of biyouyanagin A. *Angew Chem Int Ed Engl* **2007,** *46* (25), 4708-11.

3. Srikrishna, A.; Ramasastry, S.S.V., Enantiospecific Total Synthesis of Phytoalexins, (+)-Solanascone, (+)-Dehydrosolanascone, and (+)-Anydro-β-rotunol. *Tetrahedron Lett* **2005,** *46* (43), 7373-7376.

4. Dauben, W. G. K., M.S.; Seeman, J.I.; Spitzer, W.A., Photochemical rearrangement of an acyclic beta, gamma-unsaturated ketone to a conjugated cyclopropyl ketone. An oxa-di-pi-methane rearrangement. *J Am Chem Soc* **1970,** *92* (6), 1786-1787.

5. Stevens, K. E.; Yates, P. Cedrenoid sesquiterpenes. Synthesis of the (+-0 Stork-Clarke β-diketone. *Journal of the chemical Society* **1980,** *21*, 990-991.

6. Weller, A., Innermolekularer protonenübergang im angeregten zustand. *Zeitschrift für Elektrochemie, Berichte der Bunsengesellschaft für physikalische Chemie* **1956,** *60*, 9-10.

7. Formosinho, S. J. A., L.G., Excited-state proton transfer reactions II. Intramolecular reactions. *J Photoch Photobio A* **1993,** *1* (15), 21-48.

8. Arnaut, L. G. S., J.F., Excited-state proton transfer reactions I. Fundamentals and intermolecular reactions. *J Photoch Photobio A* **1993,** *75* (1), 1-20.

9. Sedgwick, A. C.; Wu, L.; Han, H. H.; Bull, S. D.; He, X. P.; James, T. D.; Sessler, J. L.; Tang, B. Z.; Tian, H.; Yoon, J., Excited-state intramolecular proton-transfer (ESIPT) based fluorescence sensors and imaging agents. *Chem Soc Rev* **2018,** *47* (23), 8842-8880.

10. Cava, M. P. N., D.R., Condensed cyclobutane aromatic systems. II. Dihalo derivatives of benzocyclobutene and benzocyclobutadiene dimer. *J. Am. Chem. Soc.* **1957,** *79*, 1701-1705.

11. Oppolzer, W., Intramolecular Cycloaddition Reactions of ortho-quinodimethanes in organic synthesis. *Synthesis* **1978**, 793-802.

12. Charlton, J. L. A., M.M., Orthoquinodimethanes. *Tetrahedron* **1987,** *43*, 2873-2889.

13. Segura, J. L.; Martin, N., o-Quinodimethanes: Efficient Intermediates in Organic Synthesis. *Chem Rev* **1999,** *99* (11), 3199-246.

14. Sammes, P. G., Photoenolisation. *Tetrahedron* **1976,** *32* (3), 405-422.

15. Quinkert, G. Q. S., U.; Stark, H.; Weber, W.D.; Baier, H.; Adam, F.; Durner, G., Asymmetric Total Synthesis of Estrone. *Angew Chem Int Ed Engl* **1980,** *19* (12), 1029-1030.

16. Kraus, G. A. W., Y., Hydrogen atom abstaction reactions in organic synthesis. A formal total synthesis of racemic podophyllotoxin. *The Journal of Organic Chemistry* **1992,** *57* (10), 2922-2925.

17. Cronk, W. C.; Mukhina, O. A.; Kutateladze, A. G., Intramolecular photoassisted cycloadditions of azaxylylenes and postphotochemical capstone modifications via Suzuki

coupling provide access to complex polyheterocyclic biaryls. *J Org Chem* **2014,** *79* (3), 1235-46.

18. Kumar, N. N. B.; Kutateladze, A. G., Photoassisted Diversity-Oriented Synthesis: Intramolecular Cycloadditions of Photogenerated Azaxylylenes with Oxazole Pendants, and Subsequent Postphotochemical Multicomponent Modifications. *Org Lett* **2016,** *18* (3), 460-463.

19. Kuznetsov, D. M.; Kutateladze, A. G., Step-Economical Photoassisted Diversity-Oriented Synthesis: Sustaining Cascade Photoreactions in Oxalyl Anilides to Access Complex Polyheterocyclic Molecular Architectures. *J Am Chem Soc* **2017,** *139* (46), 16584-16590.

20. Kuznetsov, D. M.; Mukhina, O. A.; Kutateladze, A. G., Photoassisted Synthesis of Complex Molecular Architectures: Dearomatization of Benzenoid Arenes with Aza-o-xylylenes via an Unprecedented [2+4] Reaction Topology. *Angew Chem Int Ed Engl* **2016,** *55* (24), 6988-91.

21. Mukhina, O. A.; Cronk, W. C.; Kumar, N. N.; Sekhar, M. C.; Samanta, A.; Kutateladze, A. G., Intramolecular cycloadditions of photogenerated azaxylylenes: an experimental and theoretical study. *J Phys Chem A* **2014,** *118* (45), 10487-96.

22. Mukhina, O. A.; Kumar, N. N. B.; Arisco, T. M.; Valiulin, R. A.; Metzel, G. A.; Kutateladze, A. G., Rapid Photoassisted Access to N,O,S-Polyheterocycles with Benzoazocine and Hydroquinoline Cores: Intramolecular Cycloadditions of Photogenerated Azaxylylenes. *Angew Chem Int Edit* **2011,** *50* (40), 9423-9428.

23. Mukhina, O. A.; Kutateladze, A. G., Oxazolines as Dual-Function Traceless Chromophores and Chiral Auxiliaries: Enantioselective Photoassisted Synthesis of Polyheterocyclic Ketones. *J Am Chem Soc* **2016,** *138* (7), 2110-3.

24. Mukhina, O. A.; Kuznetsov, D. M.; Cowger, T. M.; Kutateladze, A. G., Amino Azaxylylenes Photogenerated from o-Amido Imines: Photoassisted Access to Complex Spiro-Poly-Heterocycles. *Angew Chem Int Ed Engl* **2015,** *54* (39), 11516-20.

25. Nandurkar, N. S.; Kumar, N. N.; Mukhina, O. A.; Kutateladze, A. G., Photoassisted access to enantiopure conformationally locked ribofuranosylamines spiro-linked to oxazolidino-diketopiperazines. *ACS Comb Sci* **2013,** *15* (1), 73-6.

26. Reddy, D. S.; Kutateladze, A. G., Photoinitiated Cascade for Rapid Access to Pyrroloquinazolinone Core of Vasicinone, Luotonins, and Related Alkaloids. *Org Lett* **2019,** *21* (8), 2855-2858.

27. Reddy, D. S. N., I.V.; Kutateladze, A.G., Maximizing Step-Normalized Increases in Molecular Complexity: Formal [4+2+2+2] Photoinduced Cyclization Cascade to Access Polyheterocycles Possessing Privileged Substructures. *Angew Chem Int Ed Engl* **2021,** *61* (4).

28. Umstead, W. J.; Mukhina, O. A.; Kutateladze, A. G., Photoassisted access to complex polyheterocycles containing a beta-lactam moiety. *J Photochem Photobiol A Chem* **2016,** *329*, 182-188.

29. Umstead, W. J.; Mukhina, O. A.; Kutateladze, D. A., Conformationally Constrained Penta(hetero)cyclic Molecular Architectures via Photoassisted Diversity-Oriented Synthesis. *European J Org Chem* **2015,** *2015* (10), 2205-2213.

30. Cronk, W. C.; Mukhina, O. A.; Kutateladze, A. G., Photoinduced "Double Click" Cascade Offers Access to Complex Polyheterocycles from Readily Available Isatin-Based Photoprecursors. *Org Lett* **2016,** *18* (15), 3750-3.

31. Lovering, F.; Bikker, J.; Humblet, C., Escape from flatland: increasing saturation as an approach to improving clinical success. *J Med Chem* **2009,** *52* (21), 6752-6.

32. Hietala, P. K., Virtanen, A.I., Precursors of Benzoxazolinone in Rye Plants. *Acta. Chem. Scand.* **1960,** *14*, 502-504.

33. Niemeyer, H. M., Hydroxamic acids (4-hydroxy-1,4-benzoxazin-3-ones) defense chemicals in Gramineae. *Phytochemistry* **1988,** *27*, 3349-3358.

34. Meihls, L. N.; Kaur, H.; Jander, G., Natural variation in maize defense against insect herbivores. *Cold Spring Harb Symp Quant Biol* **2012,** *77*, 269-83.

35. Queirolo, C. B. A., T.H.; Niemeyer, H.M.; Corcuera, L.J., Inhibition of ATPase from chloroplasts by a hydroxamic acid from the gramineae. *Phytochemistry* **1983,** *22* (11), 2455-2458.

36. Cuevas. L.; Niemeyer, H. M., Effect of hydroxamic acids from cereals on aphid cholinesterases. *Phytochemistry* **1993,** (34), 983-985.

37. Cuevas, L. N., H.M.; Perez, F.J., Reaction of DIMBOA, a resistance factor from cereals, with a-chymotrypsin. *Phytochemistry* **1990,** (29), 1429-1432.

38. de Bruijn, W. J. C.; Gruppen, H.; Vincken, J. P., Structure and biosynthesis of benzoxazinoids: Plant defence metabolites with potential as antimicrobial scaffolds. *Phytochemistry* **2018,** *155*, 233-243.

39. Zaynab, M.; Fatima, M.; Abbas, S.; Sharif, Y.; Umair, M.; Zafar, M. H.; Bahadar, K., Role of secondary metabolites in plant defense against pathogens. *Microb Pathog* **2018,** *124*, 198-202.

40. Abramov, A.; Hoffmann, T.; Stark, T. D.; Zheng, L.; Lenk, S.; Hammerl, R.; Lanzl, T.; Dawid, C.; Schon, C. C.; Schwab, W.; Gierl, A.; Frey, M., Engineering of benzoxazinoid biosynthesis in Arabidopsis thaliana: Metabolic and physiological challenges. *Phytochemistry* **2021,** *192*, 112947.

41. Glensk, M.; Gajda, B.; Franiczek, R.; Krzyzanowska, B.; Biskup, I.; Wlodarczyk, M., In vitro evaluation of the antioxidant and antimicrobial activity of DIMBOA [2,4-dihydroxy-7-methoxy-2H-1,4-benzoxazin-3(4H)-one]. *Nat Prod Res* **2016,** *30* (11), 1305-8.

42. Jiang, S.; Awadasseid, A.; Narva, S.; Cao, S.; Tanaka, Y.; Wu, Y.; Fu, W.; Zhao, X.; Wei, C.; Zhang, W., Anti-cancer activity of benzoxazinone derivatives via targeting c-Myc G-quadruplex structure. *Life Sci* **2020,** *258*, 118252.

43. Veerasamy, R. S., D.K.; Chean, O.C.; Ying, N.M., Designing hypothesis of substituted benzoxazinones as HIV-1 reverse transcriptase inhibitors: QSAR Approach. *Journal of Enzyme Inhibition and Medicinal Chemistry* **2011,** *27* (5), 693-707.

44. Borate, H. B. M., S.R.; Swargave, S.P.; Kelkar, R.G.; Wakharkar, R.D.; Chandavarkar, M.A.; Vaiude, S.R.; Joshi, V.A., Antifungal Compounds Containing Benzothiazinone, Benzoxazinone or Benzoxazolinone and Process Thereof. *Google Patents* **2012,** *USOO8129369B2*.

45. Ishizaki, T. H., Y.; Shudo, K.; Okamoto, T., Reaction of 4-acetoxy-1,4-benzoxazin-3-one with DNA. A possible chemical mechanism for the antifungal and mutagenic activites. *Tetrahedron Lett* **1982,** *23* (39), 4055-4056.

46. Jana, S.; Yang, Z.; Pei, C.; Xu, X.; Koenigs, R. M., Photochemical ring expansion reactions: synthesis of tetrahydrofuran derivatives and mechanism studies. *Chem Sci* **2019,** *10* (43), 10129-10134.

47. Neidle, S., Quadruplex Nucleic Acids as Novel Therapeutic Targets. *Jounal of Medicinal Chemistry* **2016,** *59* (13), 5987-6011.

48. Atkinson, P. J.; Bromidge, S. M.; Duxon, M. S.; Gaster, L. M.; Hadley, M. S.; Hammond, B.; Johnson, C. N.; Middlemiss, D. N.; North, S. E.; Price, G. W.; Rami, H. K.; Riley, G. J.; Scott, C. M.; Shaw, T. E.; Starr, K. R.; Stemp, G.; Thewlis, K. M.; Thomas, D. R.; Thompson, M.; Vong, A. K.; Watson, J. M., 3,4-Dihydro-2H-benzoxazinones are 5-HT(1A) receptor antagonists with potent 5-HT reuptake inhibitory activity. *Bioorg Med Chem Lett* **2005,** *15* (3), 737-41.

49. Hirschfeld, R. M., History and evolution of the monoamine hypothesis of depression. *J Clin Psychiatry* **2000,** *61 Suppl 6*, 4-6.

50. Hedstrom, L.; Moorman, A. R.; Dobbs, J.; Abeles, R. H., Suicide inactivation of chymotrypsin by benzoxazinones. *Biochemistry* **1984,** *23* (8), 1753-9.

51. Jarvest, R. L. P., M.J.; Debouck, C.M.; Gorniak, J.G.; Jennings, L.J.; Serafinowska, H.T.; Strickler, J.E., Inhibition of HSV-1 Protease by Benzoxazinones. *Bioorganic & Medicinal Chemistry Letters* **1996,** *6* (20), 2463-2466.

52. Hsieh, P. W.; Hwang, T. L.; Wu, C. C.; Chang, F. R.; Wang, T. W.; Wu, Y. C., The evaluation of 2,8-disubstituted benzoxazinone derivatives as anti-inflammatory and anti-platelet aggregation agents. *Bioorg Med Chem Lett* **2005,** *15* (11), 2786-9.

53. Bastos, M. M.; Costa, C. C. P.; Bezerra, T. C.; da Silva, F. C.; Boechat, N., Efavirenz a nonnucleoside reverse transcriptase inhibitor of first-generation: Approaches based on its medicinal chemistry. *Eur J Med Chem* **2016,** *108*, 455-465.

54. Rakhmanina, N. Y.; van den Anker, J. N., Efavirenz in the therapy of HIV infection. *Expert Opin Drug Metab Toxicol* **2010,** *6* (1), 95-103.

55. Lanzafame, M.; Bonora, S.; Lattuada, E.; Vento, S., Efavirenz dose reduction in HIV-infected patients. *HIV Med* **2012,** *13* (4), 252-3.

56. Ford, N.; Calmy, A.; Mofenson, L., Safety of efavirenz in the first trimester of pregnancy: an updated systematic review and meta-analysis. *AIDS* **2011,** *25* (18), 2301-4.

57. Ford, N.; Mofenson, L.; Kranzer, K.; Medu, L.; Frigati, L.; Mills, E. J.; Calmy, A., Safety of efavirenz in first-trimester of pregnancy: a systematic review and meta-analysis of outcomes from observational cohorts. *AIDS* **2010,** *24* (10), 1461-70.

58. Ford, N.; Mofenson, L.; Shubber, Z.; Calmy, A.; Andrieux-Meyer, I.; Vitoria, M.; Shaffer, N.; Renaud, F., Safety of efavirenz in the first trimester of pregnancy: an updated systematic review and meta-analysis. *AIDS* **2014,** *28 Suppl 2*, S123-31.

59. Nguyen, A.; Calmy, A.; Delhumeau, C.; Mercier, I.; Cavassini, M.; Mello, A. F.; Elzi, L.; Rauch, A.; Bernasconi, E.; Schmid, P.; Hirschel, B., A randomized cross-over study to compare raltegravir and efavirenz (SWITCH-ER study). *AIDS* **2011,** *25* (12), 1481-7.

60. Shridhar, D. R. J., M.; Krishnan, V.S.H., A general and convenient synthesis of 2H-1,4-benzoxazin-3(4H)-ones. *The New Journal for Organic Synthesis* **1982,** *14* (3), 195-197.

61. Frechette, R. F. B., M.J., The Preparation of 2-hydroxyethyl-2,3-dihydro-2H-1,4-benzoxazin-3(4H)-one derivatives. *Synthetic Commun* **1998,** *28* (18), 3471-3478.

62. Hernandez, E.; Velez, J. M.; Vlaar, C. P., Synthesis of 1,4-dihydro-benzo[d][1,3]oxazin-2-ones from phthalides via an aminolysis-Hofmann rearrangement protocol. *Tetrahedron Lett* **2007,** *48* (51), 8972-8975.

63. Pierce, M. E. C., A.; Lawrence, R.; Radesca, L.A. US Patent # 5932726. 1999.

64. Mehlman, M. A., Health effects and toxicity of phosgene: Scientific Review. *Def Sci J* **1987,** *37* (2), 269-279.

65. Li, T. R.; Cheng, B. Y.; Wang, Y. N.; Zhang, M. M.; Lu, L. Q.; Xiao, W. J., A Copper-Catalyzed Decarboxylative Amination/Hydroamination Sequence: Switchable Synthesis of Functionalized Indoles. *Angew Chem Int Ed Engl* **2016,** *55* (40), 12422-6.

66. Kruger, K. T., A. Beller, M., Catalytic Synthesis of Indoles from Alkynes. *Advanced Synthesis & Catalysis* **2008,** *350* (14), 2153-2167.

67. Humphrey, G. R.; Kuethe, J. T., Practical methodologies for the synthesis of indoles. *Chem Rev* **2006,** *106* (7), 2875-911.

68. Penoni, A.; Nicholas, K. M., A novel and direct synthesis of indoles via catalytic reductive annulation of nitroaromatics with alkynes. *Chem Commun (Camb)* **2002,** (5), 484-5.

69. Taber, D. F.; Tirunahari, P. K., Indole synthesis: a review and proposed classification. *Tetrahedron* **2011,** *67* (38), 7195-7210.

70. Platon, M.; Amardeil, R.; Djakovitch, L.; Hierso, J. C., Progress in palladium-based catalytic systems for the sustainable synthesis of annulated heterocycles: a focus on indole backbones. *Chem Soc Rev* **2012,** *41* (10), 3929-68.

71. Li, T. R.; Cheng, B. Y.; Wang, Y. N.; Zhang, M. M.; Lu, L. Q.; Xiao, W. J., A Copper-Catalyzed Decarboxylative Amination/Hydroamination Sequence: Switchable Synthesis of Functionalized Indoles. *Angew Chem Int Ed Engl* **2016,** *55* (40), 12422-6.

72. Wang, S.; Liu, M.; Chen, X.; Wang, H.; Zhai, H., Copper-catalyzed decarboxylative propargylation/hydroamination reactions: access to C3 beta-ketoester-functionalized indoles. *Chem Commun (Camb)* **2018,** *54* (60), 8375-8378.

73. Li, T. R.; Zhang, M. M.; Wang, B. C.; Lu, L. Q.; Xiao, W. J., Synthesis of 3,3'-Biindoles through a Copper-Catalyzed Friedel-Crafts Propargylation/Hydroamination/Aromatization Sequence. *Org Lett* **2018,** *20* (11), 3237-3240.

74. Yuan, W. K. S., S.S.; Zhang, L.B., Wen, L.R.; Li, M., A concise construction of 4-alkynylquinazolines via [4+2] annulation of 4-alkynylbenzoxazinanones with acylhydroxamates under transition-metal-free conditions. *Organic Chemistry Frontiers* **2019,** *6*, 2892-2896.

75. Kuznetsov, D. M.; Kutateladze, A. G., Step-Economical Photoassisted Diversity-Oriented Synthesis: Sustaining Cascade Photoreactions in Oxalyl Anilides to Access

Complex Polyheterocyclic Molecular Architectures. *J Am Chem Soc* **2017,** *139* (46), 16584-16590.

76. Wilkinson, F. M., J.; Olea, A.F., Excited Triplet State Interactions with Molecular Oxygen: Influence of Charge Transfer on the Bimolecular Quenching Rate Constants and the Yields of Singlet Oxygen [O*2(1.DELTA.g)] for Substituted Naphthalenes in Various Solvents. *J. Phys. Chem.* **1994,** *98* (14), 3762-3769.

77. Galloway, W. R.; Isidro-Llobet, A.; Spring, D. R., Diversity-oriented synthesis as a tool for the discovery of novel biologically active small molecules. *Nat Commun* **2010,** *1*, 80.

78. Kumar, N. N. B.; Kutateladze, A. G., Photoassisted Diversity-Oriented Synthesis: Intramolecular Cycloadditions of Photogenerated Azaxylylenes with Oxazole Pendants, and Subsequent Postphotochemical Multicomponent Modifications. *Org Lett* **2016,** *18* (3), 460-463.

79. Schreiber, S. L., Target-oriented and diversity-oriented organic synthesis in drug discovery. *Science* **2000,** *287* (5460), 1964-9.

80. Gelat, F.; Richard, V.; Berger, O.; Montchamp, J. L., Development of a new family of chiral auxiliaries. Org Lett 2015, 17 (8), 1819-21.

5. APPENDIX

5.1 SPECTRA

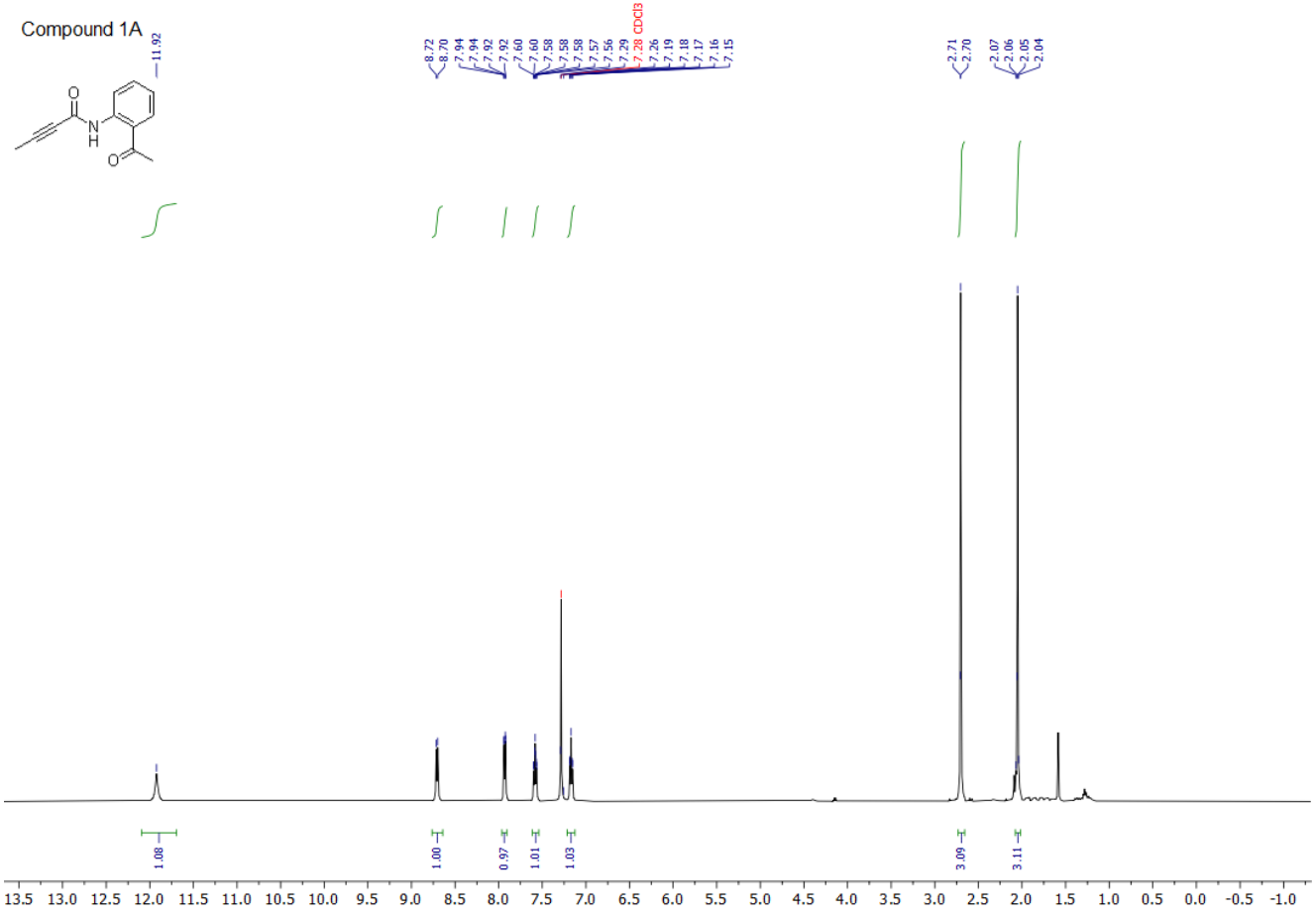

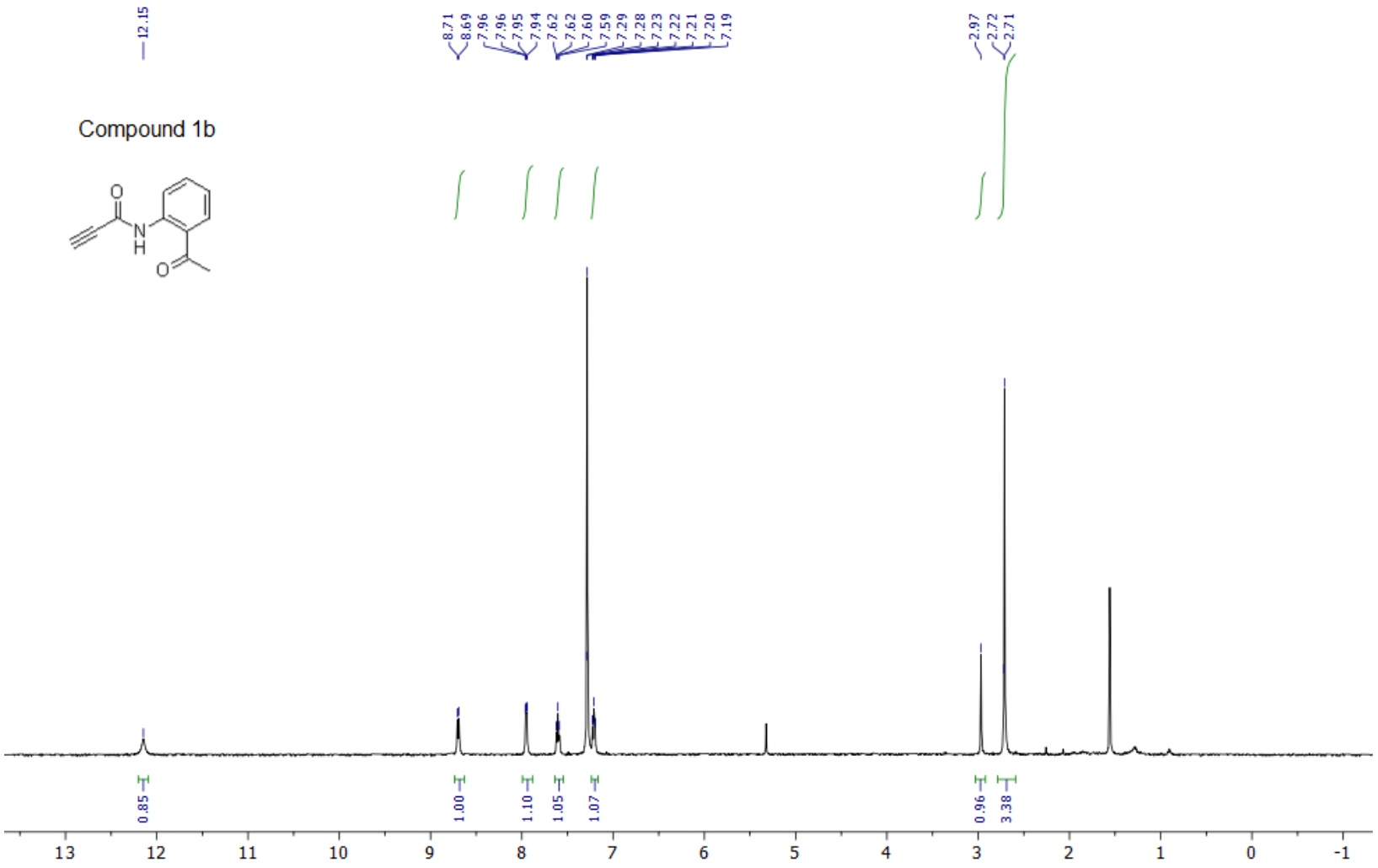
12.15
8.71
8.69
7.96
7.96
7.95
7.94
7.62
7.62
7.60
7.59
7.29
7.28
7.23
7.22
7.21
7.20
7.19
2.97
2.72
2.71
Compound 1b
O
N
H
O
0.85
1.00
1.10
1.05
1.07
0.96
3.38
13
12
11
10
9
8
7
6
5
4
3
2
1
0
-1

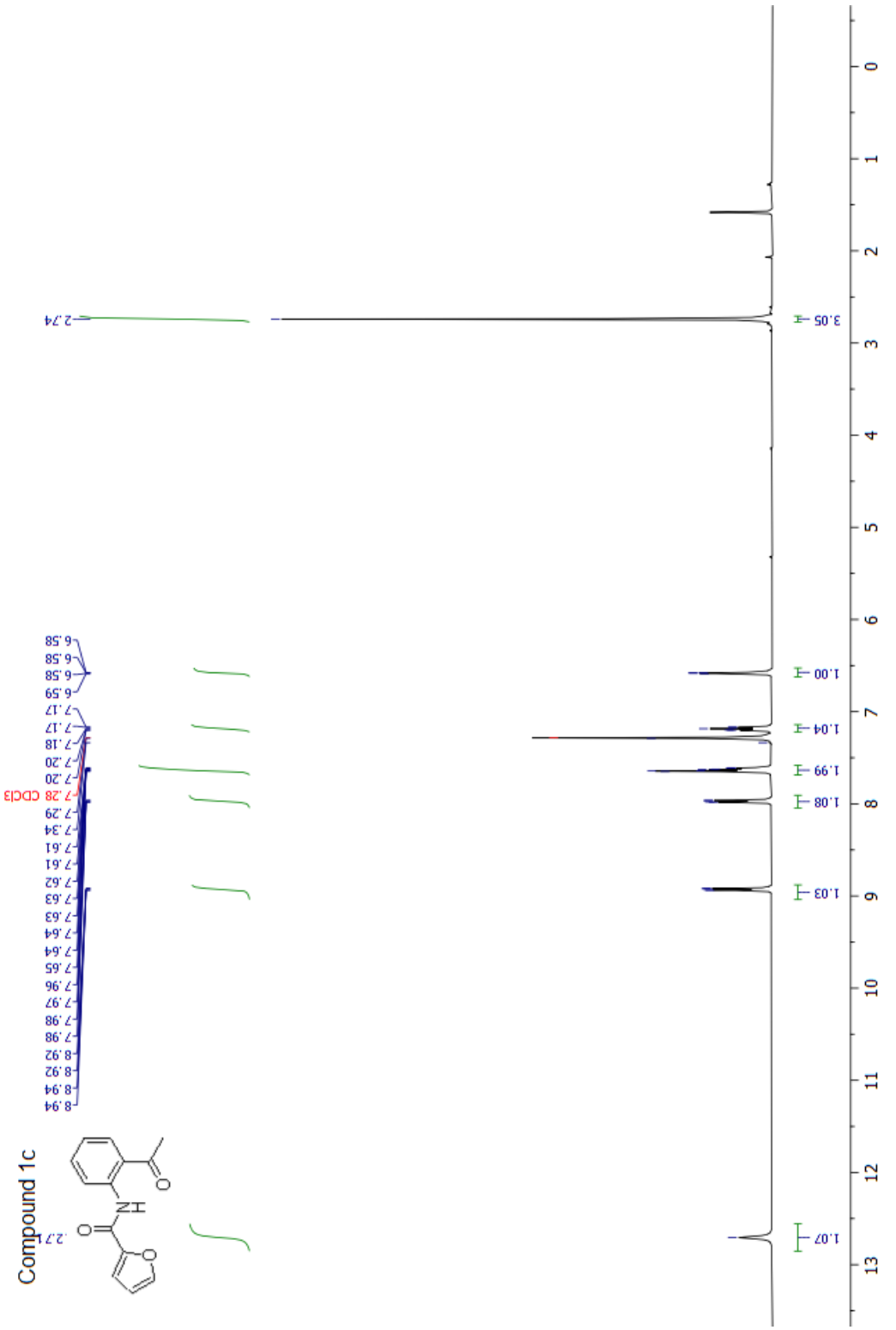
Compound 1c
8.94
8.94
8.92
8.92
7.98
7.97
7.96
7.65
7.64
7.64
7.63
7.63
7.62
7.61
7.61
7.34
7.29
7.28 CDCl3
7.20
7.20
7.18
7.17
7.17
7.17
6.59
6.58
6.58
6.58
2.74
2.71
3.05
1.00
1.04
1.99
1.08
1.03
1.07

Compound 1d

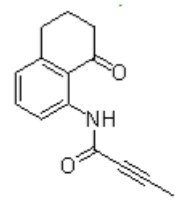
O
NH
O

12.39
8.57
8.55
7.49
7.48
7.47
7.45
6.99
6.97
3.01
3.00
2.99
2.74
2.73
2.72
2.14
2.13
2.12
2.11
2.09
2.04
2.03
0.90
0.94
0.99
1.00
1.98
1.99
2.02
2.99
13
12
11
10
9
8
7
6
5
4
3
2
1
0
-1

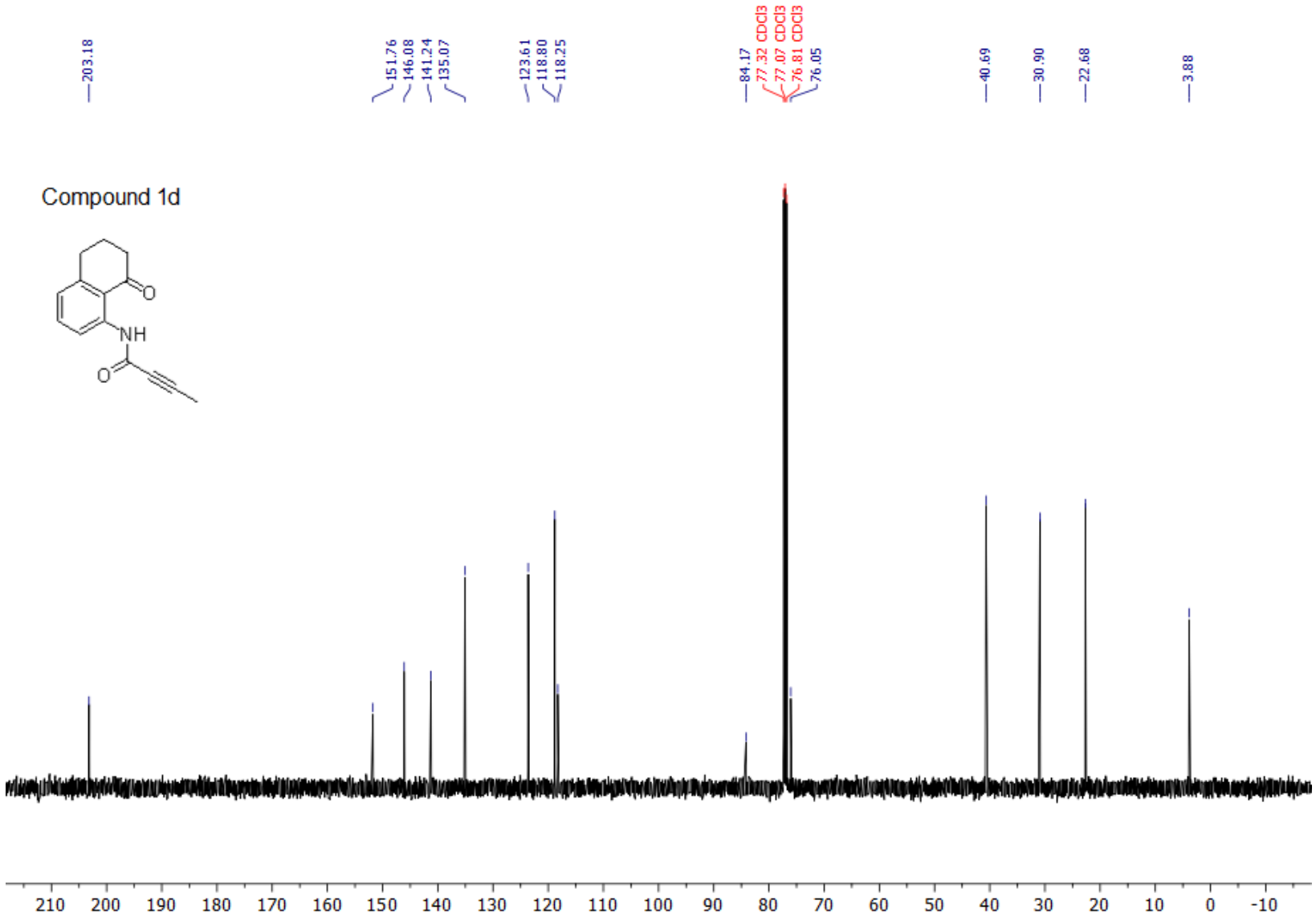
203.18
151.76
146.08
141.24
135.07
123.61
118.80
118.25
84.17
77.32 CDCl3
77.07 CDCl3
76.81 CDCl3
76.05
40.69
30.90
22.68
3.88
Compound 1d
O
NH
O
210 200 190 180 170 160 150 140 130 120 110 100 90 80 70 60 50 40 30 20 10 0 -10

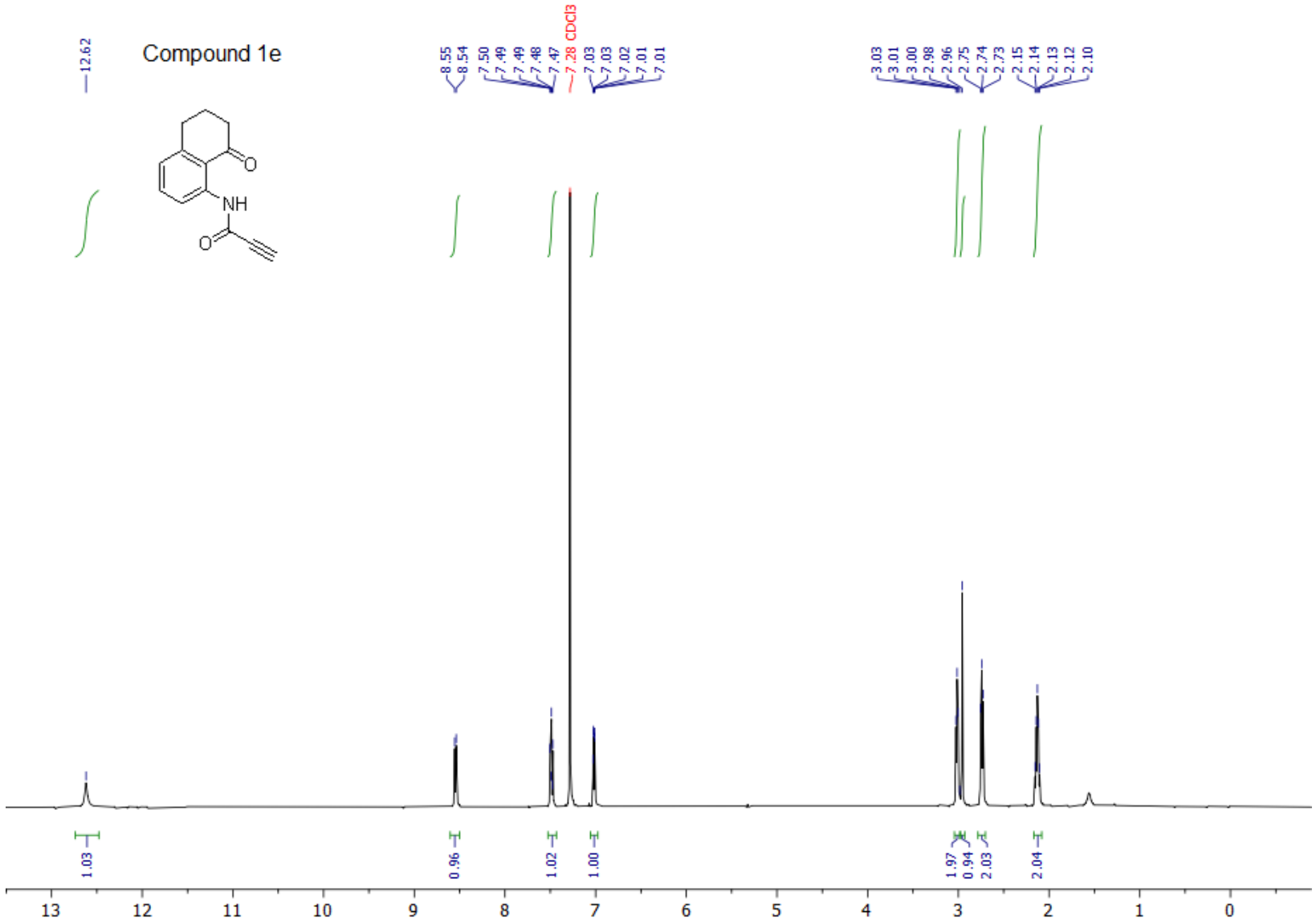
Compound 1e
12.62
8.55
8.54
7.50
7.49
7.49
7.48
7.47
7.28 CDCl3
7.03
7.03
7.02
7.01
7.01
3.03
3.01
3.00
2.98
2.96
2.75
2.74
2.73
2.15
2.14
2.13
2.12
2.10
NH
O
O
1.03
0.96
1.02
1.00
1.97
0.94
2.03
2.04
13
12
11
10
9
8
7
6
5
4
3
2
1
0

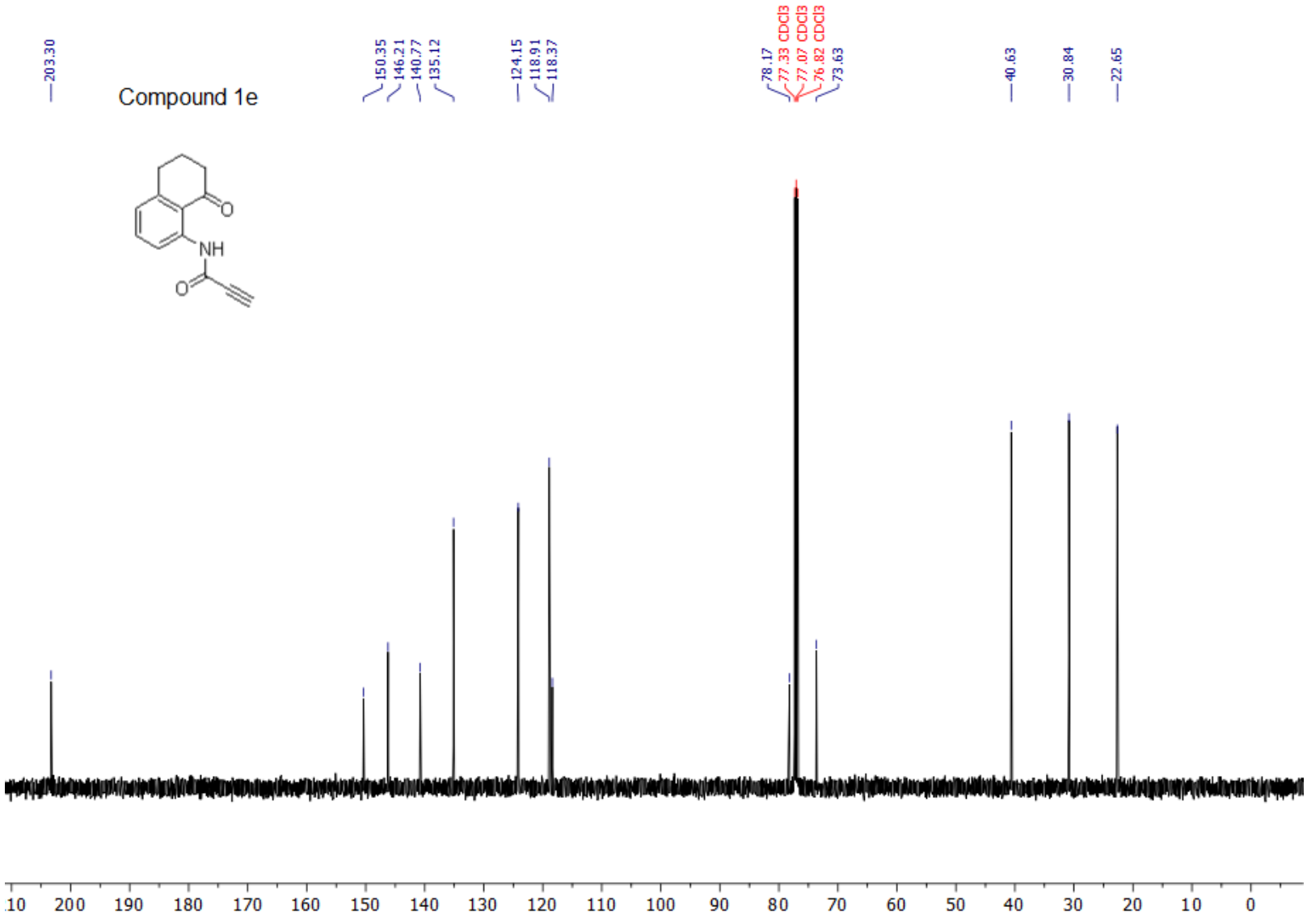
Compound 1e
203.30
150.35
146.21
140.77
135.12
124.15
118.91
118.37
78.17
77.33 CDCl3
77.07 CDCl3
76.82 CDCl3
73.63
40.63
30.84
22.65
O
NH
O
210 200 190 180 170 160 150 140 130 120 110 100 90 80 70 60 50 40 30 20 10 0

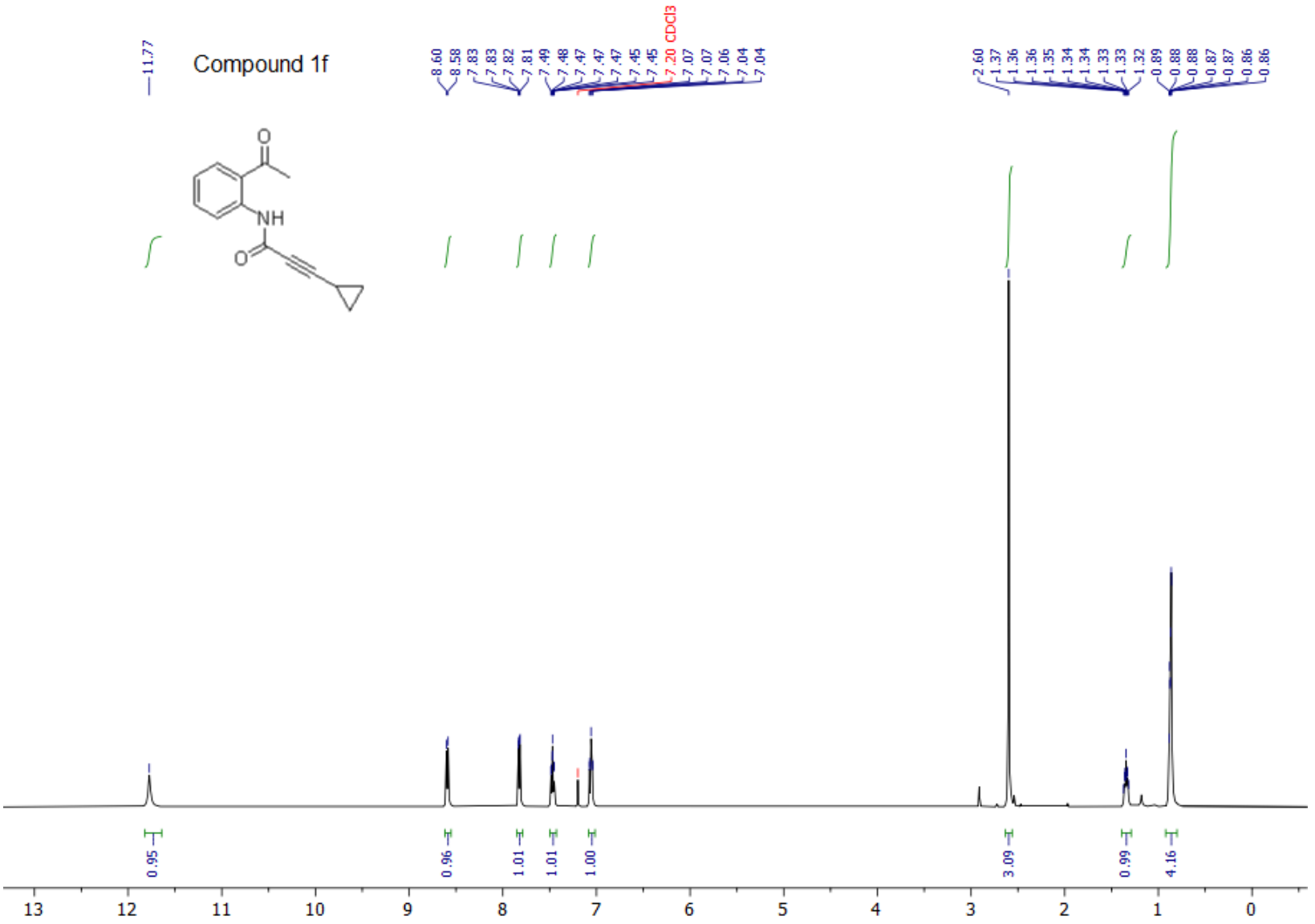
Compound 1f
11.77
8.60
8.58
7.83
7.83
7.82
7.81
7.49
7.48
7.47
7.47
7.47
7.45
7.45
7.20 CDCl3
7.07
7.07
7.06
7.04
7.04
2.60
1.37
1.36
1.36
1.35
1.34
1.34
1.33
1.33
1.32
0.89
0.88
0.88
0.87
0.87
0.86
0.86
NH
O
O
0.95
0.96
1.01
1.01
1.00
3.09
0.99
4.16
13
12
11
10
9
8
7
6
5
4
3
2
1
0

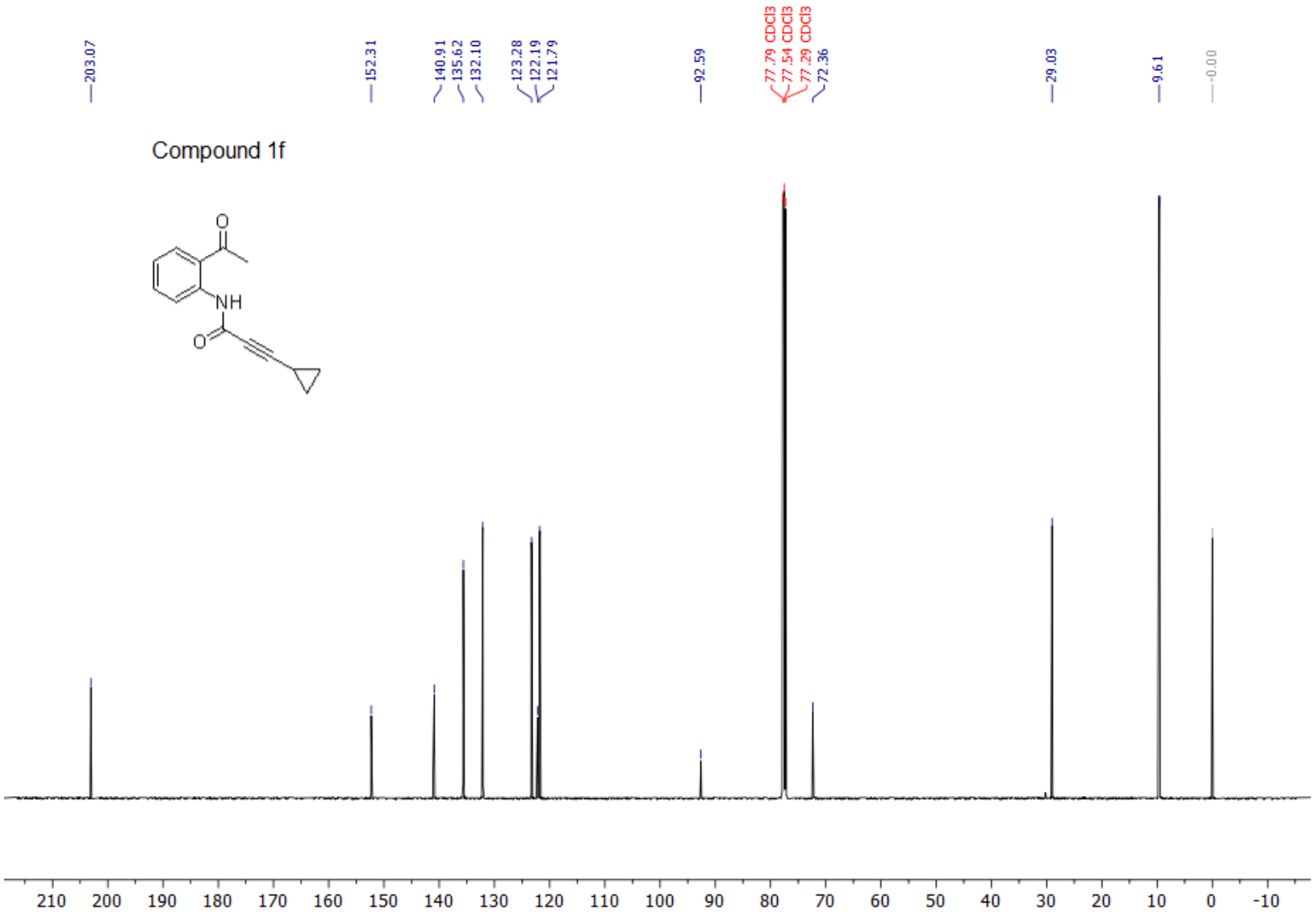
203.07
152.31
140.91
135.62
132.10
123.28
122.19
121.79
92.59
77.79 CDCl3
77.54 CDCl3
77.29 CDCl3
72.36
29.03
9.61
-0.00
Compound 1f
O
NH
O
210
200
190
180
170
160
150
140
130
120
110
100
90
80
70
60
50
40
30
20
10
0
-10

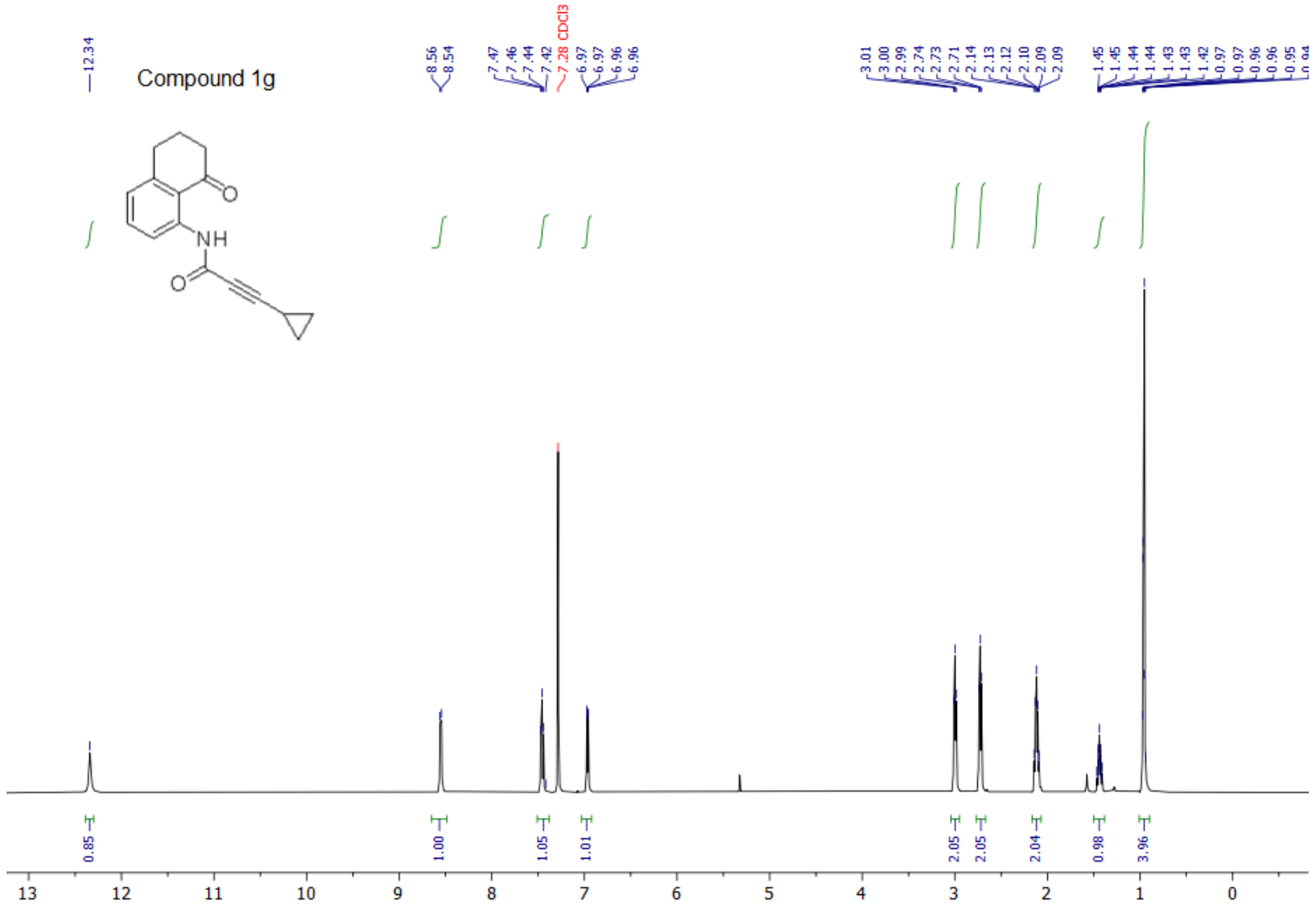
Compound 1g
12.34
8.56
8.54
7.47
7.46
7.44
7.42
7.28 CDCl3
6.97
6.96
6.96
3.01
3.00
2.99
2.74
2.73
2.71
2.14
2.13
2.12
2.10
2.09
2.09
1.45
1.45
1.44
1.44
1.43
1.43
1.42
0.97
0.97
0.96
0.96
0.95
NH
O
O
0.85
1.00
1.05
1.01
2.05
2.05
2.04
0.98
3.96
13
12
11
10
9
8
7
6
5
4
3
2
1
0

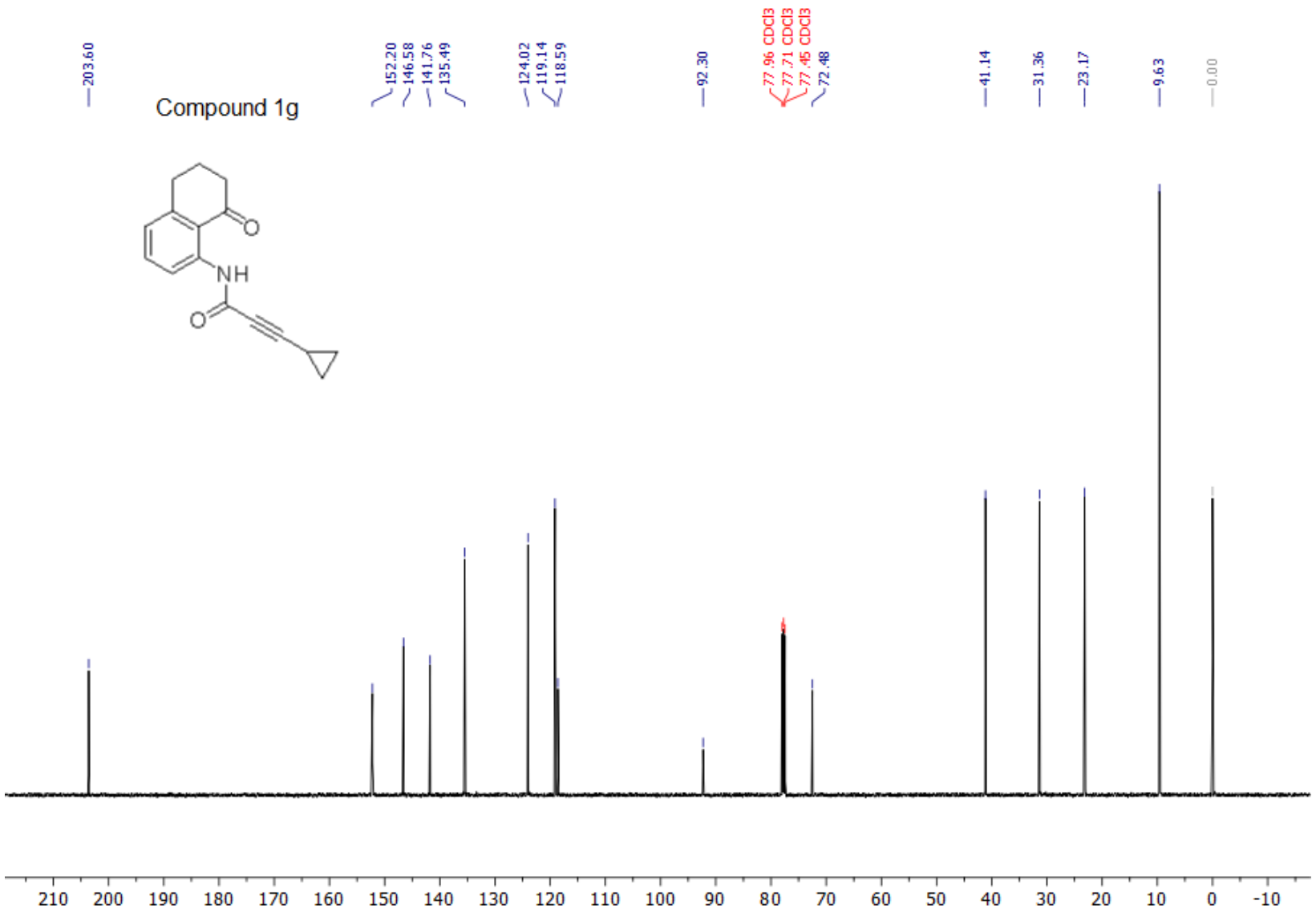
203.60
152.20
146.58
141.76
135.49
124.02
119.14
118.59
92.30
77.96 CDCl3
77.71 CDCl3
77.45 CDCl3
72.48
41.14
31.36
23.17
9.63
0.00
Compound 1g
O
NH
O
210 200 190 180 170 160 150 140 130 120 110 100 90 80 70 60 50 40 30 20 10 0 -10

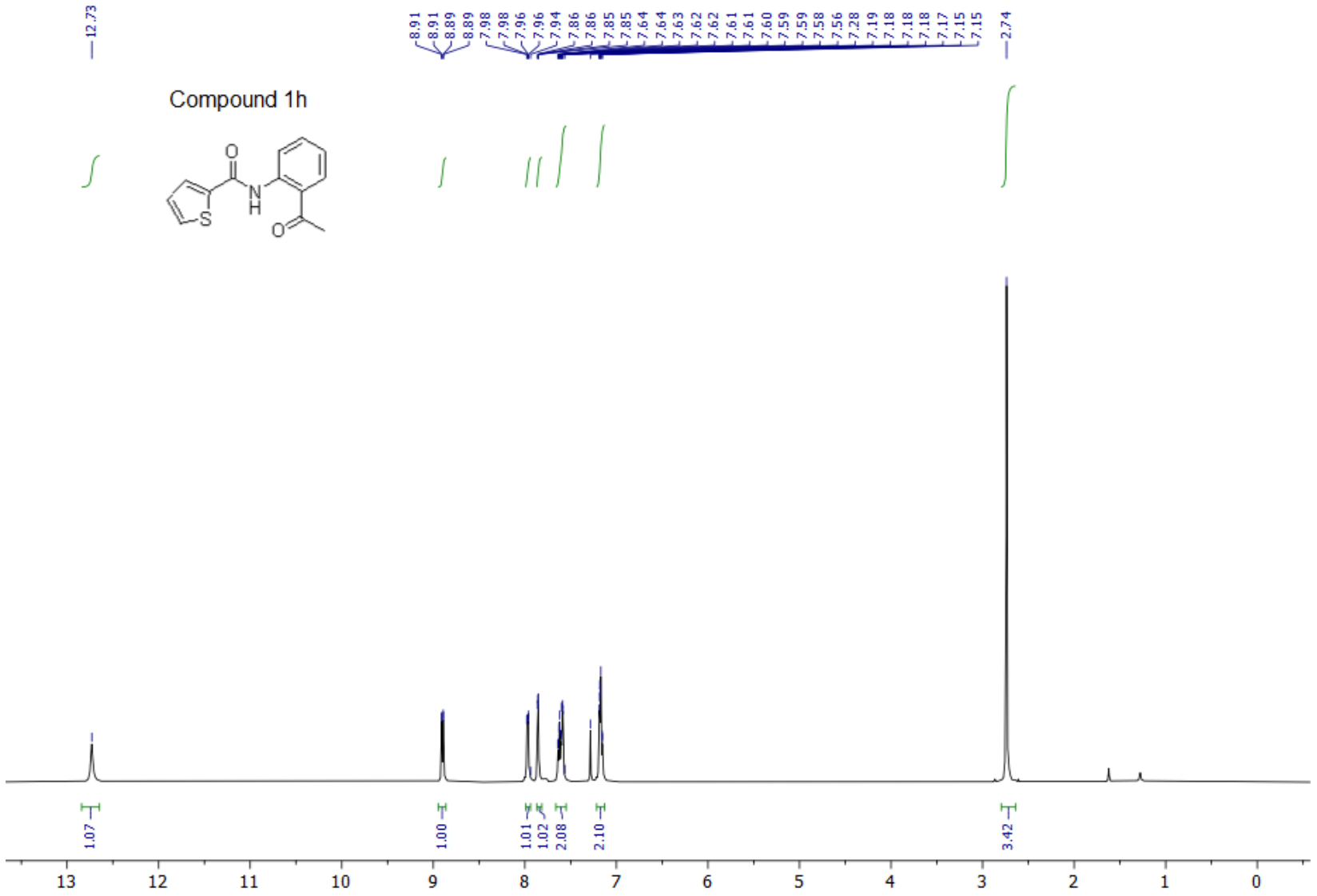
12.73
8.91
8.91
8.89
8.89
7.98
7.98
7.96
7.96
7.94
7.86
7.86
7.85
7.85
7.64
7.64
7.63
7.62
7.62
7.61
7.61
7.60
7.59
7.59
7.58
7.56
7.28
7.19
7.18
7.18
7.18
7.17
7.15
7.15
2.74
Compound 1h
O
N
H
S
O
1.07
1.00
1.01
1.02
2.08
2.10
3.42
13
12
11
10
9
8
7
6
5
4
3
2
1
0

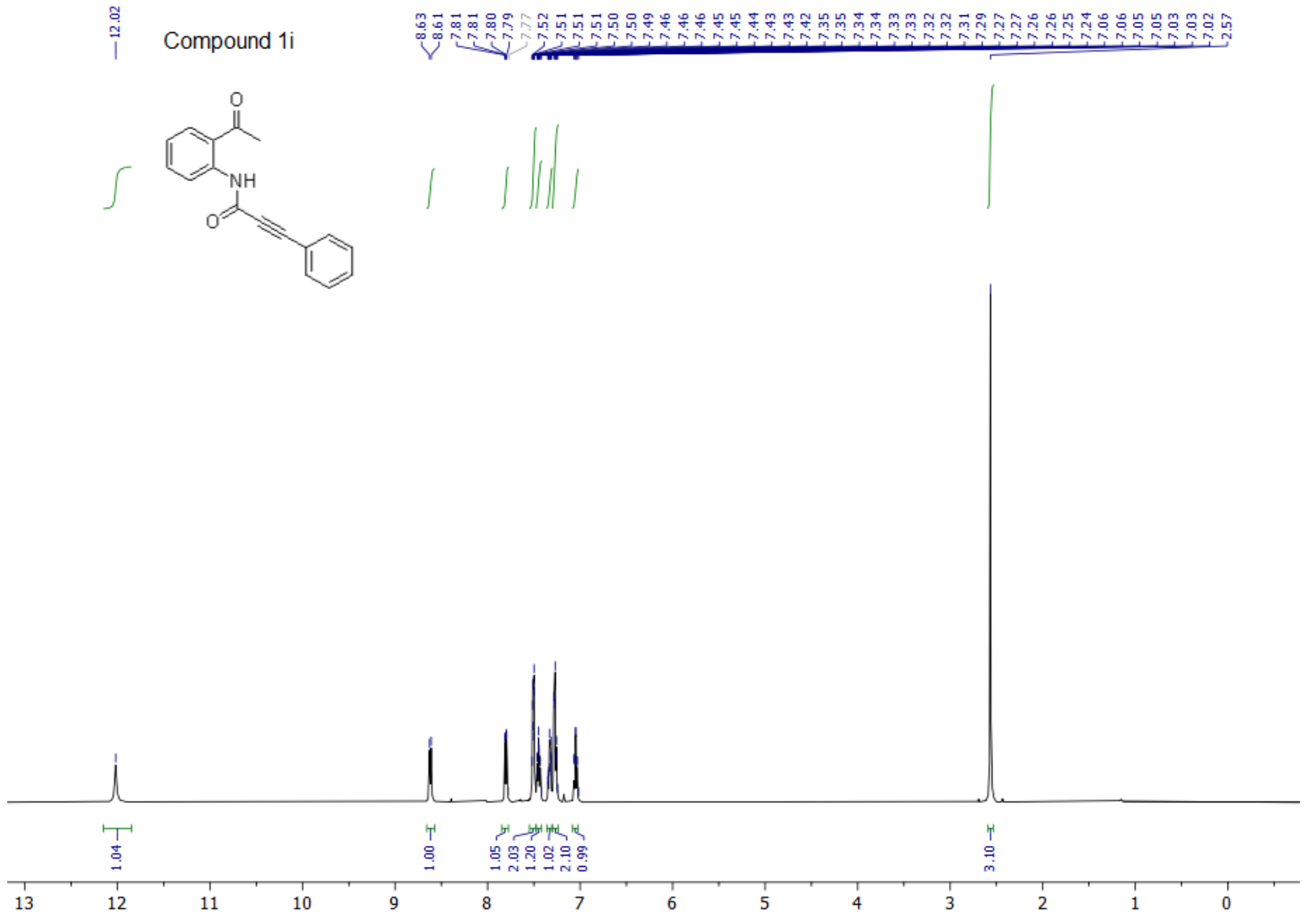
Compound 1i
12.02
8.63
8.61
7.81
7.81
7.80
7.79
7.77
7.52
7.51
7.51
7.51
7.50
7.50
7.49
7.46
7.46
7.45
7.45
7.44
7.43
7.43
7.42
7.35
7.35
7.34
7.34
7.33
7.33
7.32
7.32
7.31
7.29
7.27
7.27
7.26
7.26
7.25
7.24
7.06
7.06
7.05
7.05
7.03
7.03
7.02
2.57
O
NH
O
1.04
1.00
1.05
2.03
1.20
1.02
2.10
0.99
3.10
13
12
11
10
9
8
7
6
5
4
3
2
1
0

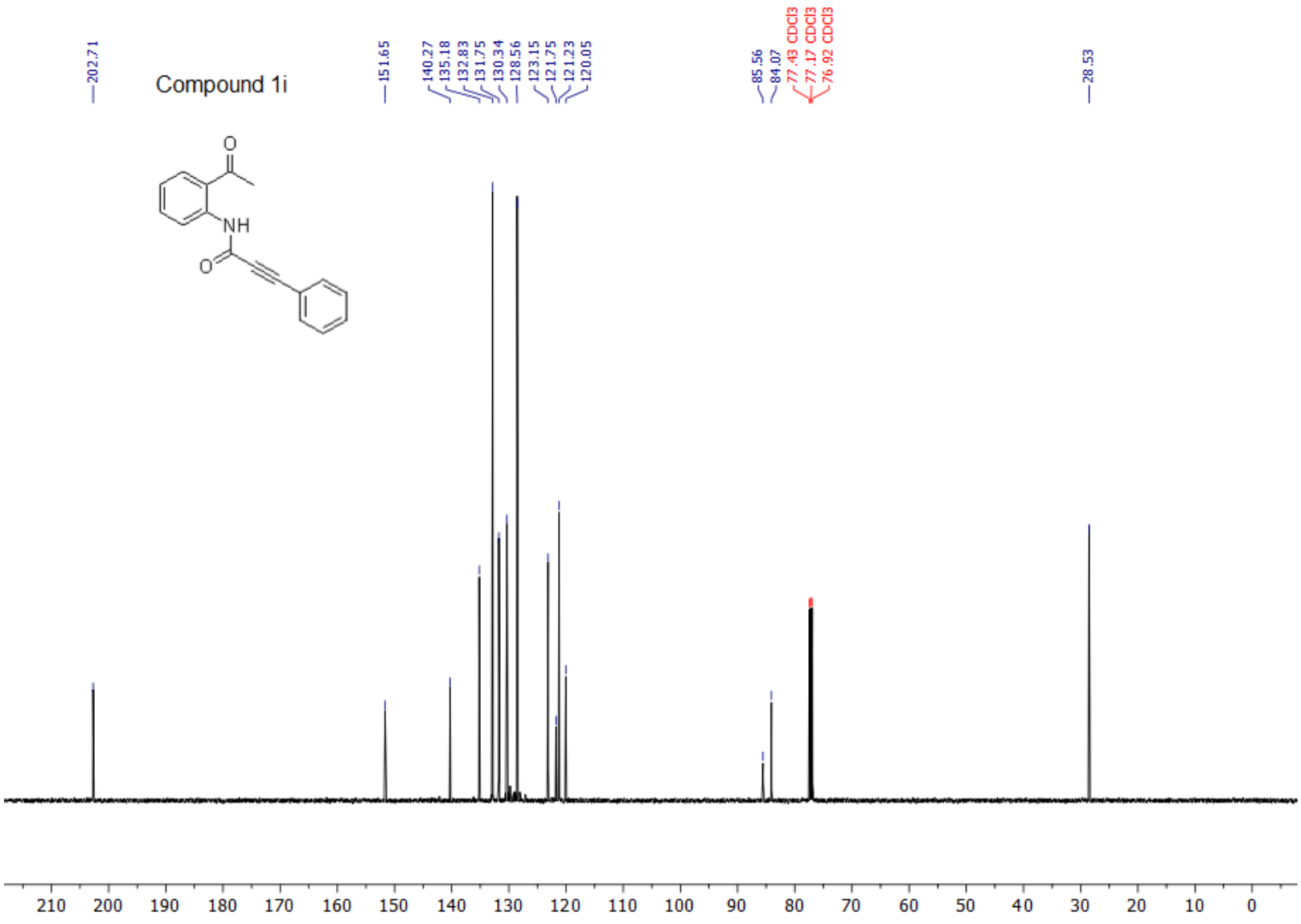
Compound 1i
O
NH
O
202.71
151.65
140.27
135.18
132.83
131.75
130.34
128.56
123.15
121.75
121.23
120.05
85.56
84.07
77.43 CDCl3
77.17 CDCl3
76.92 CDCl3
28.53
210 200 190 180 170 160 150 140 130 120 110 100 90 80 70 60 50 40 30 20 10 0

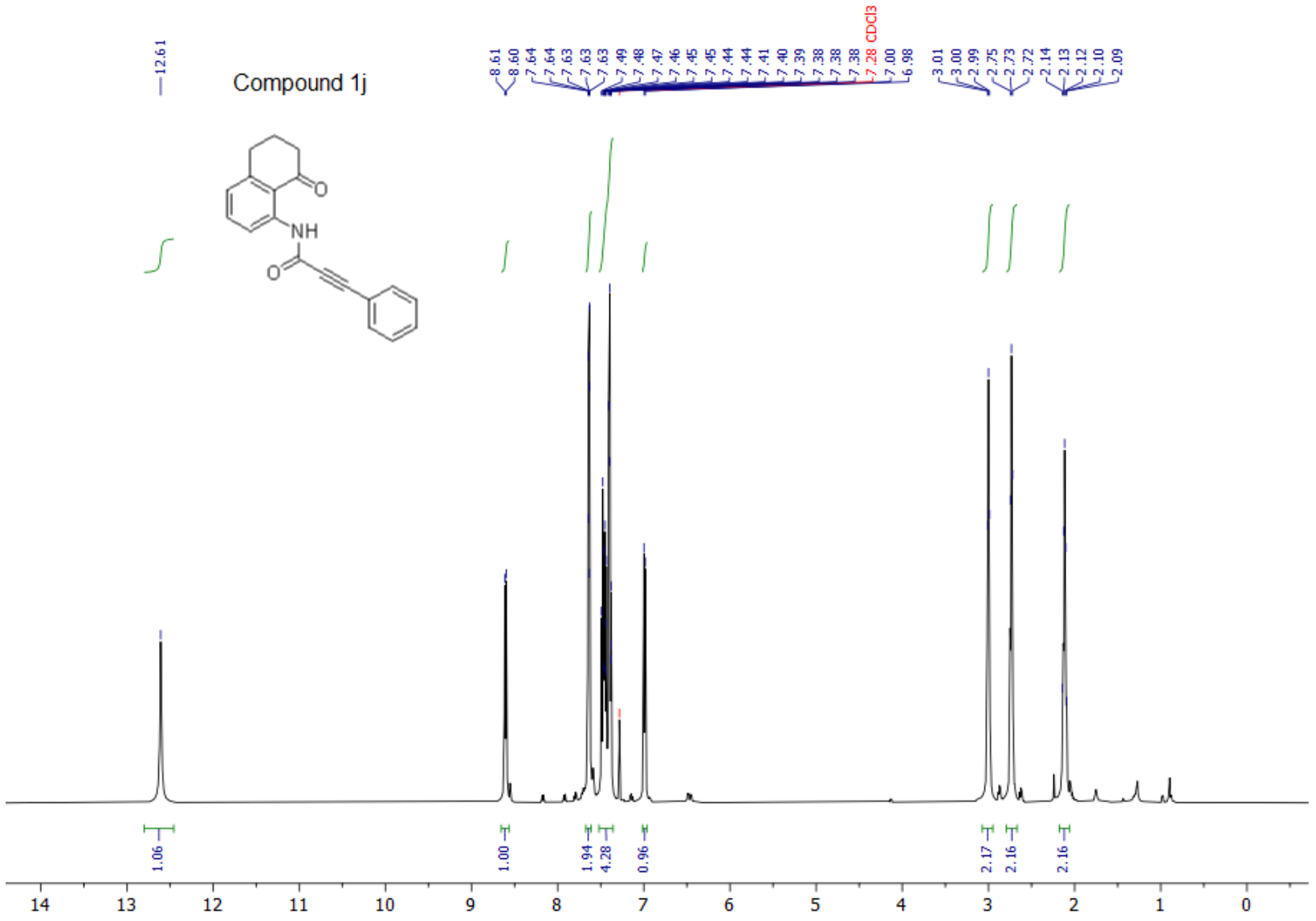
Compound 1j
12.61
8.61
8.60
7.64
7.64
7.63
7.63
7.63
7.49
7.48
7.47
7.46
7.45
7.45
7.44
7.44
7.41
7.40
7.39
7.38
7.38
7.38
7.28 CDCl3
7.00
6.98
3.01
3.00
2.99
2.75
2.73
2.72
2.14
2.13
2.12
2.10
2.09
NH
O
O
1.06
1.00
1.94
4.28
0.96
2.17
2.16
2.16
14
13
12
11
10
9
8
7
6
5
4
3
2
1
0

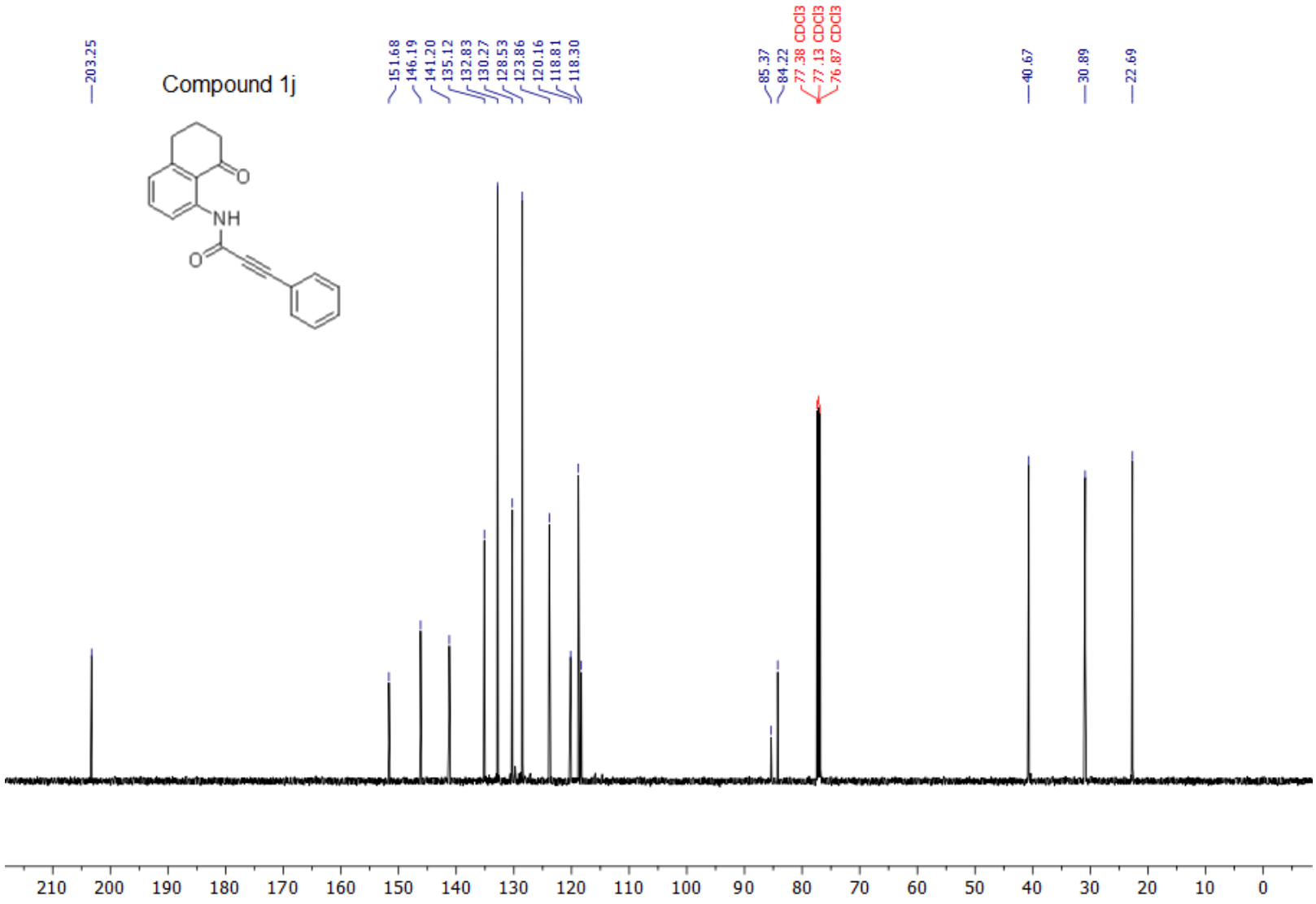
Compound 1j
203.25
151.68
146.19
141.20
135.12
132.83
130.27
128.53
123.86
120.16
118.81
118.30
85.37
84.22
77.38 CDCl3
77.13 CDCl3
76.87 CDCl3
40.67
30.89
22.69
NH
O
O
210
200
190
180
170
160
150
140
130
120
110
100
90
80
70
60
50
40
30
20
10
0

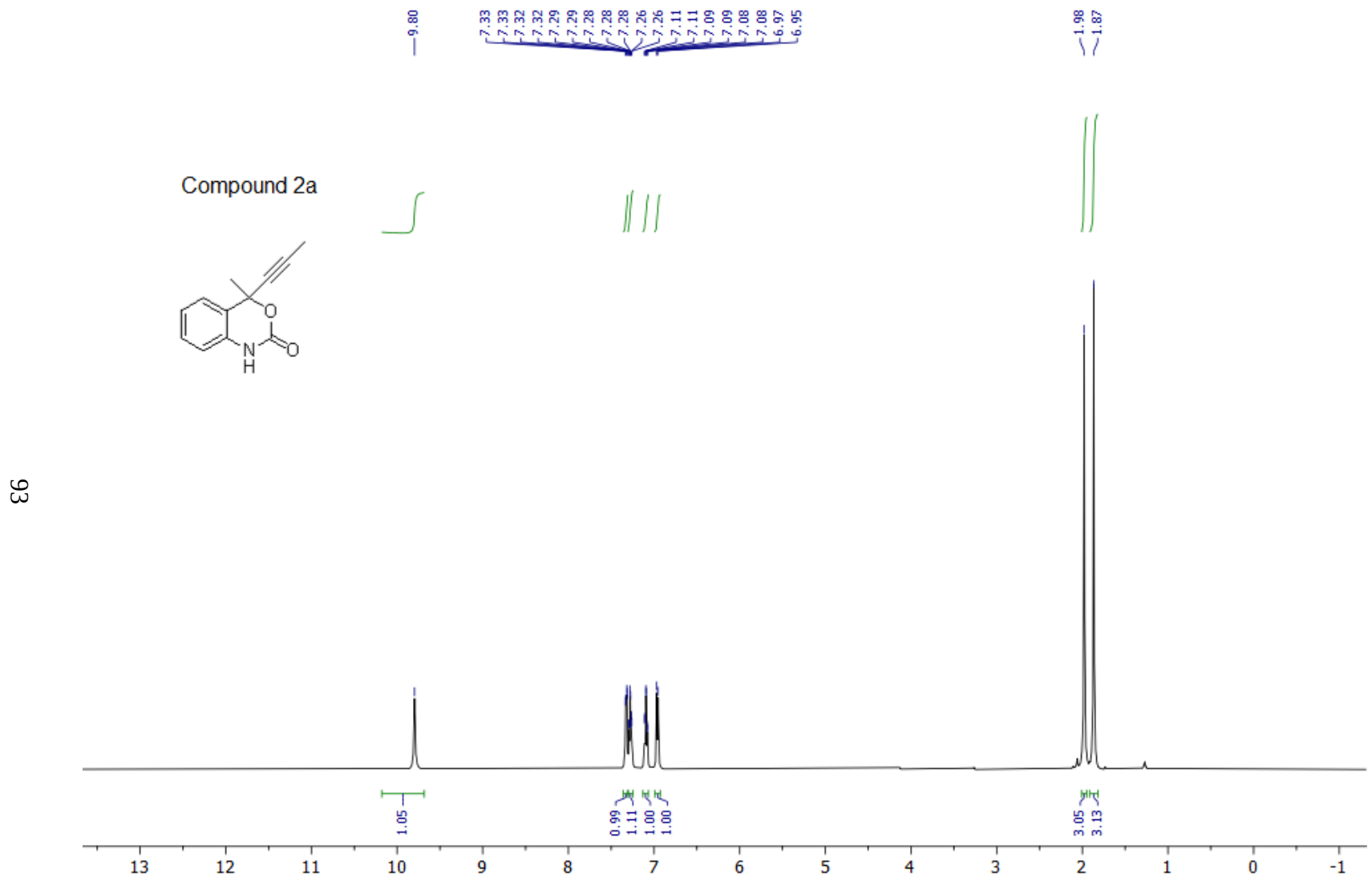
Compound 2a
9.80
7.33
7.33
7.32
7.32
7.29
7.28
7.28
7.28
7.26
7.26
7.11
7.11
7.09
7.09
7.08
7.08
6.97
6.95
1.98
1.87
1.05
0.99
1.11
1.00
1.00
3.05
3.13
13
12
11
10
9
8
7
6
5
4
3
2
1
0
-1

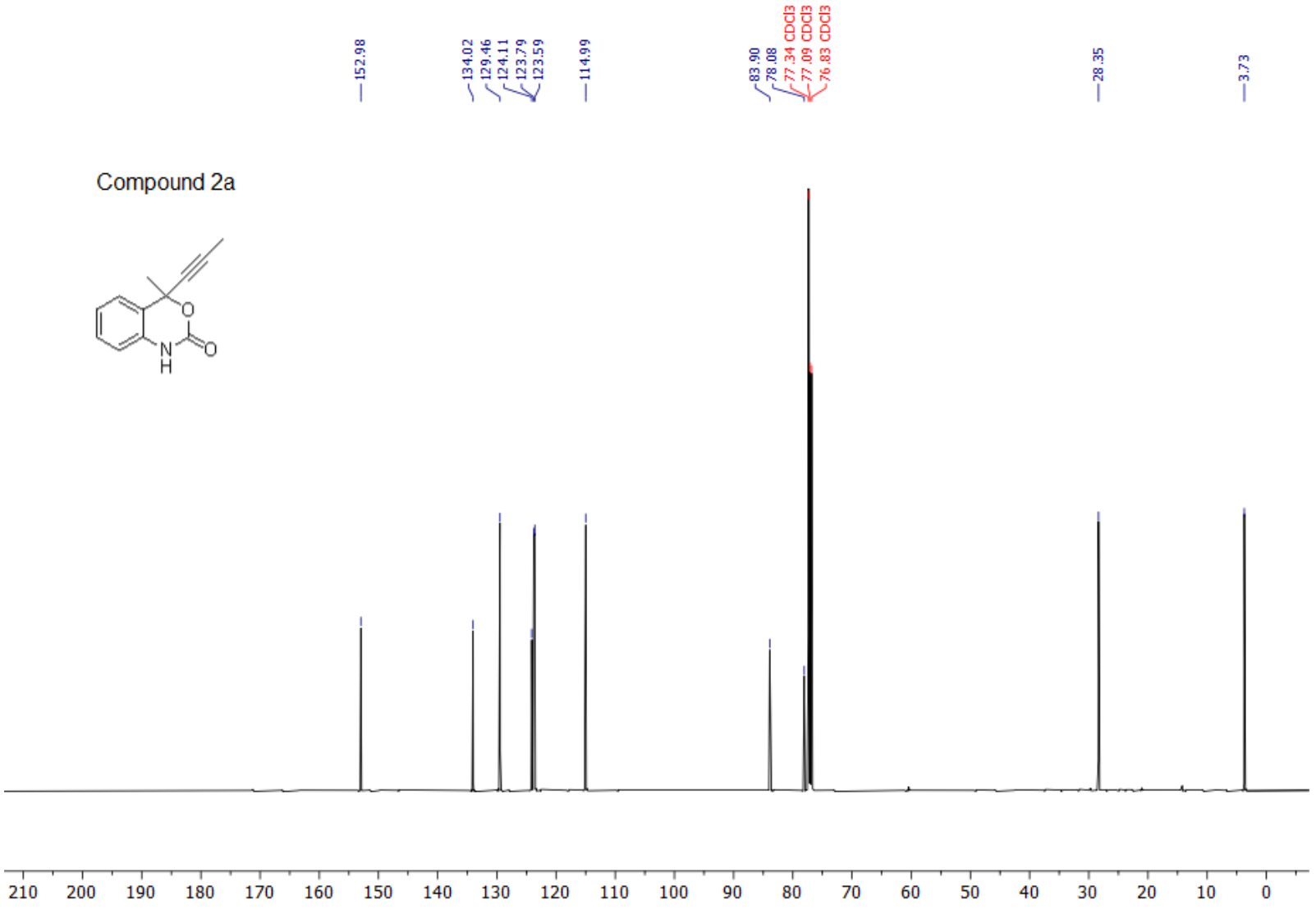
152.98
134.02
129.46
124.11
123.79
123.59
114.99
83.90
78.08
77.34 CDCl3
77.09 CDCl3
76.83 CDCl3
28.35
3.73
Compound 2a
O
N
H
O
210
200
190
180
170
160
150
140
130
120
110
100
90
80
70
60
50
40
30
20
10
0

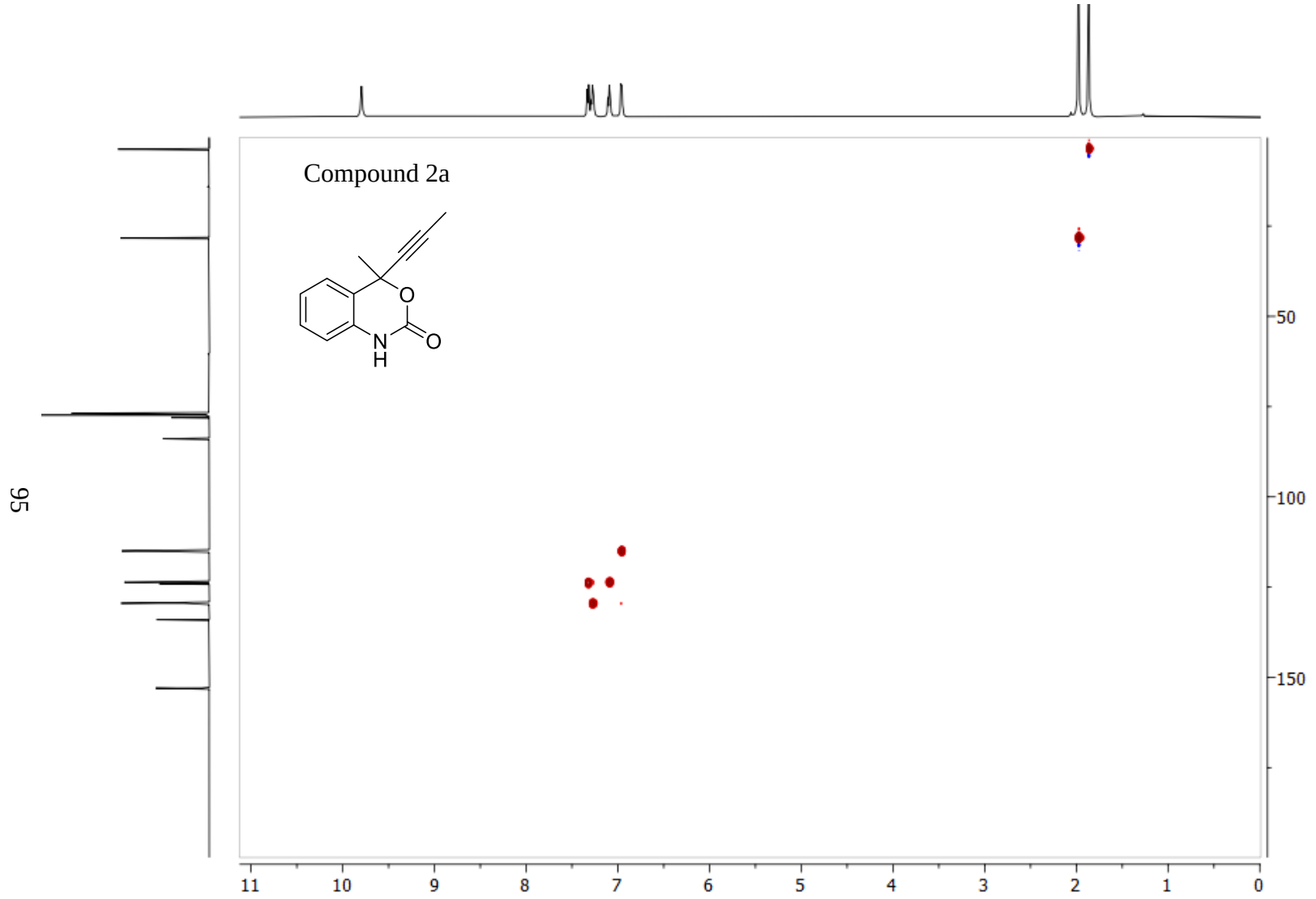
Compound 2a
O
N
H
O
50
100
150
11
10
9
8
7
6
5
4
3
2
1
0

Compound 2b

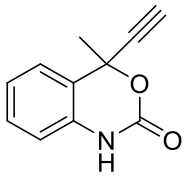
O
N
H
O

9.49
7.37
7.35
7.34
7.33
7.32
7.32
7.31
7.30
7.28 CDCl3
7.14
7.13
7.11
6.97
6.95
2.77
2.76
2.04
1.08
2.06
1.01
1.00
0.97
3.23
12
11
10
9
8
7
6
5
4
3
2
1
0

Compound 2b

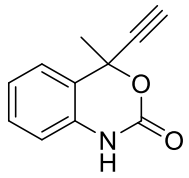
O
N
H
O

152.24
133.98
129.87
123.88
123.84
123.07
114.99
82.00
77.29 CDCl3
77.03 CDCl3
76.78 CDCl3
76.64
75.27
28.05
210
200
190
180
170
160
150
140
130
120
110
100
90
80
70
60
50
40
30
20
10
0

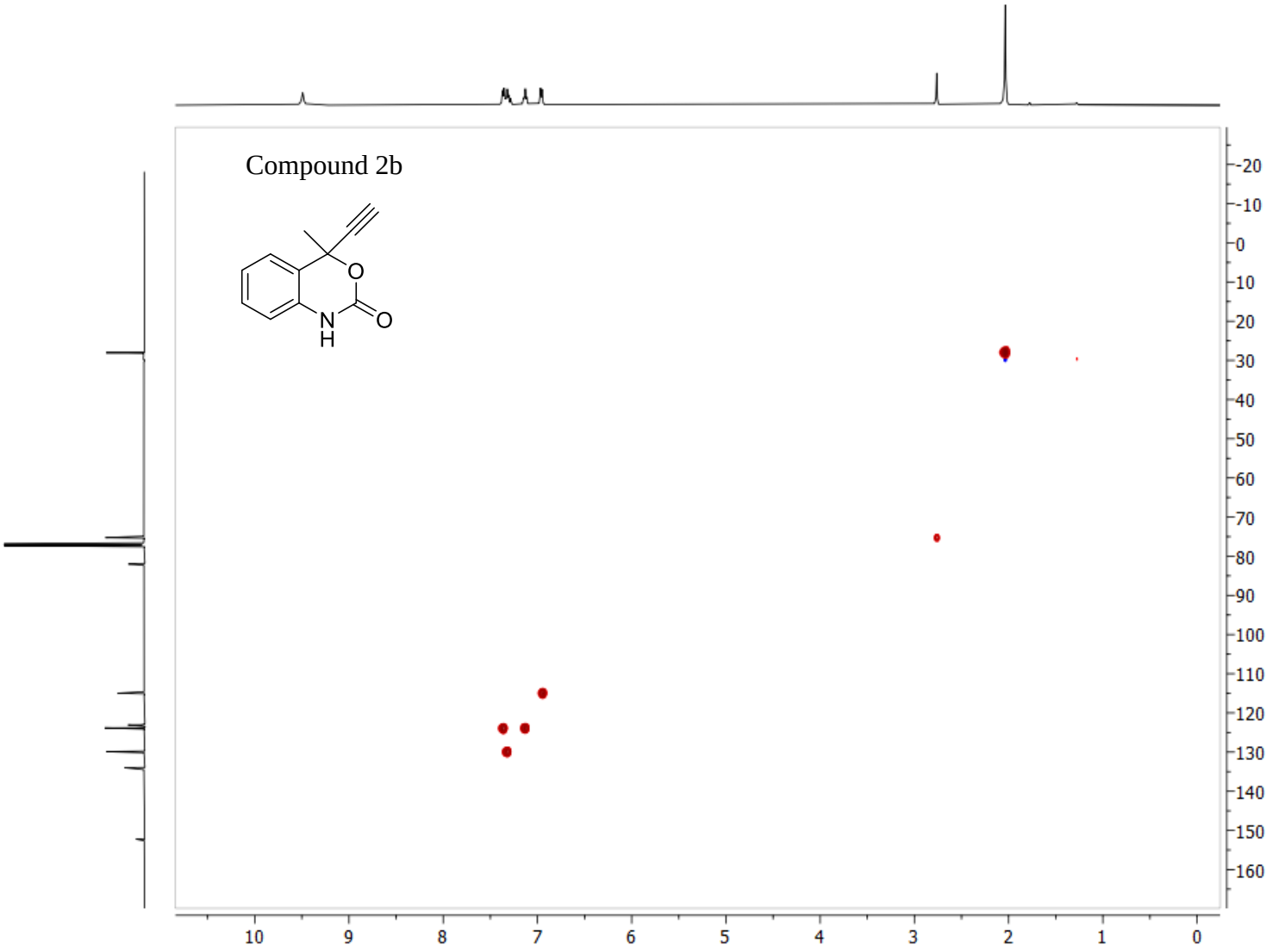
Compound 2b
O
N
H
O
10
9
8
7
6
5
4
3
2
1
0
-20
-10
0
10
20
30
40
50
60
70
80
90
100
110
120
130
140
150
160

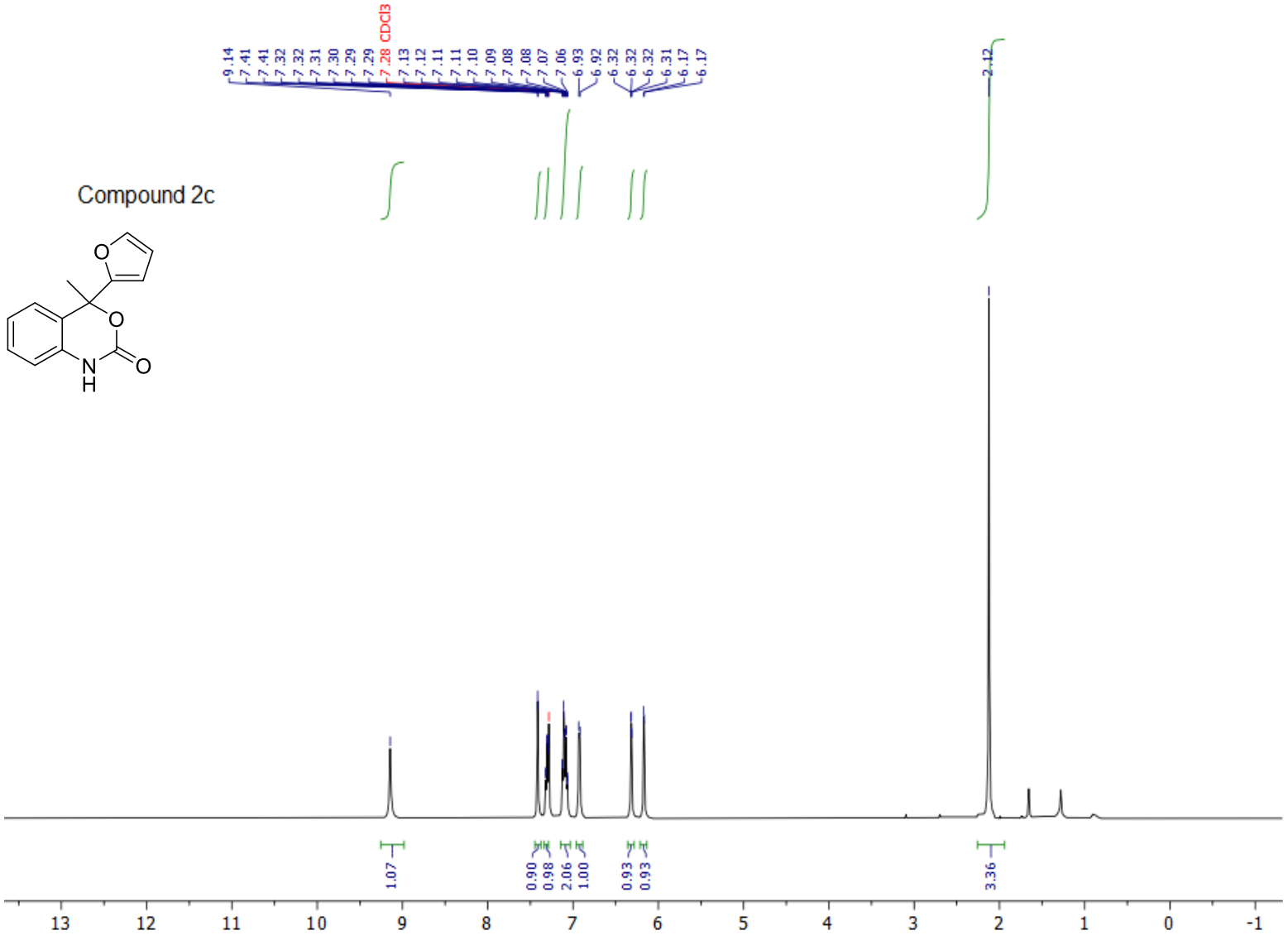
9.14
7.41
7.41
7.32
7.32
7.31
7.30
7.29
7.29
7.28 CDCl3
7.13
7.12
7.11
7.11
7.10
7.09
7.08
7.08
7.07
7.06
6.93
6.92
6.32
6.32
6.32
6.31
6.17
6.17
2.12
Compound 2c
O
O
N
H
O
1.07
0.90
0.98
2.06
1.00
0.93
0.93
3.36
13
12
11
10
9
8
7
6
5
4
3
2
1
0
-1

Compound 2c

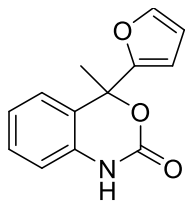
O
O
N
H
O

153.76
152.33
143.42
134.62
129.61
124.80
123.46
122.93
114.73
110.21
108.43
80.95
77.27 CDCl3
76.77 CDCl3
25.29
100
210 200 190 180 170 160 150 140 130 120 110 100 90 80 70 60 50 40 30 20 10 0 -10

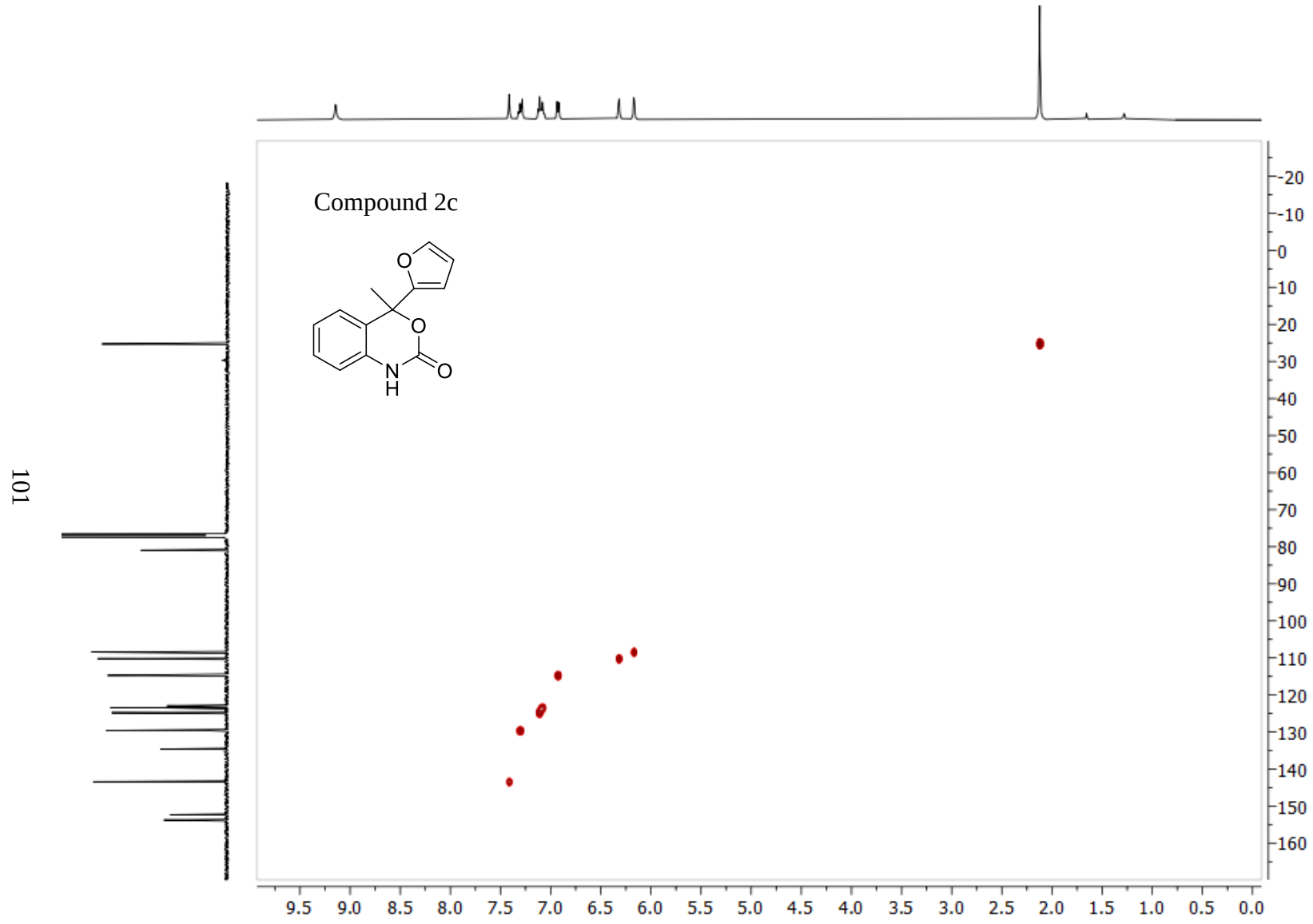
Compound 2c
O
O
N
H
O
-20
-10
0
10
20
30
40
50
60
70
80
90
100
110
120
130
140
150
160
9.5
9.0
8.5
8.0
7.5
7.0
6.5
6.0
5.5
5.0
4.5
4.0
3.5
3.0
2.5
2.0
1.5
1.0
0.5
0.0

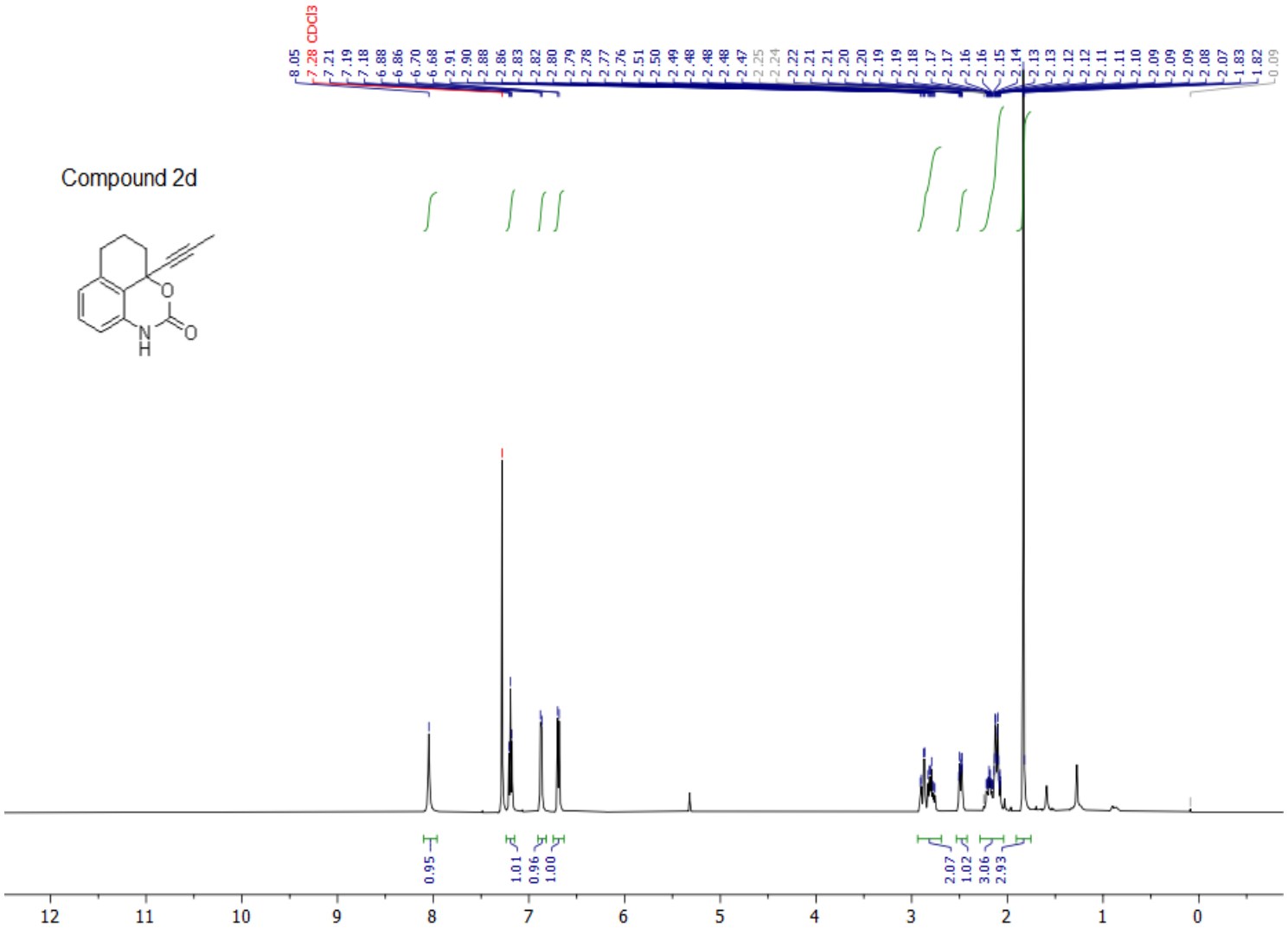
Compound 2d
8.05
7.28 CDCl3
7.21
7.19
7.18
6.88
6.86
6.70
6.68
2.91
2.90
2.88
2.86
2.83
2.82
2.80
2.79
2.78
2.77
2.76
2.51
2.50
2.49
2.48
2.48
2.48
2.47
2.25
2.24
2.22
2.21
2.21
2.20
2.20
2.19
2.19
2.18
2.17
2.17
2.16
2.16
2.15
2.14
2.13
2.13
2.12
2.12
2.11
2.11
2.10
2.09
2.09
2.09
2.08
2.07
1.83
1.82
0.09
0.95
1.01
0.96
1.00
2.07
1.02
3.06
2.93
12
11
10
9
8
7
6
5
4
3
2
1
0

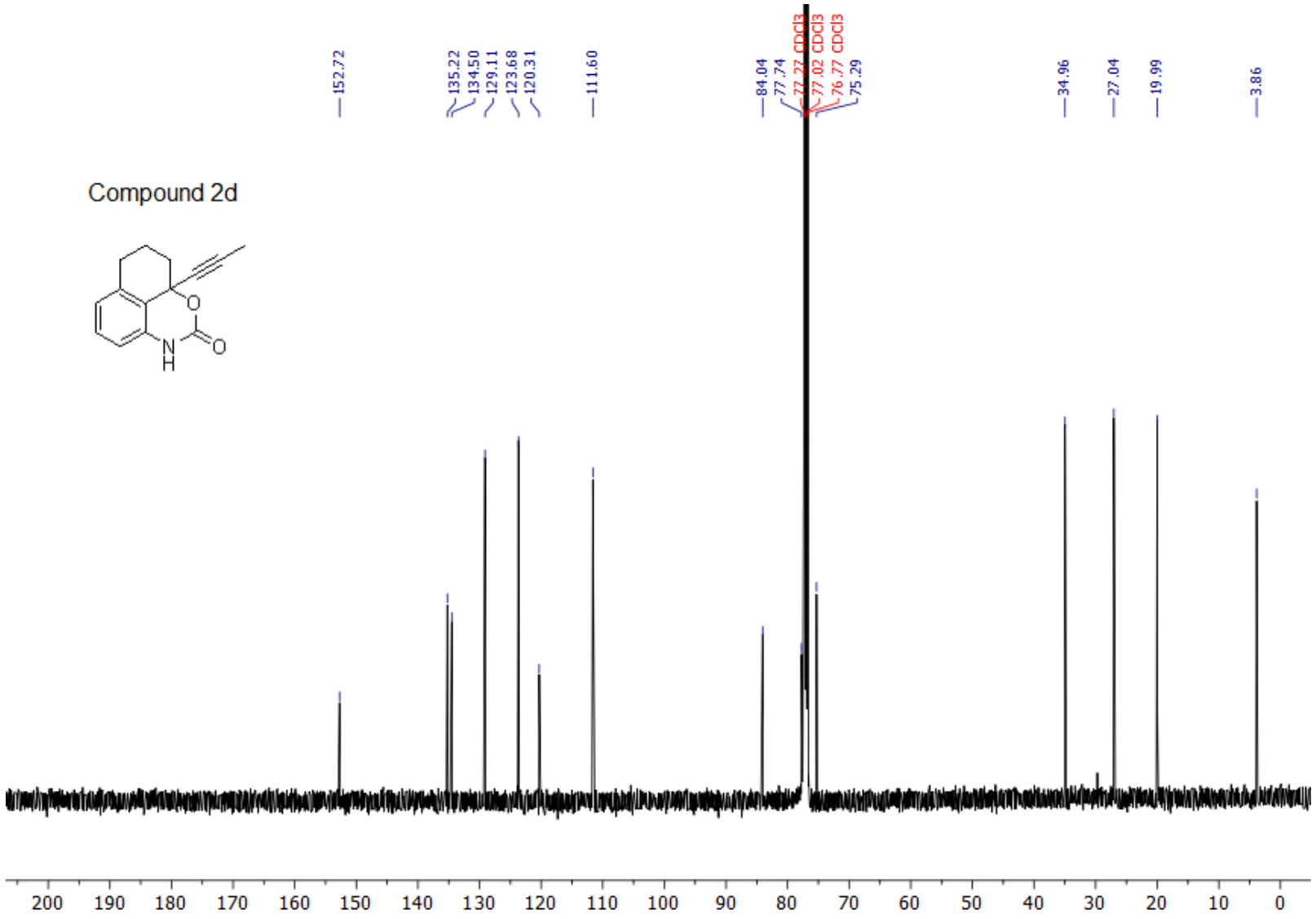
Compound 2d
152.72
135.22
134.50
129.11
123.68
120.31
111.60
84.04
77.74
77.27 CDCl3
77.02 CDCl3
76.77 CDCl3
75.29
34.96
27.04
19.99
3.86
200
190
180
170
160
150
140
130
120
110
100
90
80
70
60
50
40
30
20
10
0

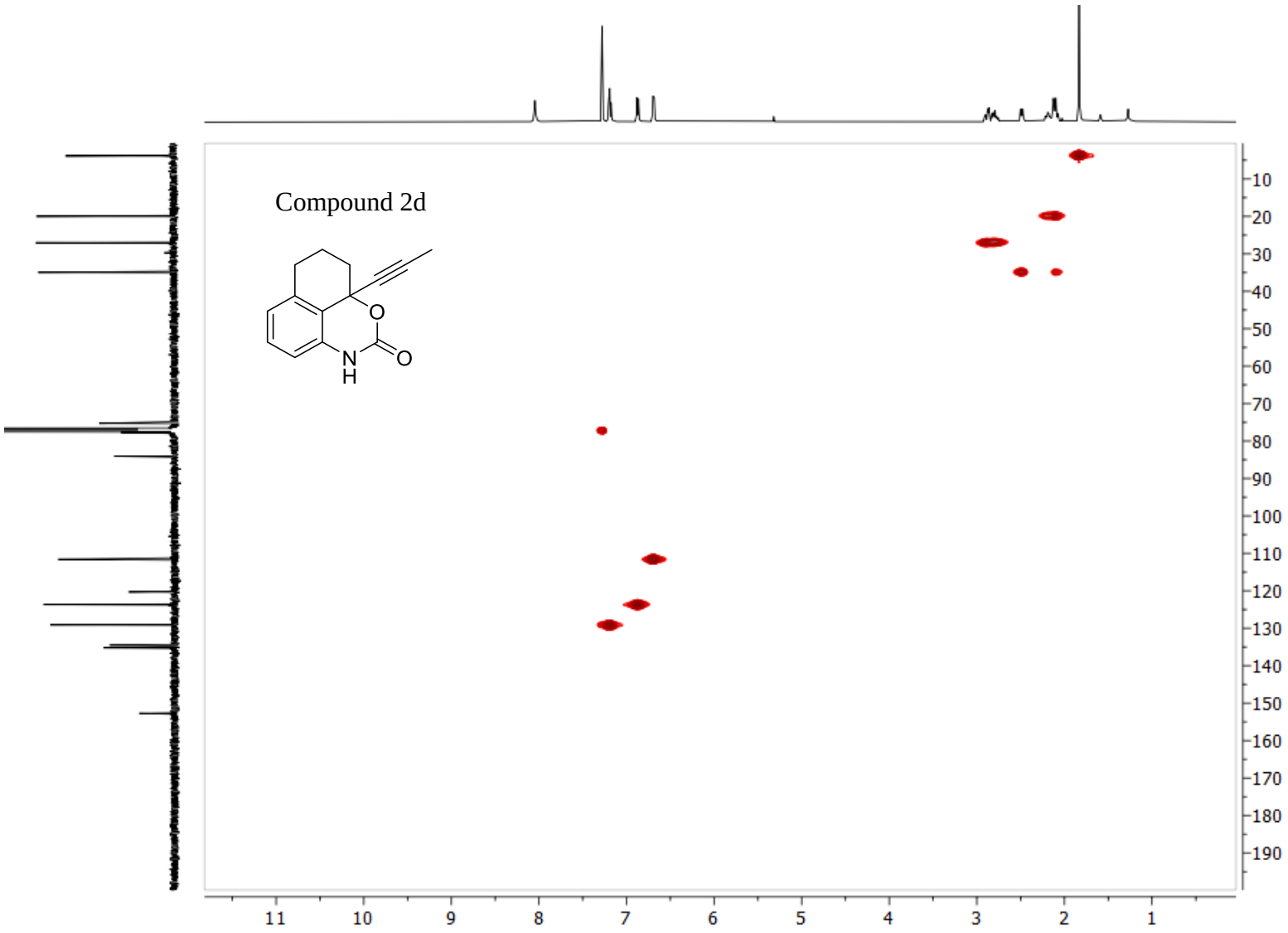
Compound 2d
O
N
H
O
10
20
30
40
50
60
70
80
90
100
110
120
130
140
150
160
170
180
190
11
10
9
8
7
6
5
4
3
2
1

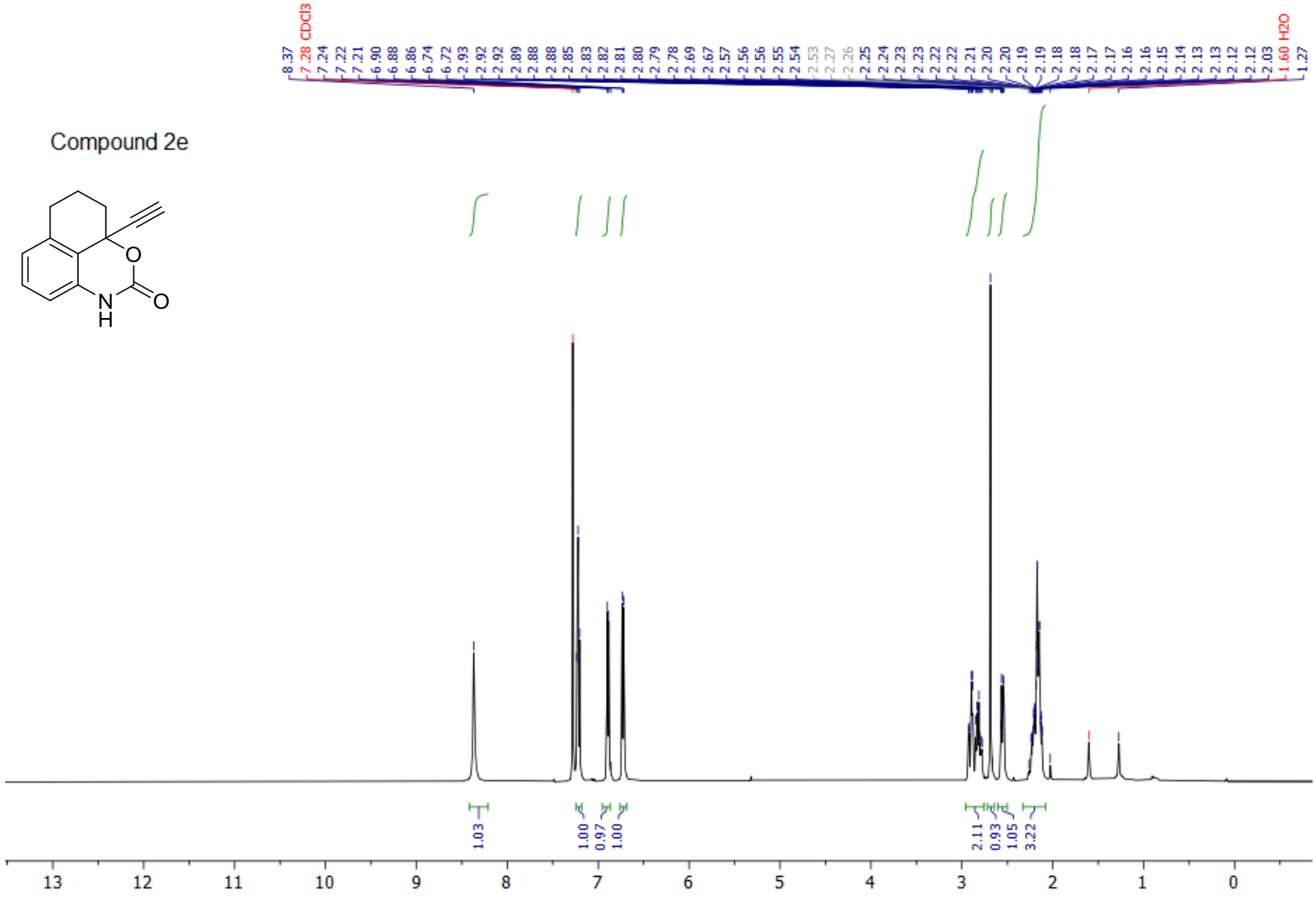
Compound 2e
8.37
7.28 CDCl3
7.24
7.22
7.21
6.90
6.88
6.86
6.74
6.72
2.93
2.92
2.92
2.89
2.88
2.88
2.85
2.83
2.82
2.81
2.80
2.79
2.78
2.69
2.67
2.57
2.56
2.56
2.55
2.54
2.53
2.27
2.26
2.25
2.24
2.23
2.23
2.22
2.22
2.21
2.20
2.20
2.19
2.19
2.18
2.18
2.17
2.17
2.16
2.16
2.15
2.14
2.13
2.13
2.12
2.12
2.03
1.60 H2O
1.27
O
O
N
H
1.03
1.00
0.97
1.00
2.11
0.93
1.05
3.22
13
12
11
10
9
8
7
6
5
4
3
2
1
0

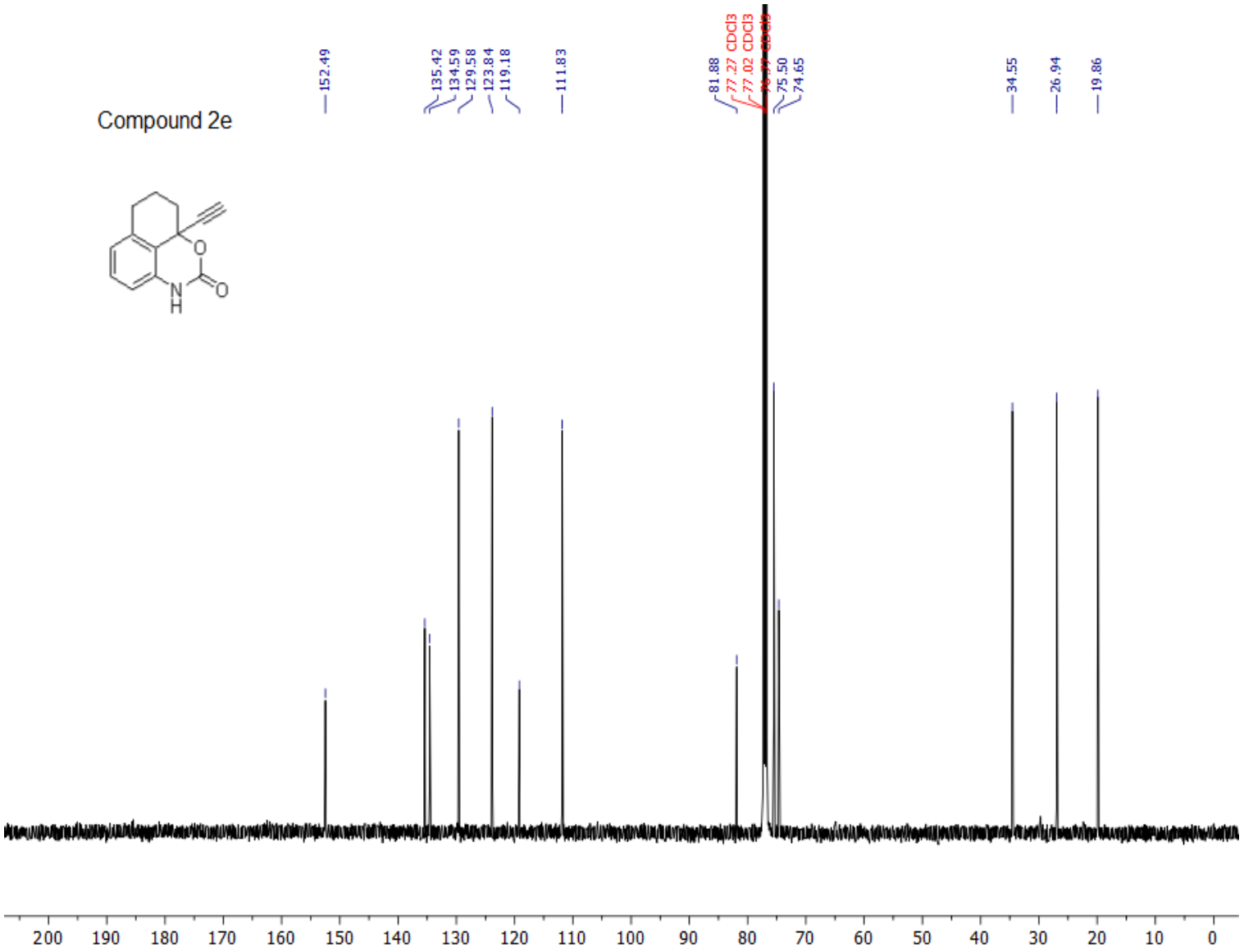
Compound 2e
152.49
135.42
134.59
129.58
123.84
119.18
111.83
81.88
77.27 CDCl3
77.02 CDCl3
75.50
74.65
34.55
26.94
19.86
O
N
H
O
200
190
180
170
160
150
140
130
120
110
100
90
80
70
60
50
40
30
20
10
0

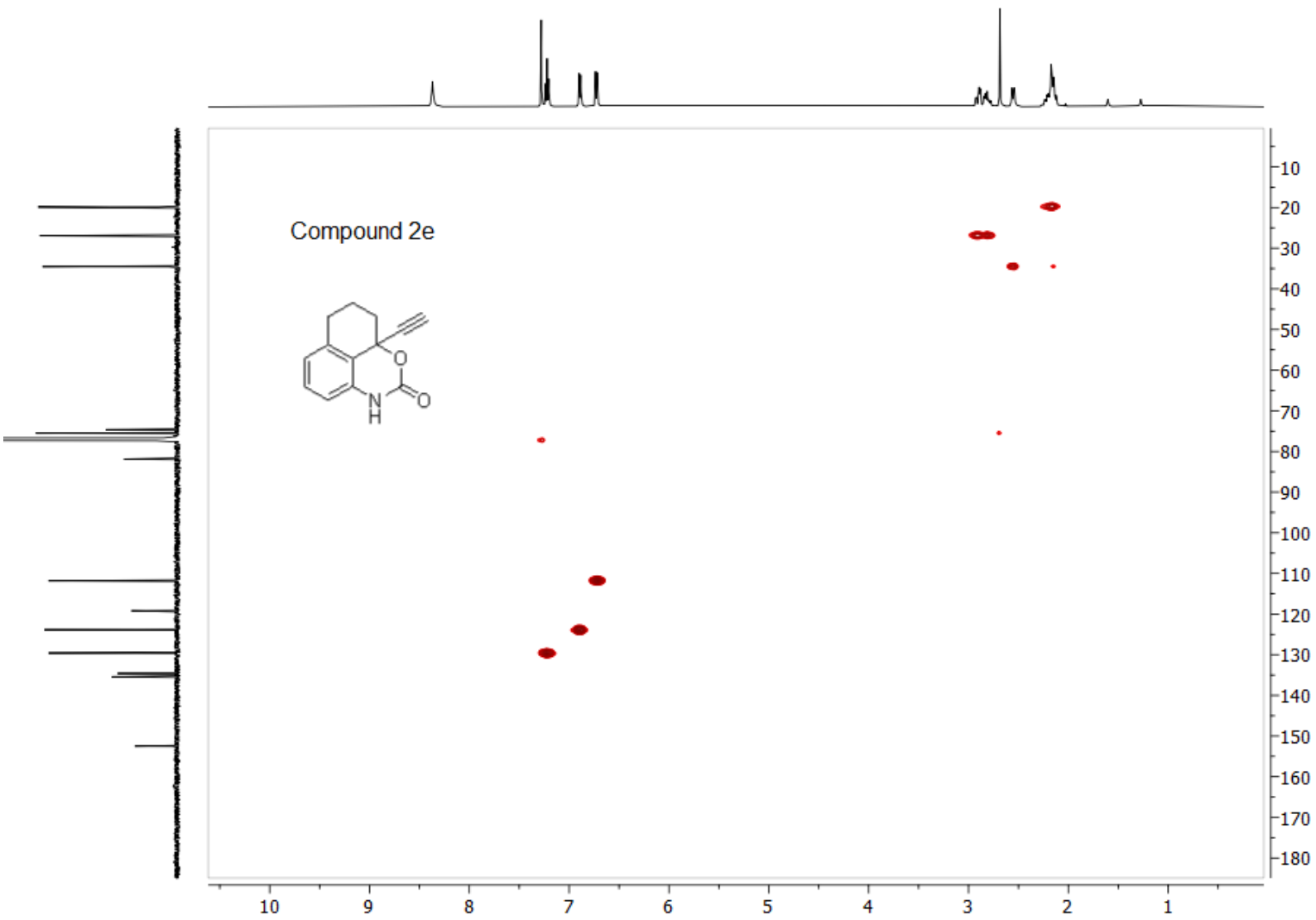
Compound 2e
O
N
H
O
10
20
30
40
50
60
70
80
90
100
110
120
130
140
150
160
170
180
10
9
8
7
6
5
4
3
2
1

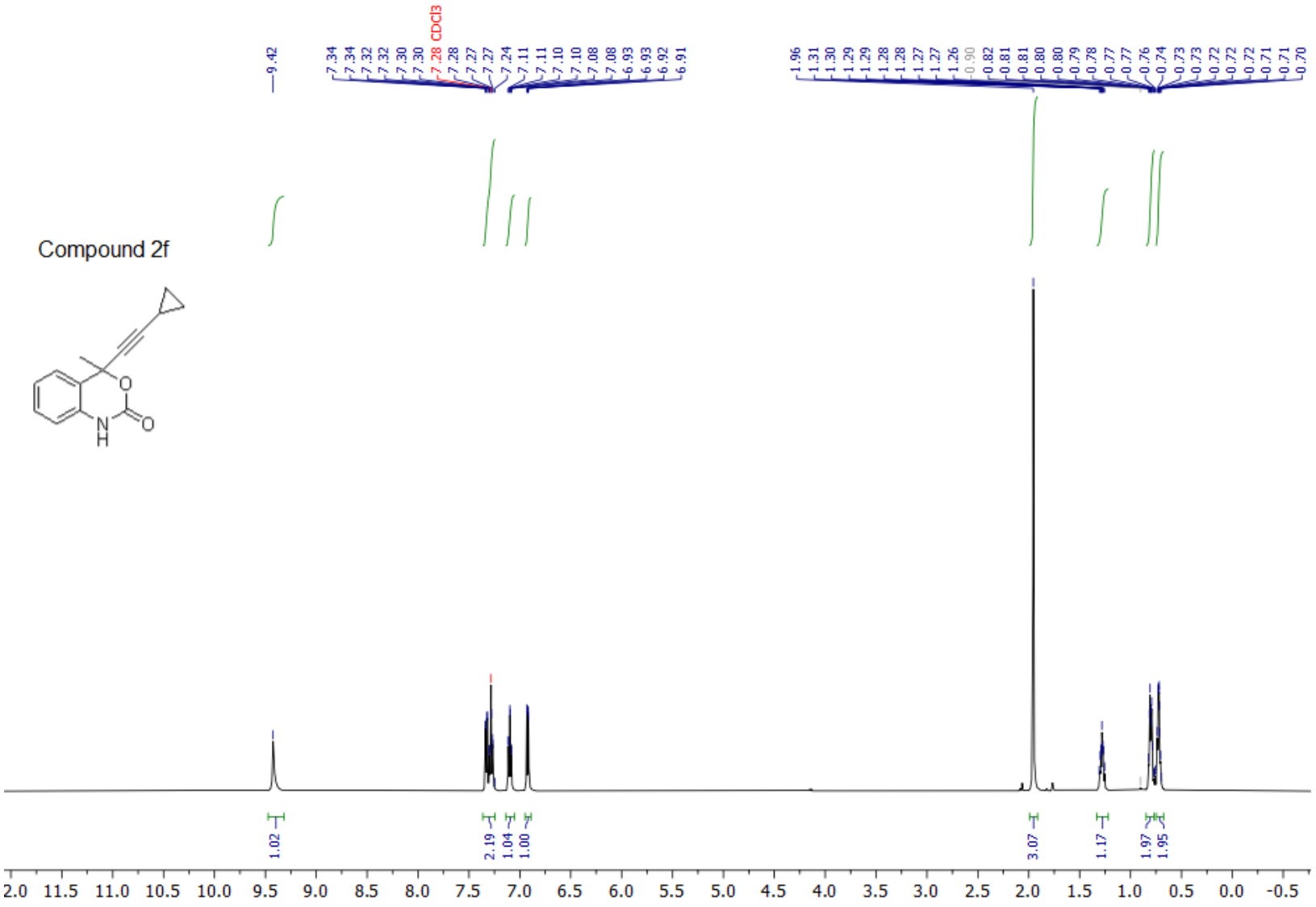
Compound 2f
CDCl3
9.42
7.34
7.34
7.32
7.32
7.30
7.30
7.28
7.28
7.27
7.27
7.24
7.11
7.11
7.10
7.10
7.08
7.08
6.93
6.92
6.91
1.96
1.31
1.30
1.29
1.29
1.28
1.28
1.27
1.27
1.26
0.90
0.82
0.81
0.81
0.80
0.80
0.79
0.78
0.77
0.77
0.76
0.74
0.73
0.73
0.72
0.72
0.72
0.71
0.71
0.70
1.02
2.19
1.04
1.00
3.07
1.17
1.97
1.95
2.0 11.5 11.0 10.5 10.0 9.5 9.0 8.5 8.0 7.5 7.0 6.5 6.0 5.5 5.0 4.5 4.0 3.5 3.0 2.5 2.0 1.5 1.0 0.5 0.0 -0.5

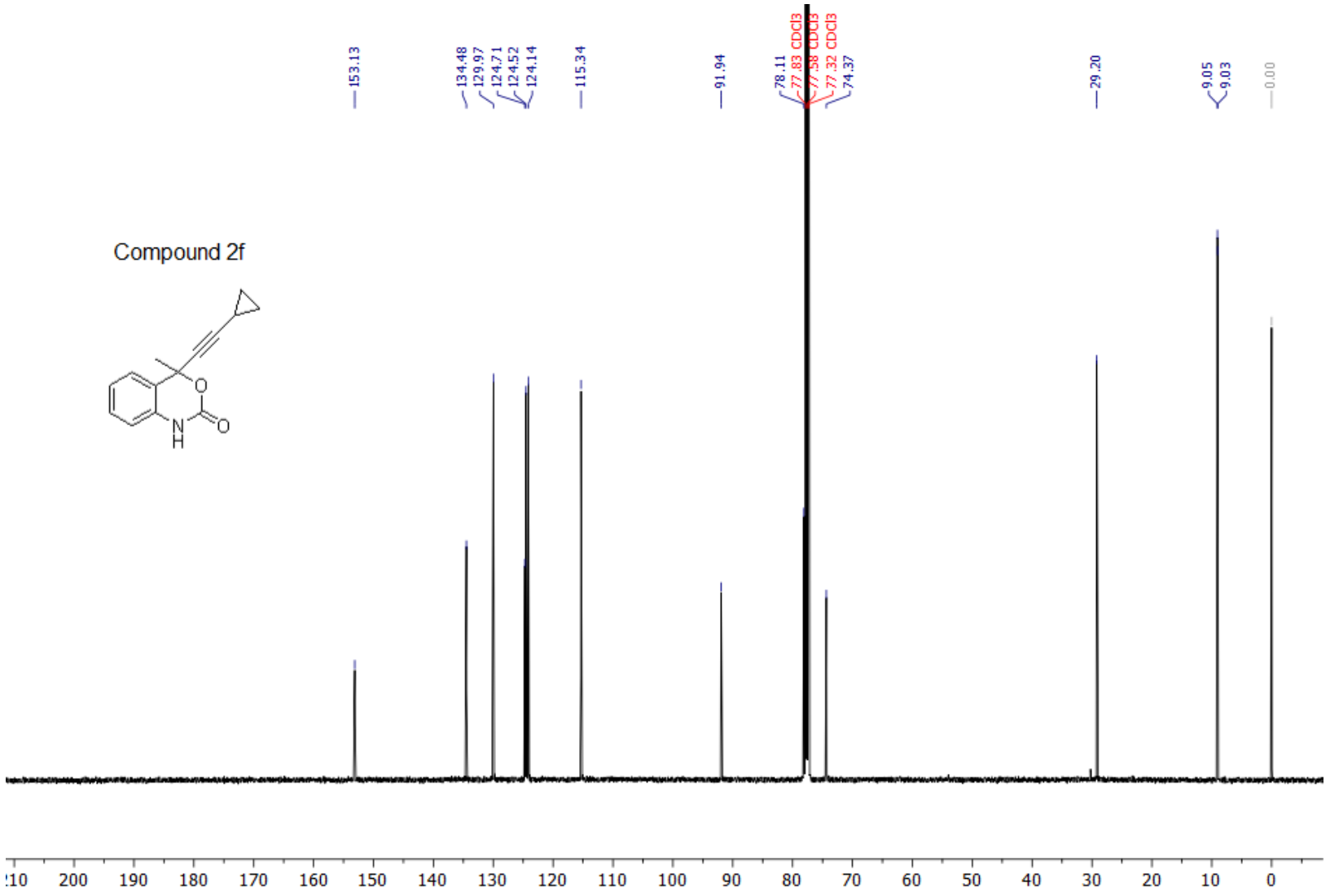
153.13
134.48
129.97
124.71
124.52
124.14
115.34
91.94
78.11
77.83 CDCl3
77.58 CDCl3
77.32 CDCl3
74.37
29.20
9.05
9.03
0.00
Compound 2f
O
N
H
O
210
200
190
180
170
160
150
140
130
120
110
100
90
80
70
60
50
40
30
20
10
0

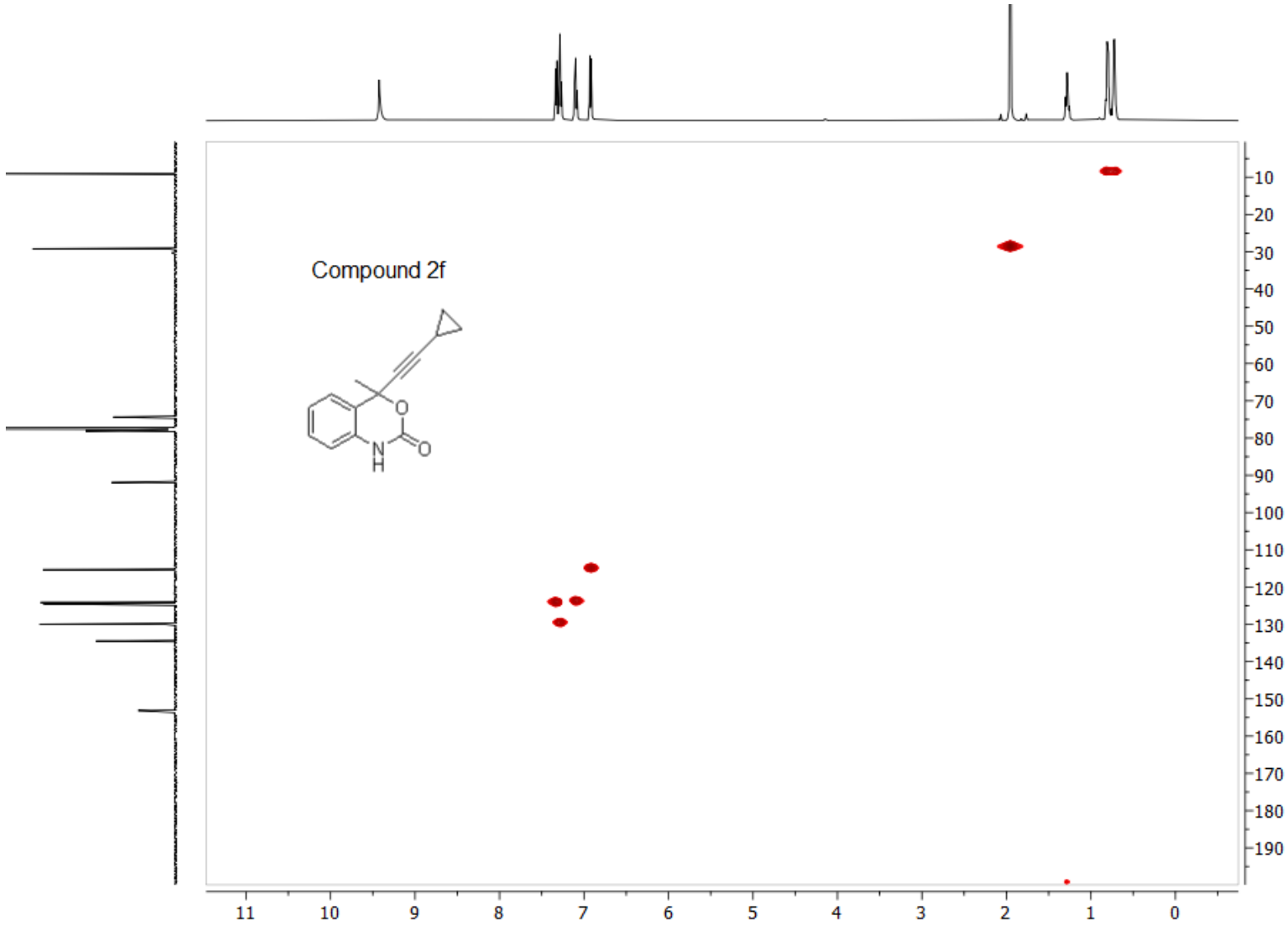
Compound 2f
O
N
H
O
10
20
30
40
50
60
70
80
90
100
110
120
130
140
150
160
170
180
190
11
10
9
8
7
6
5
4
3
2
1
0

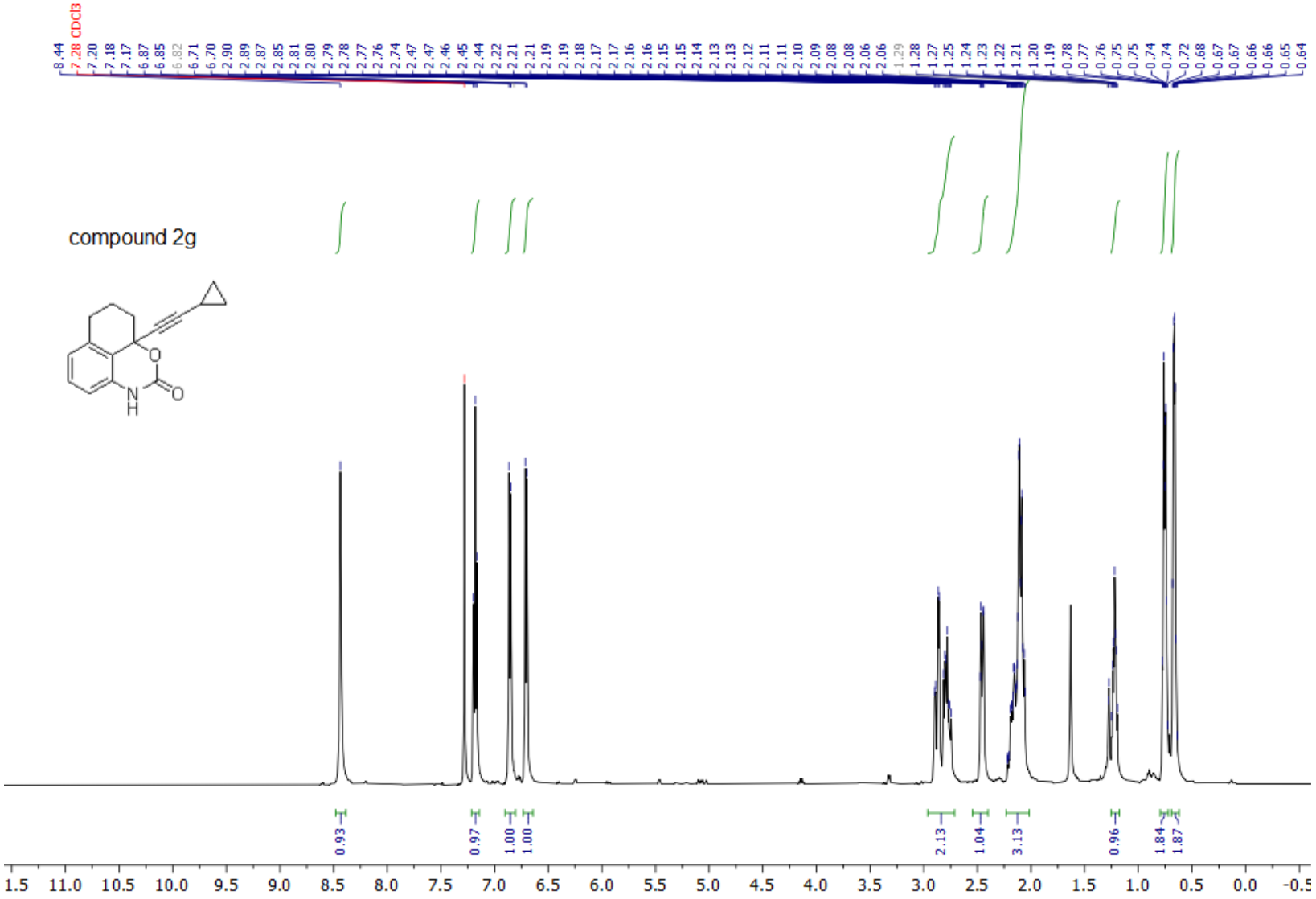
compound 2g
CDCl3
0.93
0.97
1.00
1.00
2.13
1.04
3.13
0.96
1.84
1.87

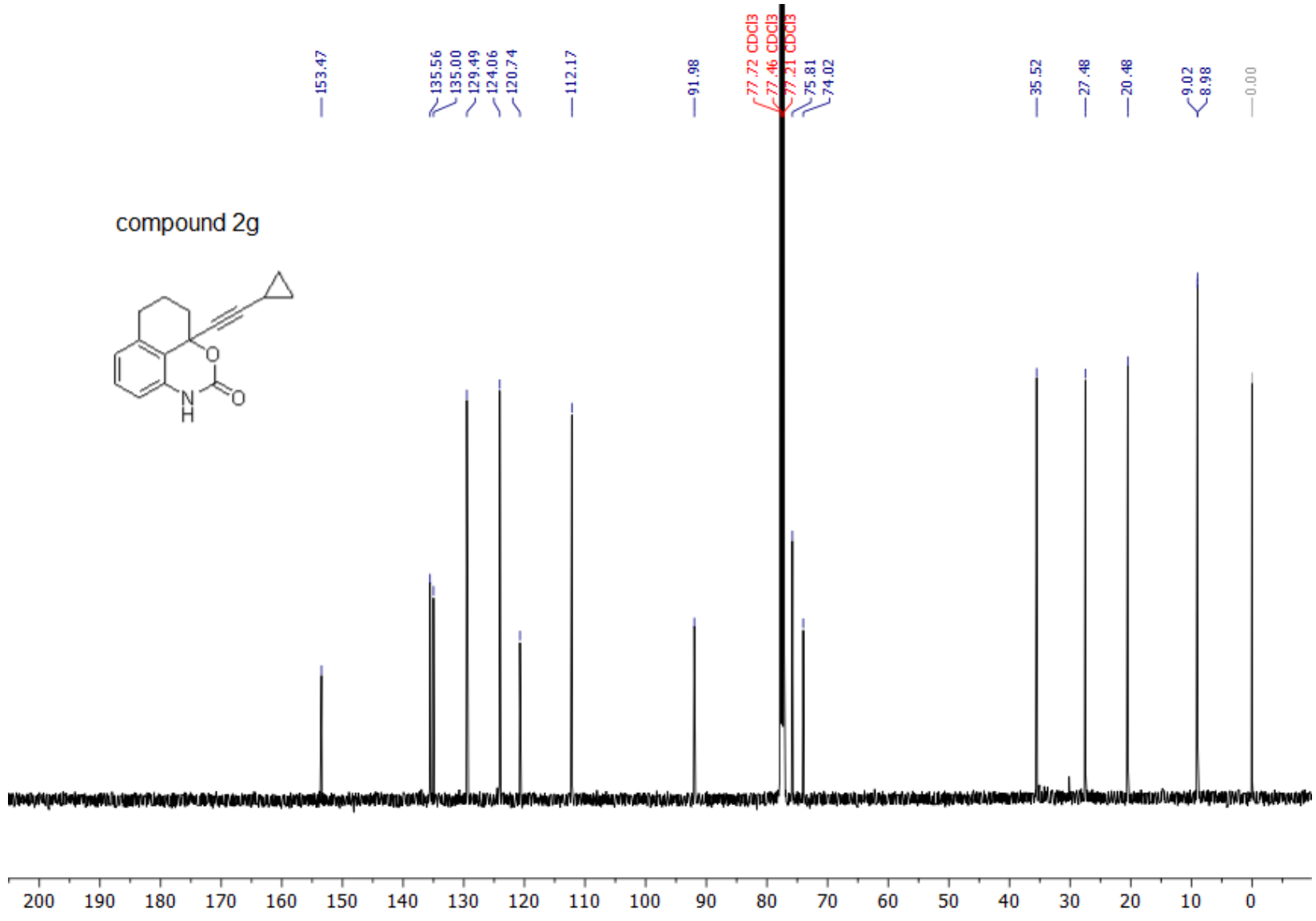
153.47
135.56
135.00
129.49
124.06
120.74
112.17
91.98
77.72 CDCl3
77.46 CDCl3
77.21 CDCl3
75.81
74.02
35.52
27.48
20.48
9.02
8.98
0.00
compound 2g
O
N
H
O
200
190
180
170
160
150
140
130
120
110
100
90
80
70
60
50
40
30
20
10
0

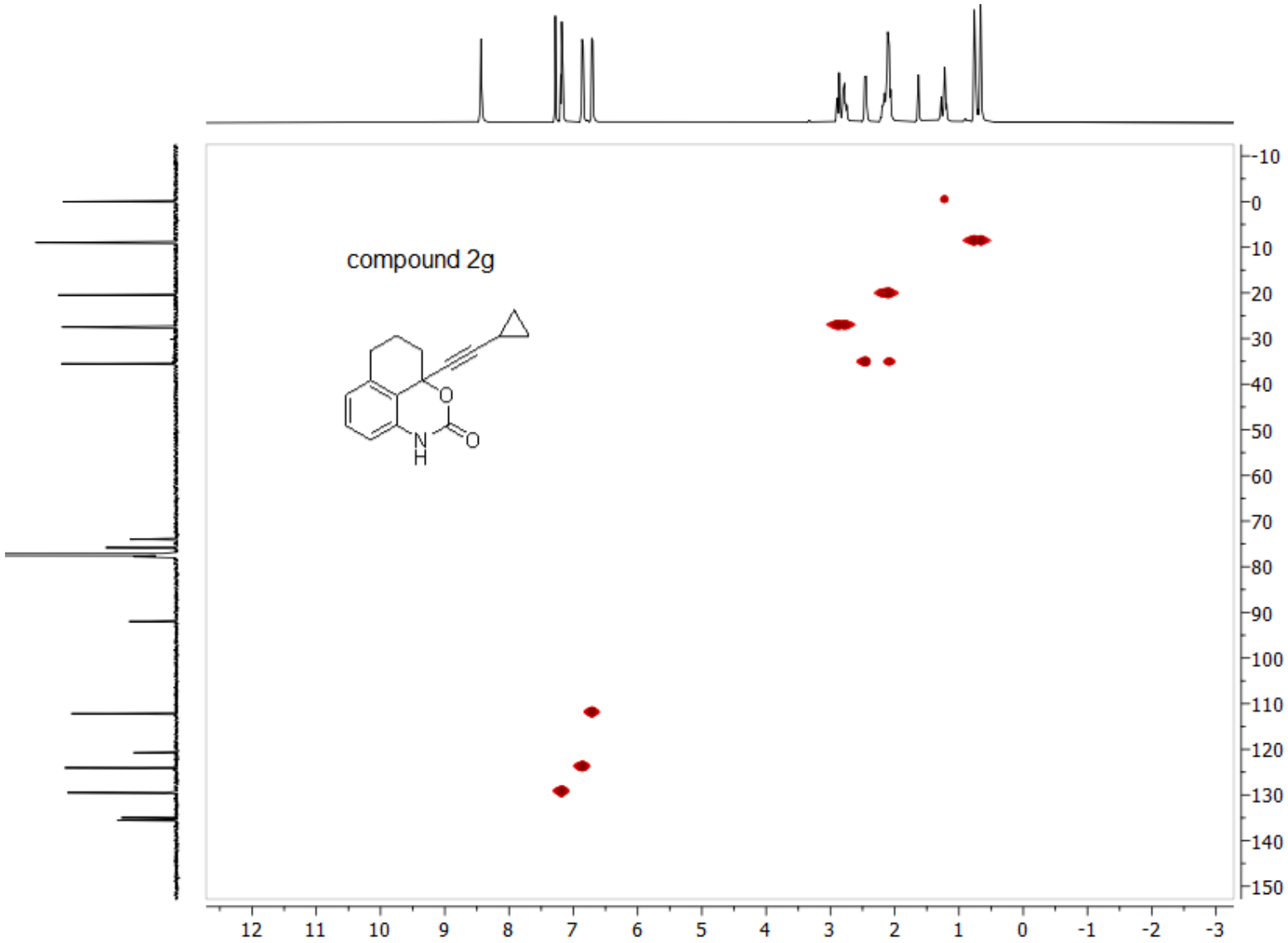
compound 2g
O
N
H
O
-10
0
10
20
30
40
50
60
70
80
90
100
110
120
130
140
150
12
11
10
9
8
7
6
5
4
3
2
1
0
-1
-2
-3

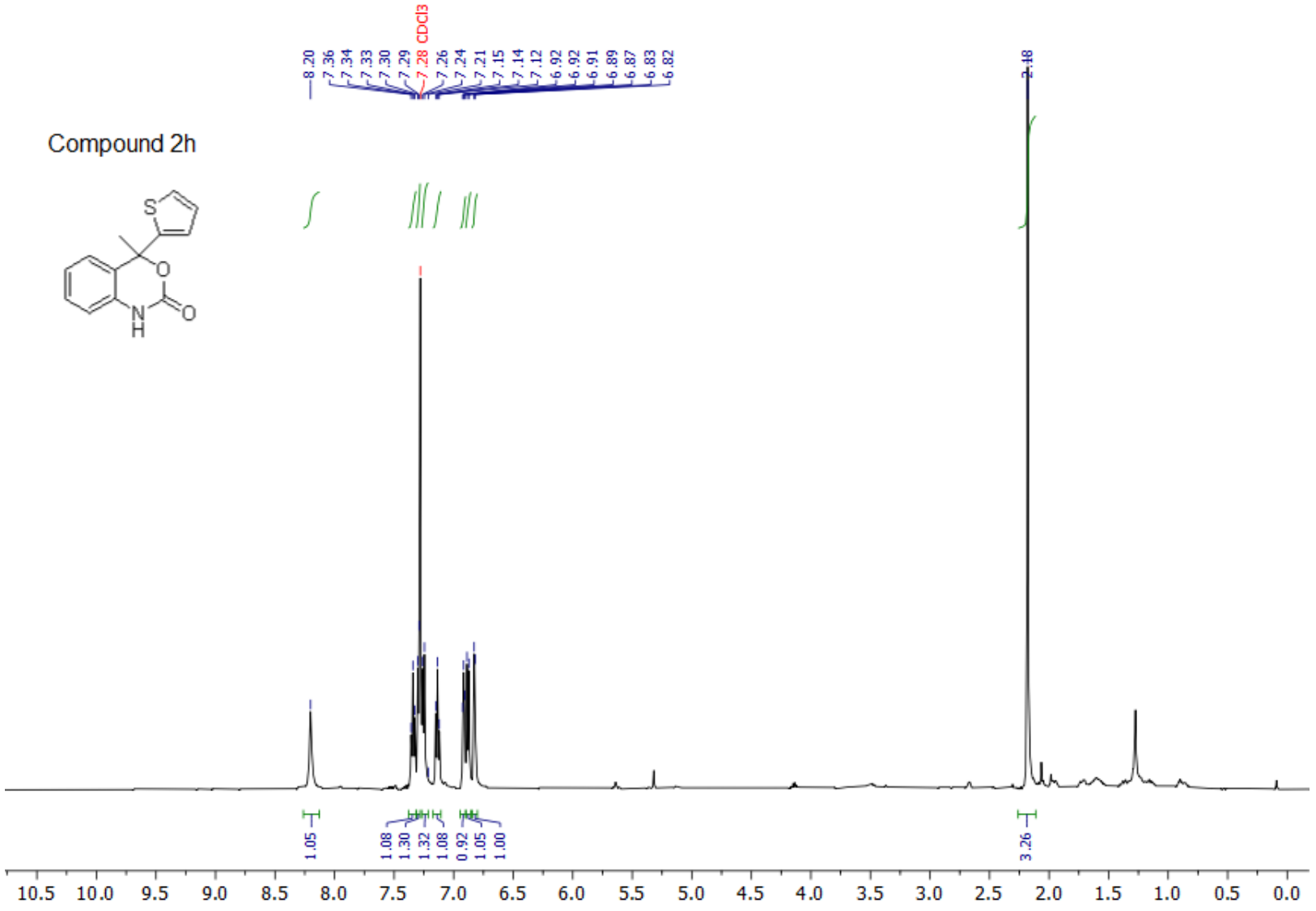
Compound 2h
8.20
7.36
7.34
7.33
7.30
7.29
7.28
CDCl3
7.26
7.24
7.21
7.15
7.14
7.12
6.92
6.92
6.91
6.89
6.87
6.83
6.82
2.48
1.05
1.08
1.30
1.32
1.08
0.92
1.05
1.00
3.26
10.5
10.0
9.5
9.0
8.5
8.0
7.5
7.0
6.5
6.0
5.5
5.0
4.5
4.0
3.5
3.0
2.5
2.0
1.5
1.0
0.5
0.0

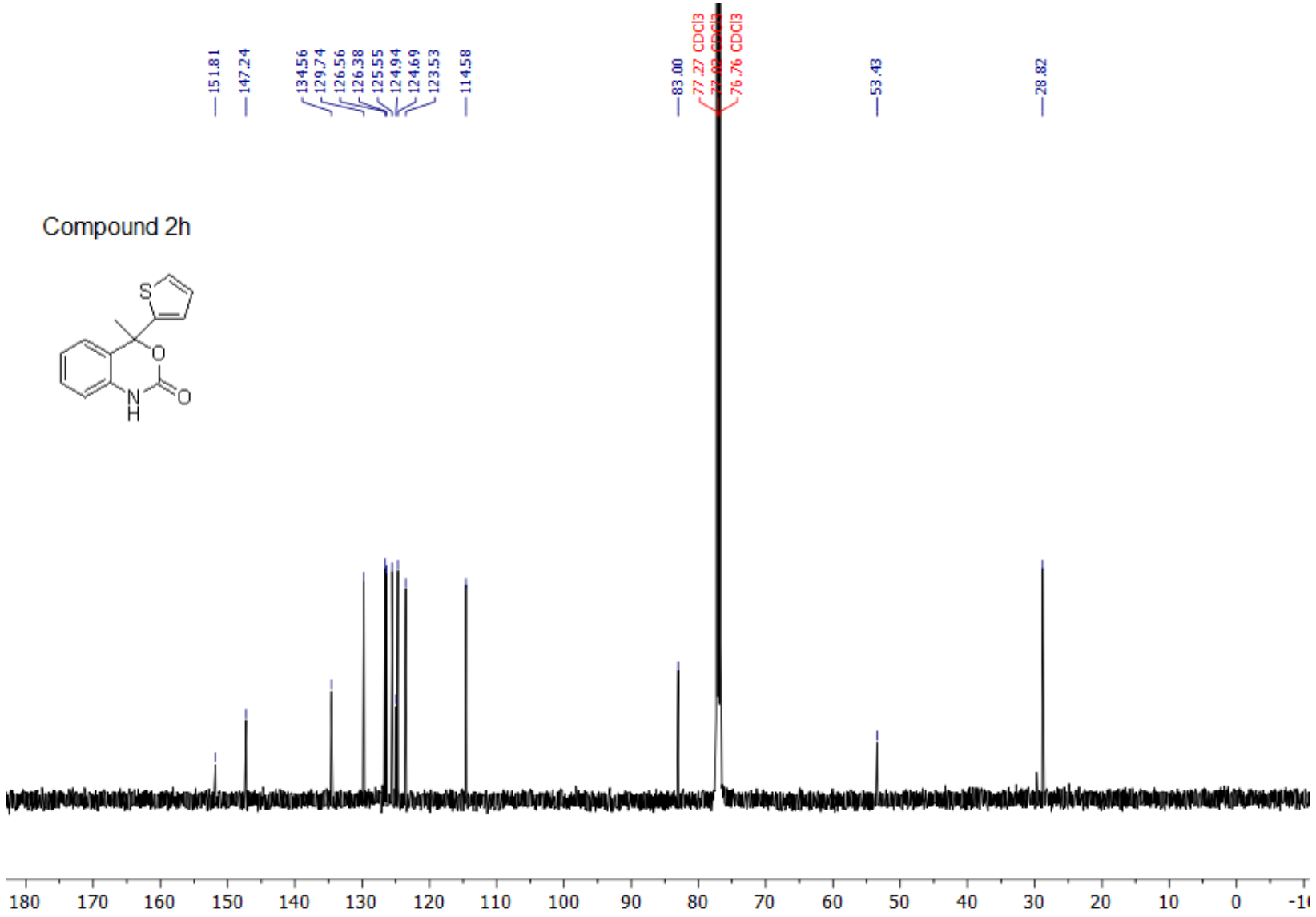
151.81
147.24
134.56
129.74
126.56
126.38
125.55
124.94
124.69
123.53
114.58
83.00
77.27 CDCl3
77.02 CDCl3
76.76 CDCl3
53.43
28.82
Compound 2h
S
O
N
H
O
180
170
160
150
140
130
120
110
100
90
80
70
60
50
40
30
20
10
0

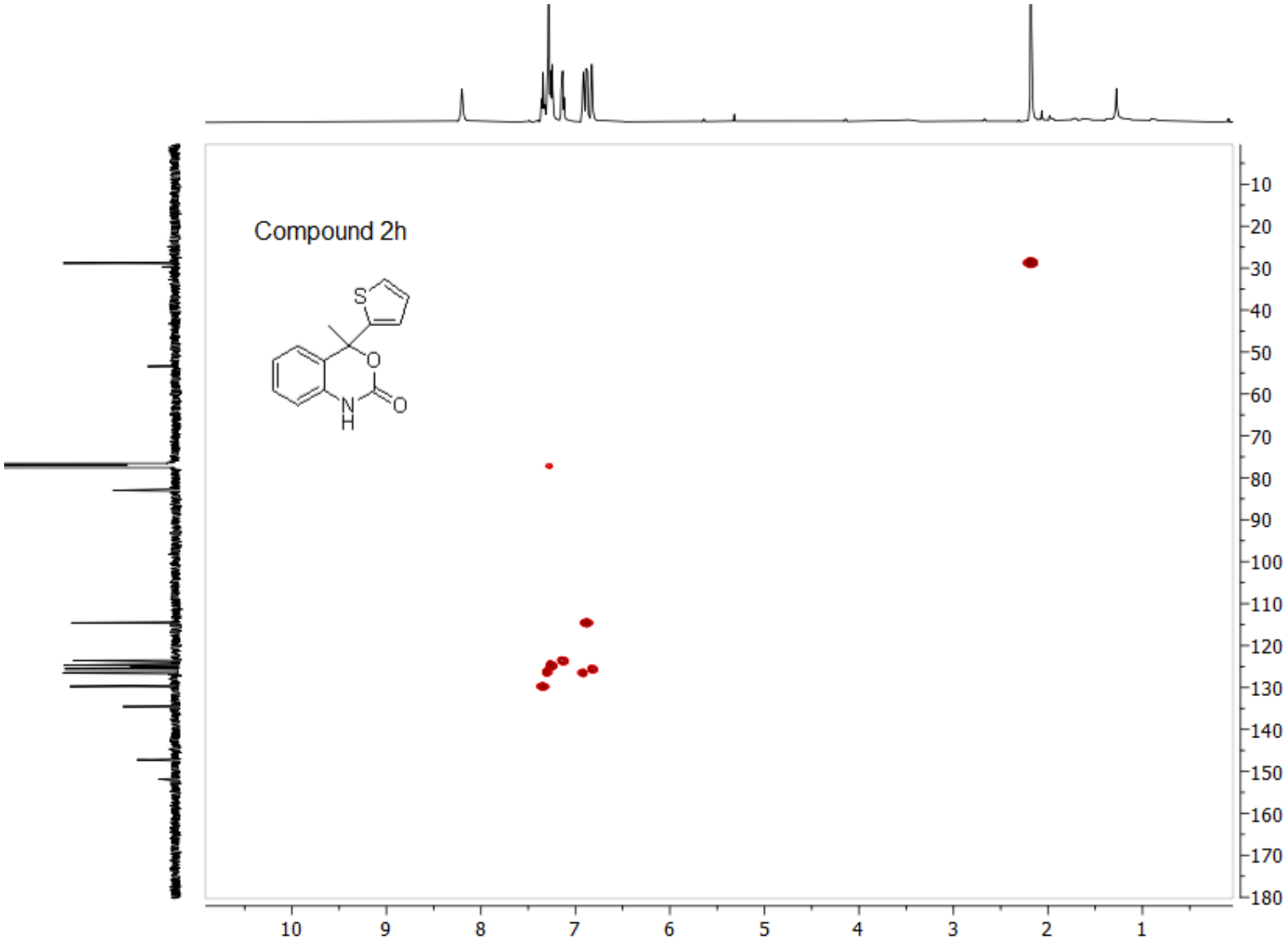
Compound 2h
S
O
N
H
O
10
20
30
40
50
60
70
80
90
100
110
120
130
140
150
160
170
180
10
9
8
7
6
5
4
3
2
1

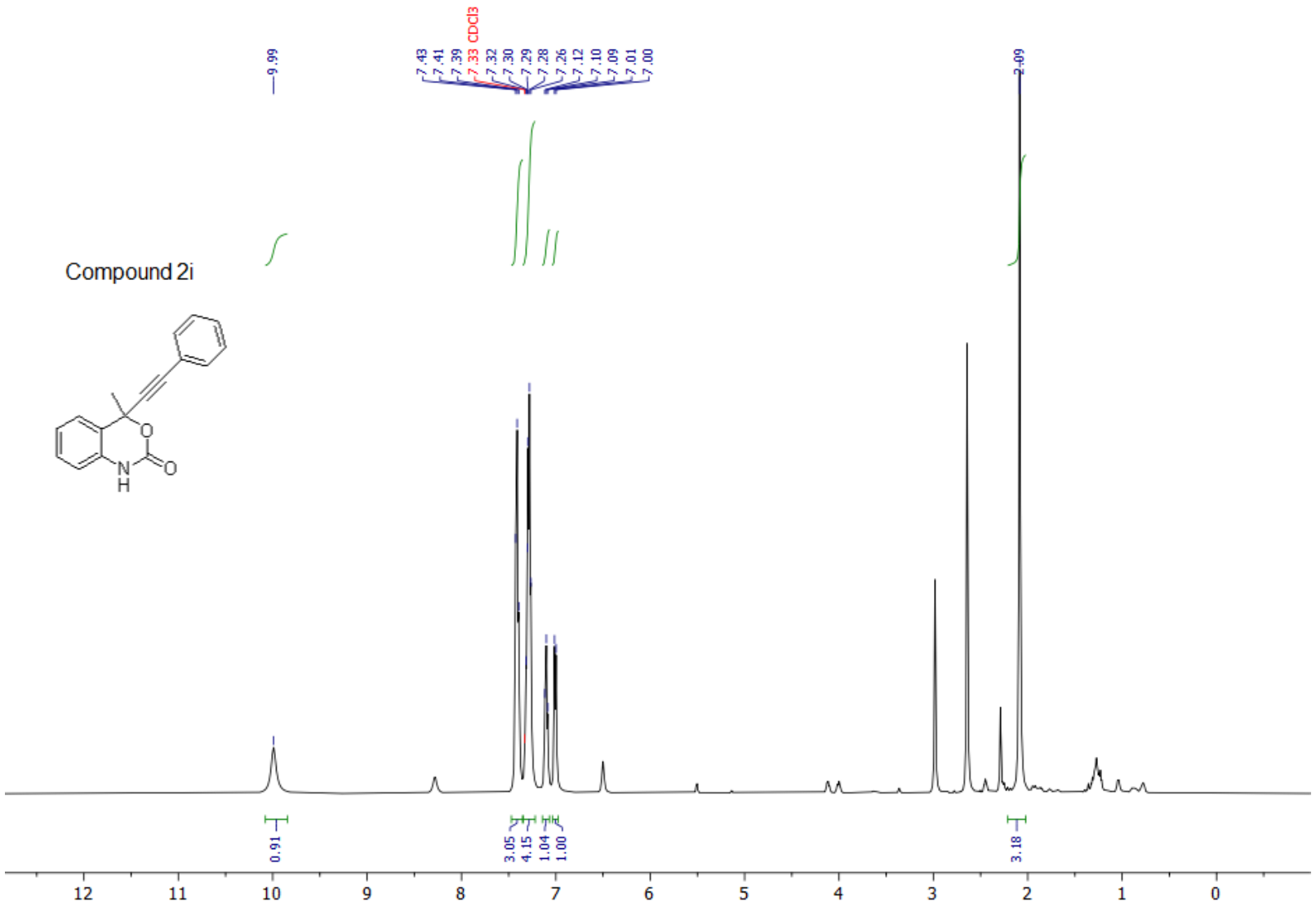
Compound 2i
9.99
7.43
7.41
7.39
7.33
CDCl3
7.32
7.30
7.29
7.28
7.26
7.12
7.10
7.09
7.01
7.00
2.09
0.91
3.05
4.15
1.04
1.00
3.18
12
11
10
9
8
7
6
5
4
3
2
1
0

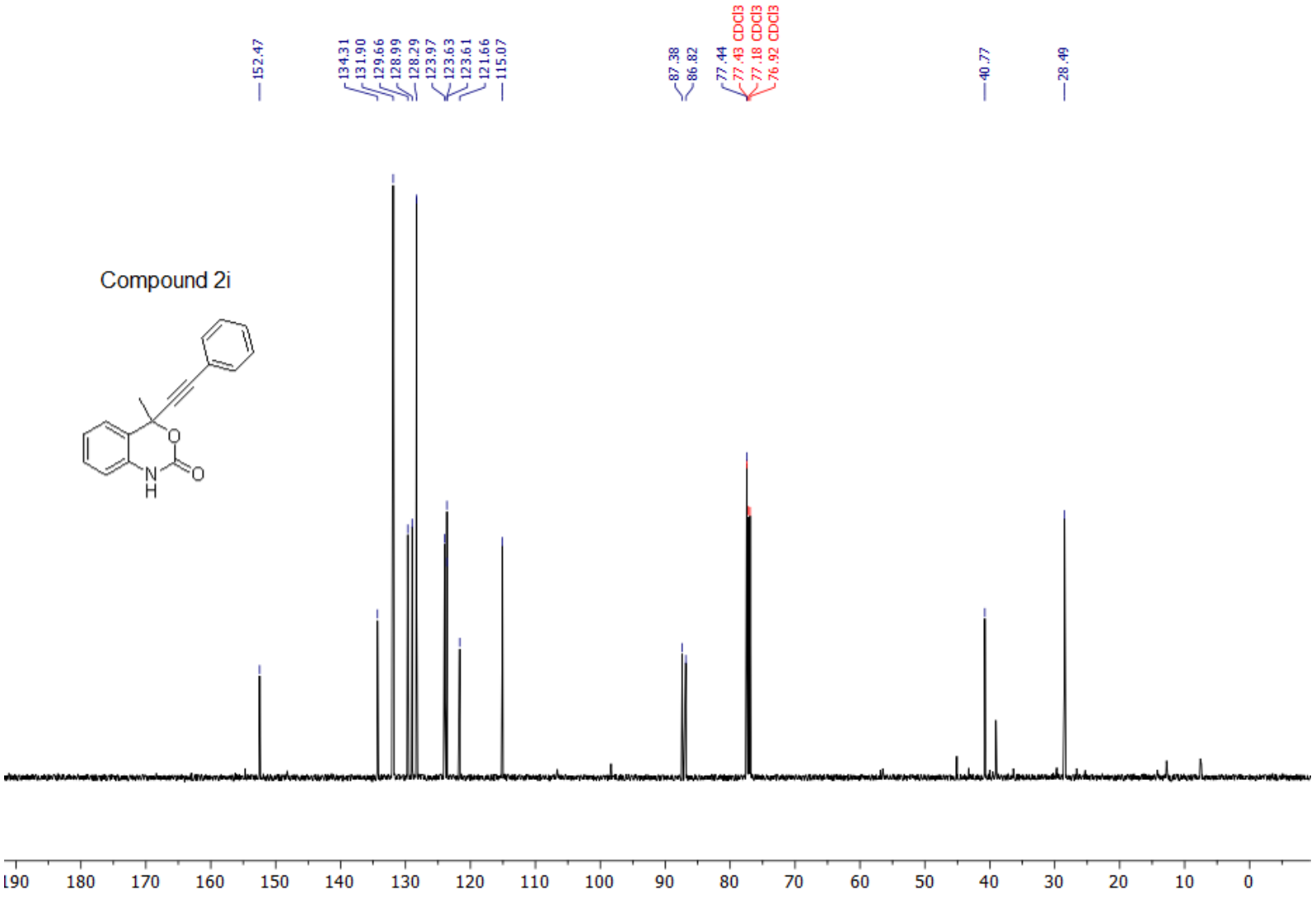
152.47
134.31
131.90
129.66
128.99
128.29
123.97
123.63
123.61
121.66
115.07
87.38
86.82
77.44
77.43 CDCl3
77.18 CDCl3
76.92 CDCl3
40.77
28.49
Compound 2i
O
N
H
O
190
180
170
160
150
140
130
120
110
100
90
80
70
60
50
40
30
20
10
0

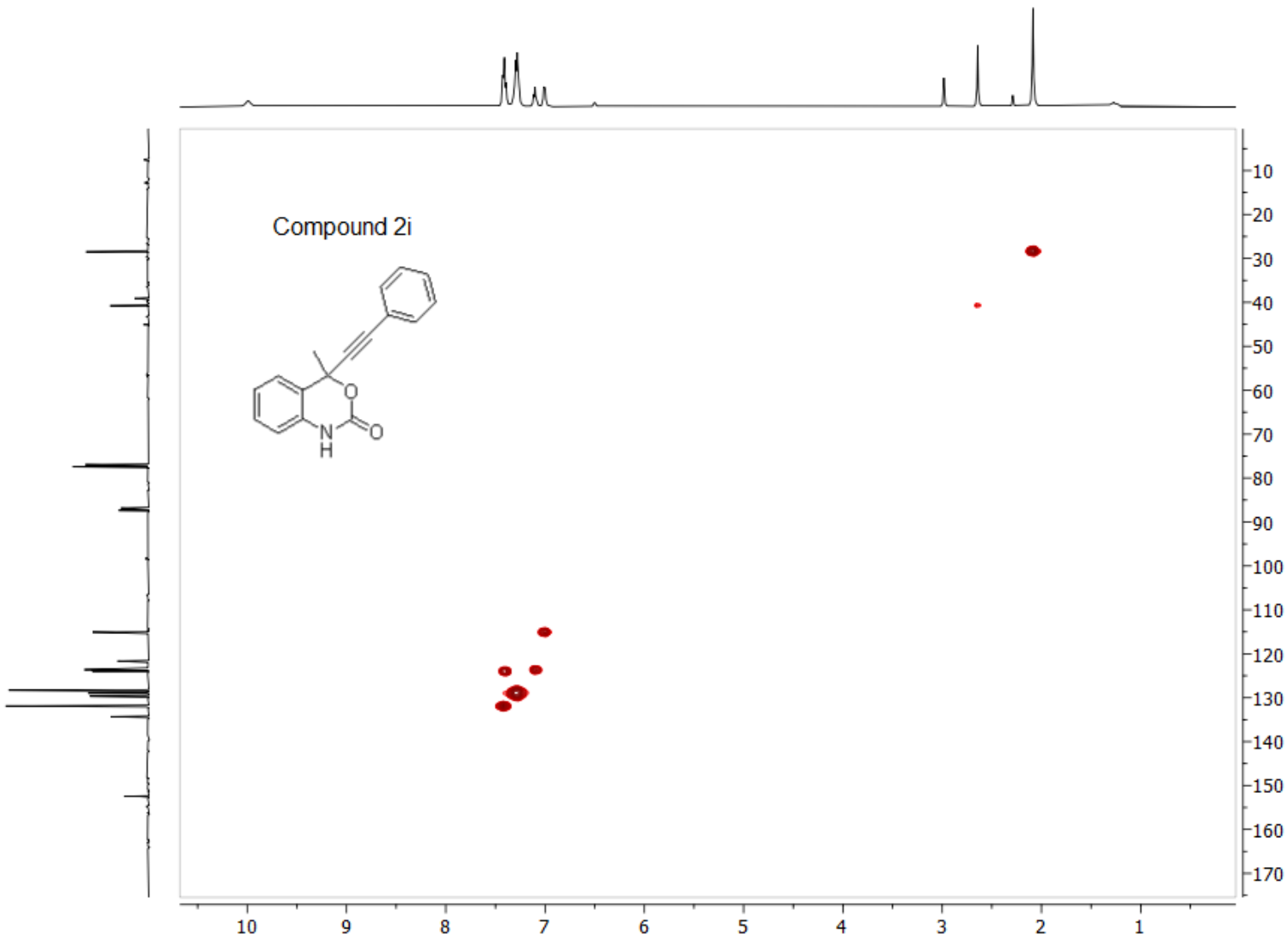
Compound 2i
O
N
H
O
10
20
30
40
50
60
70
80
90
100
110
120
130
140
150
160
170
10
9
8
7
6
5
4
3
2
1

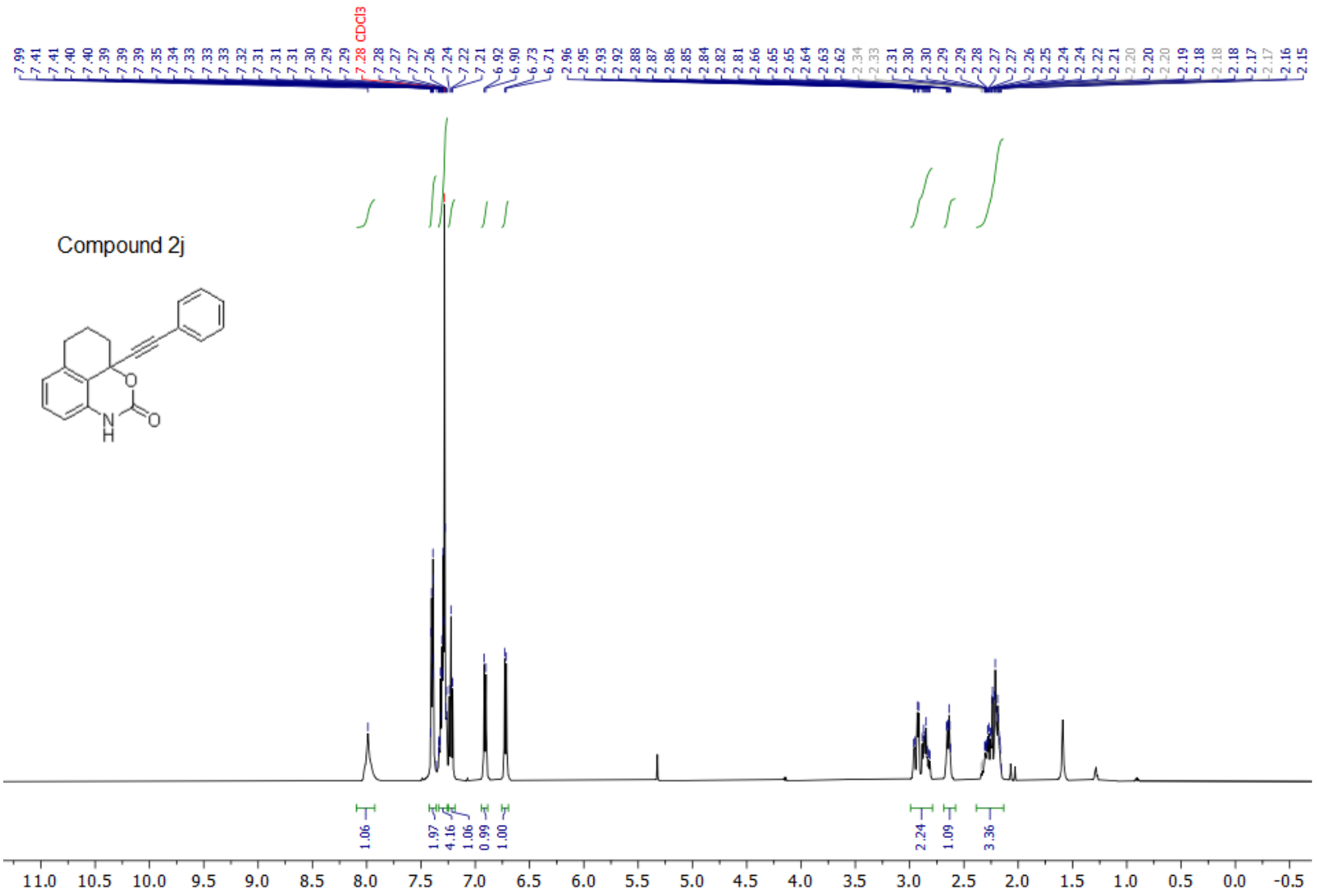
Compound 2j
CDCl3
1.06
1.97
4.16
1.06
0.99
1.00
2.24
1.09
3.36
11.0
10.5
10.0
9.5
9.0
8.5
8.0
7.5
7.0
6.5
6.0
5.5
5.0
4.5
4.0
3.5
3.0
2.5
2.0
1.5
1.0
0.5
0.0
-0.5

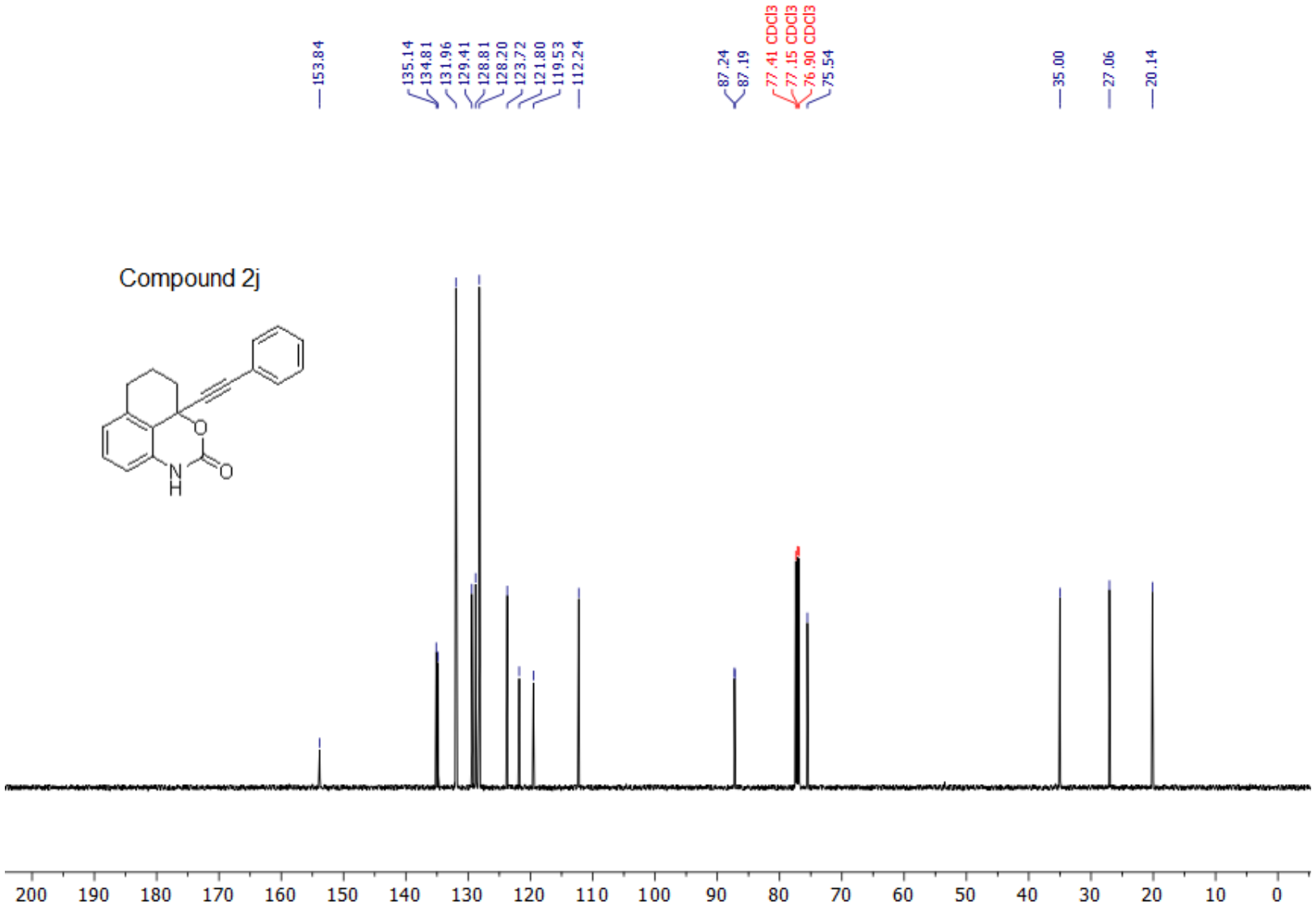
153.84
135.14
134.81
131.96
129.41
128.81
128.20
123.72
121.80
119.53
112.24
87.24
87.19
77.41 CDCl3
77.15 CDCl3
76.90 CDCl3
75.54
35.00
27.06
20.14
Compound 2j
O
O
NH
200
190
180
170
160
150
140
130
120
110
100
90
80
70
60
50
40
30
20
10
0

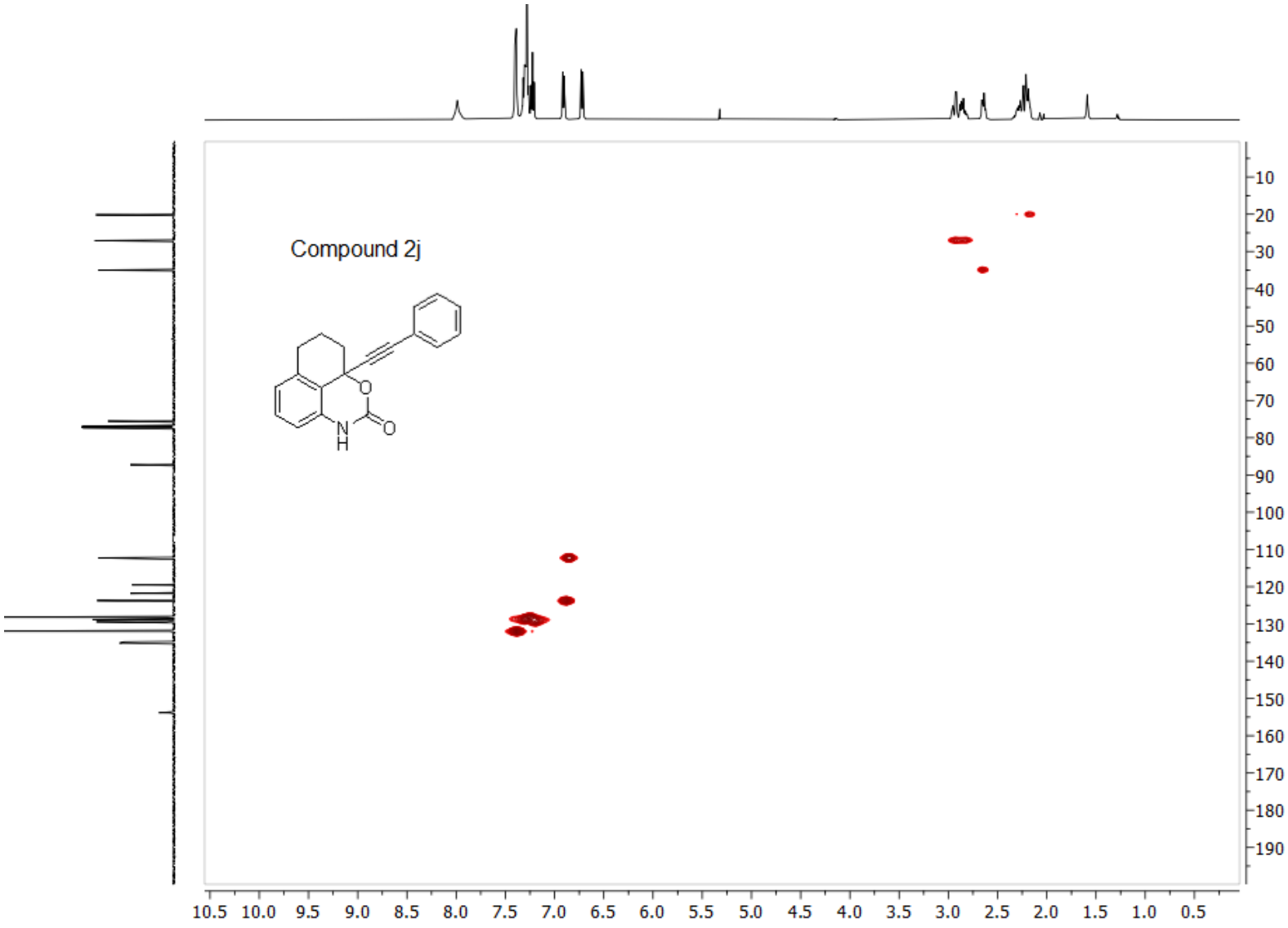
Compound 2j
O
N
H
O
10
20
30
40
50
60
70
80
90
100
110
120
130
140
150
160
170
180
190
10.5 10.0 9.5 9.0 8.5 8.0 7.5 7.0 6.5 6.0 5.5 5.0 4.5 4.0 3.5 3.0 2.5 2.0 1.5 1.0 0.5